Corrosion protection concepts for aluminium and magnesium alloys coated with silica films prepared by water-based sol-gel process

Von der Fakultät für Maschinenbau der

Technischen Universität Chemnitz

genehmigte Dissertation

zur Erlangung des akademischen Grades

Doktor-Ingenieur

Dr.-Ing.

vorgelegt von

M.Sc. Samer Darwich

geboren am 13.04.1978 in Aleppo, Syrien

eingereicht am 01.04.2012

Gutachter

Univ.-Prof. Dr.-Ing. habil. Thomas Lampke

Univ.-Prof. Dr.-rer. nat. habil. Heinrich Lang

Chemnitz, den 01.04.2012

http://nbn-resolving.de/urn:nbn:de:bsz:ch1-qucosa-93617

To my parents

My lovely wife

Dr. Laith and Dr. Taim

List of abbreviations and symbols

Aluminium-oxide	Al_2O_3
Alumina	$Al(OH)_3$
volatile organic compounds	VOC
chromic acid	$H_2Cr_2O_7$
glutathione	GSH
methoxy	OCH_3
ethoxy	OC_2H_5
alkoxy groups	-OR
Hydroxide	-OH
Hydrochloric Acid	HCl
zirconium isopropoxide	$Zr[OCH(CH_3)_2]_4$
cerium isopropoxide	$Ce[OCH(CH_3)_2]_4$
Tetraethylorthosilica	TEOS
Methyltriethoxysilane	MTES
3-glycidoxypropyltrimethoxysilane	GPTM
Silicon dioxide	SiO_2
Zirconium oxide	ZrO_2
Silicon carbide	SiC
Disilica	SiO_3^{2-}
Cycle's Voltammetric measurement	CVs
electrochemical impedance spectroscopy	EIS
Scanning Electron microscopy	SEM
1.2.3 Benzotriazole	BTAH

Curriculum Vitae

Family name:	Darwich
Name:	Samer
Birth date/ place:	13.04.1978 / Aleppo-Syria
Nationality:	Syrian
Address:	Vetterstraße 70/129, 09126 Chemnitz, Germany

Scientific education

Since 2007	PhD student at Chemnitz University of Technology, Faculty of Mechanical Engineering-Institute of Surface Technology and Functional Materials
2003-2005	Master degree in Applied Chemistry at Aleppo University-Syria

Professional activities

Since 2007	Scientific Co-Worker at the Faculty of Mechanical Engineering-Institute of Surface Technology and Functional Materials, TU-Chemnitz-Germany

Further education courses

- Team Development & Leadership at TU Chemnitz
- Creo Elements/Pro Wildfire 5 at TU Chemnitz
- Training Course in Excel-Macro for application at Aleppo University

List of Figures

List of Tables

Contents

Bibliografische Beschreibung

Darwich, Samer

Thema

Konzepte für den Korrosionsschutz von Aluminium- und Magnesiumlegierungen mit mittels Sol-Gel-Prozess hergestelltem Silikafilm auf Wasserbasis

Dissertation an der Fakultät für Maschinenbau der Technischen Universität

Chemnitz, Professur Oberflächentechnik/Funktionswerkstoffe

Seitenzahl: 141

Anzahl der Abbildungen: 86

Anzahl der Tabellen: 12

Anzahl der Literaturzitate: 165

Zusammenfassung

Die vorliegende Arbeit liefert einen Einblick in die Entwicklung von Silikafilmen, die mittels Sol-Gel-Prozess auf Wasserbasis hergestellt wurden. Die Schwächen der Beschichtungstechnologie werden dargestellt und Lösungen diskutiert. Der Silikafilm wird auf Aluminiumlegierung 6082-T6 und Magnesium-legierung AZ31 aufgebracht. Schwerpunkt dieser Arbeit ist die Entwicklung der Schichteigenschaften, wie Kosteneffizienz, Rissfreiheit, Selbstheilung so wie langfristiger Korrosionsschutz. Rissbildung ist ein wesentlicher Nachteil von Silikafilmen; rissfreie Filme wurden mittels nanopartikeldotierter Silikafilme hergestellt. Die Selbstheilung von Aluminium- und Magnesiumsubstraten mit Silikafilm wird durch den Effekt der wasserlöslichen Korrosionsinhibitoren generiert. Die Experimente haben gezeigt, dass die Proben mit inhibitordotierter Beschichtung selbst gegen Korrosion geschützt sind. Ein langfristiger Korrosionsschutz wird durch eine Mischung aus Korrosionsinhibitor-dotierten Silika-Film realisiert.

Schlüsselwörter: Wasserbasis sol, Silikafilm, Sol-Gel-Prozess, Korrosionsinhibitoren, Selbstheilung, Korrosionsschutz

Bibliographic description

Darwich, Samer

Topic

Corrosion protection concepts for aluminium and magnesium alloys coated with silica films prepared by water-based sol-gel process

Dissertation at the Faculty of Mechanical Engineering of the Technical University

Chemnitz, Institute of Surface Technology and Functional Materials

Number of pages: 141

Number of figures: 86

Number of tables: 12

Number of references: 165

Summary

The present work provides an insight in the development of silica films prepared by water-based sol-gel process. The weaknesses of the coating technology are identified, also solutions are discussed. The silica film is applied on aluminium alloy 6082-T6 and magnesium alloy AZ31. The development of the coating properties such as cost-efficiency, crack-free, self-healing and long-term corrosion protection is the main topic of this work. Cracking is the major drawback of silica films; the cracks are generated due to shrinkage of the film during the heat treatment, nanoparticles-doped silica film is successfully reduced the shrinkage which leads to crack-free silica films. The self-healing of the coated aluminium and magnesium samples is generated by corrosion inhibitors-doped silica film. When a defect appears in the film, the corrosion inhibitors leach out of the silica film to the defect area to heal the corroded surface. The long-term corrosion protection is realized by means of a mixture of corrosion inhibitors-doped silica film.

Keywords: water-based sol, silica film, sol-gel process, corrosion inhibitors, self-healing, corrosion protection

1 Introduction

Silica films prepared by sol-gel process are widely accepted as environmental friendly protective layers for aluminium and magnesium metal alloys. The keyword of this technology is the composition of the sol and the application parameters which controls the structure and the properties of the film [1; 2]. The sol consists usually of organo-silica materials, catalyst and water. The organo-silica compounds are immiscible with water in all proportions. Thus, organic solvents are needed to achieve dispersion of the water with the organo-silica compounds. The using of the organic solvent or volatile organic compounds (VOC) showed several problems in the applications such as the flammability and evaporation [3; 4]. This has shifted studies to develop the water-based sol-gel process to reduce the amount of VOCs and to obtain cost-efficient sol. The water–based sol shows also obstacles in the applications such as:

- Low hydrophobic organo-silica compounds are used to prepare the water-based sol, which leads to silica film with low hydrophobic property in comparison to the alcohol-based silica films,
- the low stability of the water-based sol, especially at intermediate pH values,
- the corrosion inhibitors-doped water-based sol has to be completely water soluble, the using of corrosion inhibitors is needed to generate the self-healing effect.

Self-healing is an important aspect to improve the stability of aluminium and magnesium samples in corrosive solution. When a defect occurs in the corrosion inhibitors-doped silica film, the corrosion inhibitors leach out of the film to the defect area, a layer of corrosion inhibitors is formed in the defect which reduces the corrosion process [5]. The solubility of the corrosion inhibitors in the water-based sol and in the corrosive media show an important influence on the self-healing ability of the aluminium and magnesium samples coated with silica film. [6; 7]

In this work, the proposed coating system consists of organo-silica compound, nanoparticles, corrosion inhibitors, acid as a catalyst and water as a solvent. No

VOCs are needed to prepare the water-based sol which demands for safety issues and cost-efficient system.

The water-based sols show a rapid hydrolysis reaction of the organo-silica compounds in acid media. The silica coating is amenable to dipping, brushing and spraying on a clean aluminium and magnesium metal alloy. The heat treatment of the film is needed to obtain a dense protective film through the cross-linking of the silica compounds.

The proposal of this thesis provides an important insight in the development of the silica film prepared by water-based sol-gel process. The weakness of the new coating technology are identified, also solutions are discussed. The development of the film properties such as cost-efficiency, crack-free films, self-healing and long-term corrosion protection is the main topic of this work, which can be achieved by:

- modifying the composition of the water-based sol and the application parameters to reach a cost-efficient protective silica film,
- investigating the effect of the nanoparticles to reduce the shrinkage of the silica film in order to obtain crack-free film,
- Improving of the self-healing of the coated aluminium and magnesium sample by using a mixture of the water-soluble corrosion inhibitors, to reach the long-term corrosion protection,
- developing the stability of the water-based sol which is important for the cost-efficiency systems,
- sealing of anodized aluminium and plasma anodized magnesium in the water-based sol for better corrosion protection.

2 State of the art

2.1 Corrosion of aluminium

Corrosion is defined as the deterioration of materials due to the reactions with their environments; materials are included metals, polymers and ceramics. Metals are produced from their natural ores and have the tendency to return to the most thermodynamically stable state which considered as corrosion. The corrosion can be physical, chemical or electrochemical. [8]

Aluminium comprises 8% of the earth's crust. The annual market of the aluminium is 25 million tons which makes it the leader in the metallurgy of non-ferrous metals [9]. The applications of aluminium alloys are vary from household to electrical engineering, packaging, transport and building. The high consumption is attributed to the properties of aluminium alloys such as lightness and corrosion resistance. The natural aluminium oxide layer can protect the aluminium alloy from atmospheric corrosion; the passive oxide layer hinders the effect of the oxygen and atmospheric pollutants on the aluminium substrate. Aluminium oxide layer is unstable in corrosive environments. When aluminium metal alloy is plunged into corrosive aqueous solution, the corrosion of the metal is controlled by the anodic and cathodic reactions. The anodic corrosion reaction of the aluminium alloy proceeds according to the equation 1. [10]

$$Al \rightarrow Al^{3+} + 3e^{-} \quad (1)$$

The aluminium metal with oxidation state (0) goes in the solution as a cation Al^{3+} and loosing three electros. The electrons results from the oxidation of the aluminium metal are picked up by H^{+} to form hydrogen gas at the cathodic site. Two cathodic reactions can be happen at moderate pH values (equations 2, 3, 4 and 5). [11; 12]

- Reduction of H^+ protons, as in equation 2:

$$3H^+ + 3e^- \rightarrow \frac{3}{2} H_2 \tag{2}$$

The H^+ are formed from the water dissolution according to the equation 3

$$2H_2O \Leftrightarrow H_3O^+ + OH^- \tag{3}$$

- Reduction of oxygen dissolved in water (equations 4 and 5):

  - Reduction in alkaline or neutral solution

$$O_2 + 2H_2O + 4e^- \rightarrow 4OH^- \tag{4}$$

  - Reduction in acid media

$$O_2 + 4H^+ + 4e^- \rightarrow 2H_2O \tag{5}$$

The corrosion of aluminium in aqueous media is the sum of the anodic and the cathodic corrosion reactions.

$$Al \rightarrow Al^{3+} + 3e^-$$
$$3H^+ + 3e^- \rightarrow \frac{3}{2} H_2$$
$$----------$$
$$Al + 3H^+ \rightarrow Al^{3+} + \frac{3}{2} H_2$$
$$or$$
$$Al + 3H_2O \rightarrow Al(OH)_3 + \frac{3}{2} H_2$$

Aluminium alloys are susceptible for different types of corrosion such as uniform corrosion, pitting corrosion and filiform corrosion. The type of corrosion depends on the aluminium alloy composition and the surrounding medium. [13; 14]

2.1.1 Uniform corrosion

The uniform corrosion is developed as pits in the size of micrometer which leads to a decrease in the thickness of the surface area of the aluminium alloy. The uniform corrosion of aluminium alloys is known in the highly acidic and basic media, where the dissolution rate of the natural aluminium oxide is higher than its formation rate [15]. The uniform corrosion rate of the aluminium alloy can be estimated by different methods such as measuring the mass loss, the quantity of the released hydrogen in pickling bath or by electrochemical methods. [16]

2.1.2 Crevice corrosion

The crevice corrosion takes place at the overlapping of joined parts, welding zones and under the deposits (corrosion products, slag, precipitates). Figure 2.1 demonstrates the crevice corrosion of the joined metal parts. Once the corrosive electrolyte penetrates between the joined parts, the corrosion process starts at the anode area. [17]

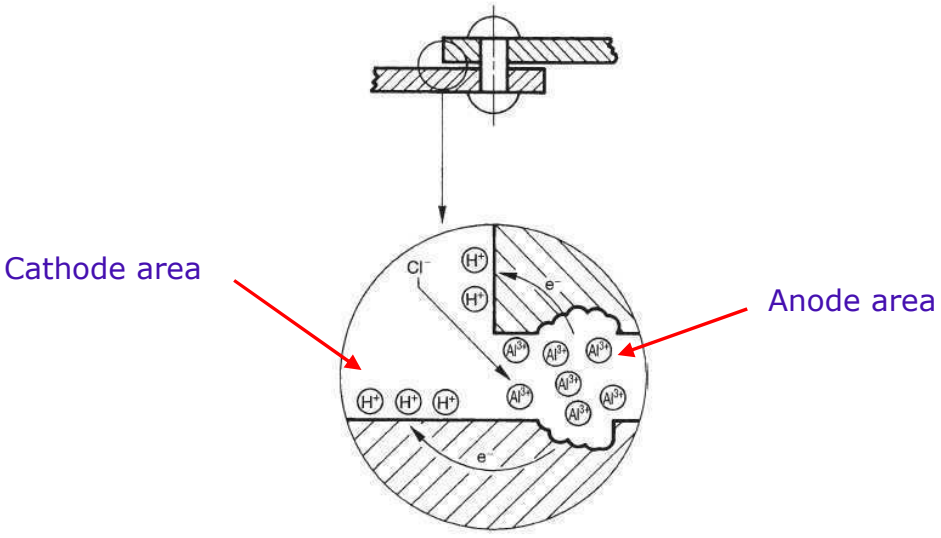

Figure 2.1: Crevice corrosion of joined metal parts at low pH value [17]

The anodic dissolution occurs in the tiny area, the chloride ions are directed to the crevice to form aluminium chloride (equations 6). [18]

$$Al^{3+} + 3Cl^{-} \rightarrow AlCl_3 \quad (6)$$

Aluminium chloride is hydrolysed to form aluminium hydroxide as in equation 7.

$$AlCl_3 + 3H_2O \rightarrow Al(OH)_3 + 3H^{+} + 3Cl^{-} \quad (7)$$

An insoluble $Al(OH)_3$ precipitates in the crevice area which hinders the further crevice corrosion of aluminium alloy. The electrons results from the anodic dissolution of the aluminium metal are picked up by the cathodic as in equations 2; 3; 4 and 5. [19; 20]

Figure 2.2 shows a crevice corrosion of aluminium screw. It is clear that the area under the nut has higher corrosion rate than the other points of the screw. The crevice corrosion can be reduced by different methods such as anodizing and phosphating.

Figure 2.2: Crevice corrosion of aluminium screw under the nut [20]

2.1.3 Pitting corrosion

Aluminium is prone to pitting corrosion in moderate and acid chloride media. The pitting corrosion is developed in the first weeks of the exposure in chloride environment [21]. Pitting corrosion can be divided into the following stages:

- Initiation stage

The initiation stage of the pitting corrosion is based on the adsorption of chloride ions on the aluminium surface. Failure in the film at the weak points of the oxide films is occurred which leads to cracks. [22]

- Propagation stage

The cracks of the initiated pits are growth in the propagation stage. The aluminium metal is oxidized to aluminium ions, which attracts the chloride ions from the surrounding environment toward the pit bottom to form aluminium chloride. The hydrolysis of the aluminium chloride reduces the pH value at the pit bottom as in the equations 6 and 7. Thus, the medium in the pit becomes very aggressive (low pH value) which promotes the growth of the pit. [23; 24]

Aluminium ions diffuse to the opening of the pit where the environment is more alkaline as in Figure 2.3, aluminium hydroxide $Al(OH)_3$ is formed at the top of the pit which reduces the entry of the corrosive electrolyte to the pit and the pits are re-passivated. [25; 26]

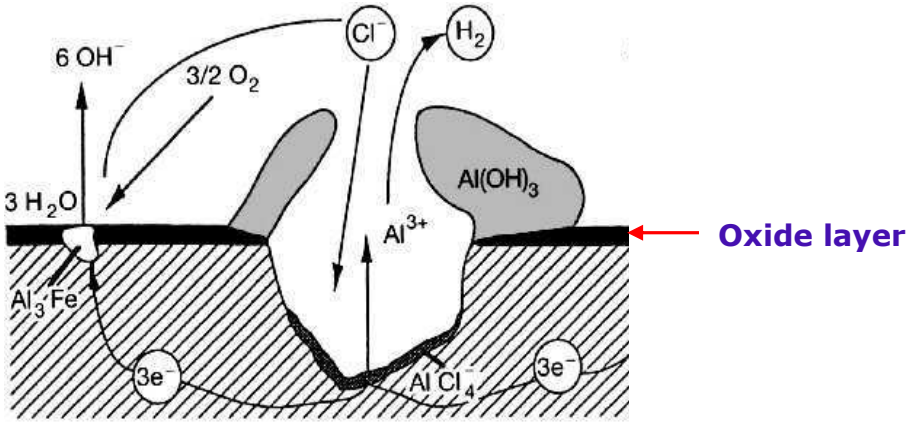

Figure 2.3: Pitting corrosion mechanism of aluminium alloy in chloride solution [26]

2.1.4 Filiform corrosion

Filiform corrosion is observed for aluminium samples coated with organic coating. The low adhesion of the coating on the aluminium substrate is the main reason for the filiform corrosion, the accumulation of the corrosion products beneath the coating leads to the coating delamination. [27; 28; 29]

Figure 2.4 describes the mechanism of the filiform corrosion which has the following characteristics: [30]

- The coating allows oxygen and water to migrate through it,
- the concentration of the dissolved oxygen increases at the open side of the coating which becomes the cathodic region,
- the region with low oxygen concentration becomes anode.

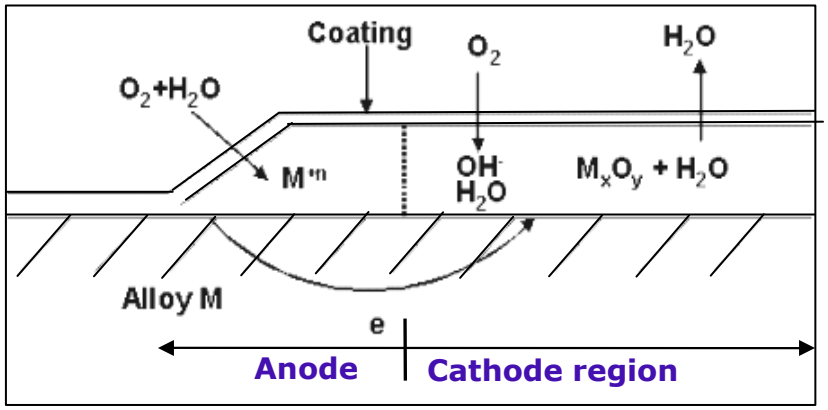

Figure 2.4: Mechanism of filiform corrosion [30]

Figure 2.5 demonstrates the filiform corrosion of aluminium metal alloy coated with organic polymer. It is clear that the filiform corrosion starts from the scratch edge of the coating and propagates to new areas under the coating. [31]

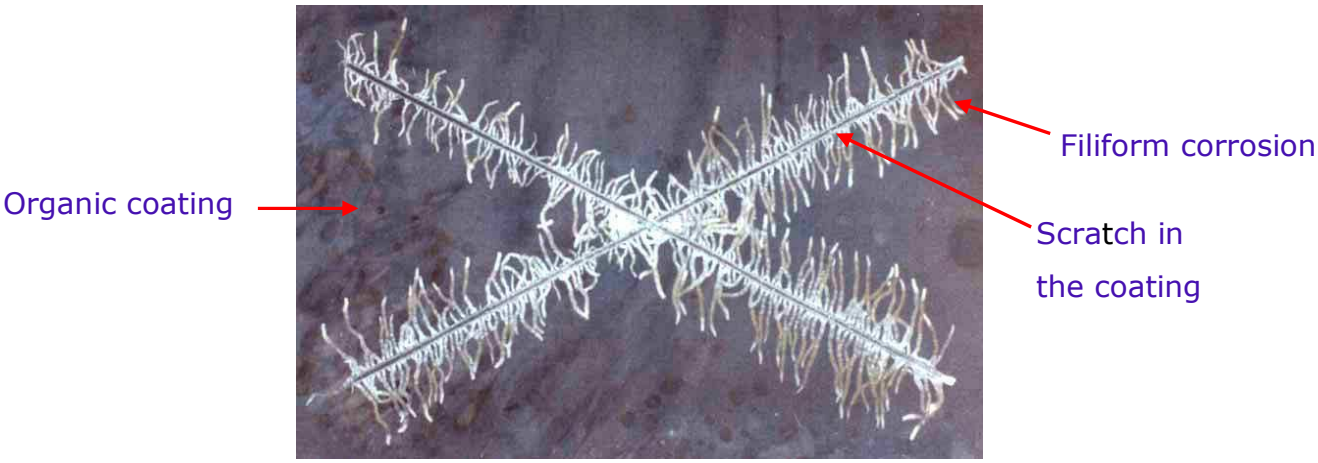

Figure 2.5: Filiform corrosion on the aluminium alloy coated with organic polymer [31]

Factors of filiform corrosion

The reasons of the filiform corrosion of the aluminium alloy can be summarized:

- The surface preparation: The filiform corrosion is developed on the poor prepared aluminium surfaces. The metal oxide or the dirt on the substrate surface results in low coating adhesion. [32]
- The cracks of the coating allowing the direct access of oxygen and corrosive anions to the substrate. The corrosion products beneath the coating lead to coating delamination, [33]
- The nature of the surrounding environment e.g. high humidity.

The appearance of the filfiform corrosion can be decreased by different approaches: [34]

- Application of multi-coatings,
- using of primer coating on the aluminium alloy such as chromate conversion coating or silica film prepared by sol-gel process,
- decreasing the humidity of the surrounding environment.

2.1.5 Galvanic corrosion cell

The galvanic corrosion cell is formed when two dissimilar metals are in direct contact and the both metals are in conducting media. One of the metals is corroded and behaves as an anode, the second metal acts as a cathode. Galvanic corrosion depends also on the metal texture and the temperature of the surrounding media which can modify the corrosion potential of the metal and accelerates the galvanic corrosion. [35; 36]

Figure 2.6 shows magnesium pipe out of gas water heater, the magnesium pipe is joined to aluminium metal parts. It is clear that the magnesium suffers an intensive corrosion, and the aluminium parts act as a cathode. [37]

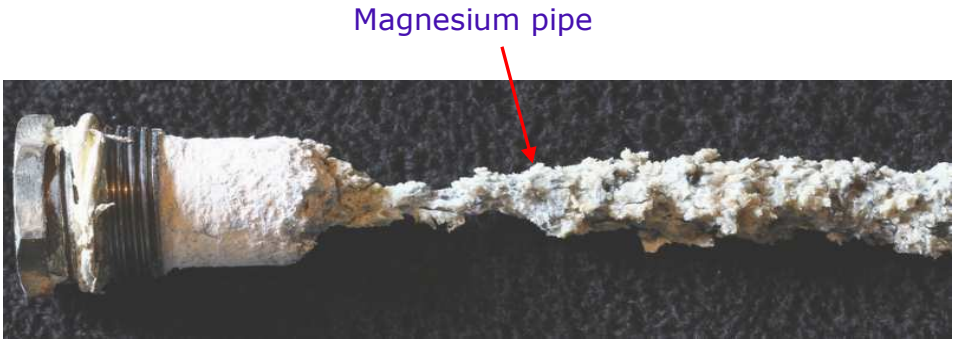

Figure 2.6: Galvanic corrosion of magnesium rod out of gas water heater joined to aluminium metal [37]

The galvanic corrosion of aluminium can be reduced by different methods like:

- Isolating the connected metal parts by high resistance materials such as polymers. [38]
- Neutralisation of the galvanic coupling, the high different in the potential between the anode and cathode should be avoided.
- Controlling the temperature of the surrounding media to hinder the change in the potential of the connected metallic parts. [39]

2.2 Corrosion of magnesium

Magnesium alloys are receiving increased attention for applications due to their light-weight. Magnesium alloys are widely used in automotive industry, computer parts, cellular phones and the aerospace industry, where weight reduction is needed. The magnesium metal oxidized to Mg^{2+} in an aqueous solution; magnesium ions react with the oxygen ions to form magnesium oxide according to the equation 8. [40; 41]

$$Mg + 2H_2O \rightarrow Mg(OH)_2 + H_2 \uparrow \quad (8)$$

In the base media, the magnesium oxide acts as a barrier layer which hinders the access of the active corrosion process at the magnesium alloy surface. Magnesium oxide layer breaks down in acid media which open pathway for the corrosion solution towards the metal substrate. The magnesium oxide loses also the barrier property when ions such as bromide, chloride and sulphate are presented in the surrounding environment. [42; 43]

Magnesium metal alloys have the same corrosion types as the aluminium alloy. Figure 2.7 demonstrates the corrosion of magnesium metal in the loudspeakers. The corrosion of magnesium occurs due to the humid environment and the galvanic corrosion cells; magnesium metal is joined with steel screws and aluminium metal parts. Several methods can be used to improve the corrosion protection of magnesium metal alloys such as chromate conversion coating, anodizing and silica coating. [44; 45]

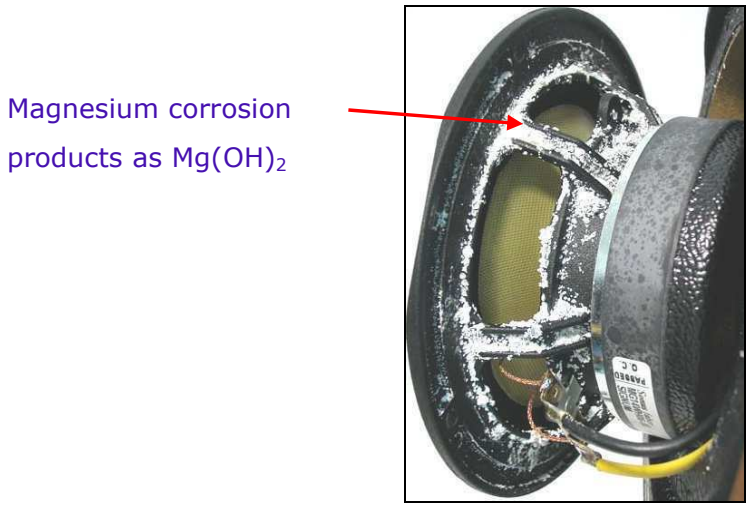

Figure 2.7: The galvanic corrosion of magnesium alloy in loudspeaker [46]

Different methods can be used to reduce the corrosion effects; they are mainly based on the formation of "Protective Coating". The coating should isolate the aluminium and magnesium metal surface from the effect of the corrosive media. The universally used protective coatings can be summarised as follow

2.3 Organic Coating

Organic coatings are commonly employed for the corrosion protection of different metal alloys. The coating suppresses (to some extent) the penetration of the corrosive media which reduces the corrosion process. Several factors are governed the protection of the organic coating such as the coating composition, the metal substrate and the pre-treatment of the sample. The chemical composition of the procurer has the major influence on the coating features. [47]

The constituents of the organic coating can be described as follow:

The binder: the binder forms the matrix of the coating; it is the polymeric phase in which all other components can be incorporated. The binder is principally responsible for the adhesion of the coating to the substrate. There are several types of binders for various applications such as alkyds, vinyls, natural resins and

oils, epoxies and urethanes. The binders can be classified into two groups depend on how they cure: [48]

- Binders are cured slowly by the solvent evaporation, which is known as thermoplastic binders.
- Binders are cured via chemical reaction through or after the application, which is known as thermosetting binders.

The pigment: the pigment serves two purposes. First, it provides the colour of the coating system. Second, it behaves as a corrosion inhibitor in the matrix. The pigments are grouped into two categories "inorganic and organic". [49]

The solvent: most of the organic coatings need solvents to 1) dissolving the binder with other components and enable their homogeneous mixing, 2) adjusting the viscosity of the mixture. The compatibility and the evaporation rate of the solvent have an important influence on the properties of the coating. For solvents evaporate too quickly, the coating can not flow into the defects and the groves of the metal surface, the film then has low adhesion. For solvents evaporate slowly, the coating fails due to the sagging, blistering and pinholing. The result can be drawn that the failure of the organic coating is attributed to the choice of the solvent. [50]

The additives: the additives are added in low concentrations to improve the features of the coating. Several additives for specific function can be added to the coating procurer such as surfactants, catalysts, defoamers, ultraviolet light absorbers, dispersing agents and zinc oxide. [51]

The fillers: the main function of the filler is to increase the volume of the coating through the incorporation of low-cost materials such as wood, dust or talc.

2.4 Inorganic coating

Inorganic coatings are prepared through the chemical or electrochemical reactions between the substrate and the selective solution. The reactions modify the aluminium and magnesium surface into oxide film or compounds which have better corrosion resistance than the natural oxide layer. Several inorganic

conversion coatings are commonly used in the industry such as anodizing and chromating. The coating hinders the transport of the corrosive electrolyte toward the substrate. [52]

2.4.1 Anodizing of light-weight metals

The anodizing is well known as an effective method to improve the wear and the corrosion resistance of light-weight metal alloys. The anodizing process is based on the oxidation of the aluminium and magnesium at the anode site; the thickness of the metal oxide is increased through the anodizing process which enhances the barrier properties of the sample.

Anodizing of aluminium

The spontaneous reaction leading to the formation of the natural aluminium oxide can be described as in the equation 9. The natural aluminium oxide layer can protect the aluminium alloy from atmospheric corrosion; it hinders the effect of oxygen and atmospheric pollutants on the aluminium substrate. [53]

$$2Al_{(s)} + 3/2O_{2(g)} \rightarrow Al_2O_{3(s)} \quad (9)$$

Natural aluminium oxide is unstable in corrosive environments. Thus, a protective coating is needed to resist the corrosion. The anodic oxidation of aluminium (ANOX) is carried out at DC or AC current in acid solution such as chromic, sulphuric or oxalic acid. The coating features depend on the application parameters like: anodizing time, temperature, concentration of the anodizing solution. The composition and the structure of the aluminium alloy have important effects on the properties of the anodizing film. [54; 55]

The anodizing of aluminium happens as in the equation 10; the metal is oxidized to form metal oxide. The electrons are picked-up by the cathodic reaction to form hydrogen gas (equation 11). [56]

$$2Al + 3H_2O \rightarrow Al_2O_3 + 6H^+ + 6e^- \quad (10)$$

$$6H^+ + 6e^- \rightarrow 3H_2 \quad (11)$$

Porous coating structure is formed through the ANOX process, this attributed to the aluminium alloy impurities and the different in the oxide growth at the substrate surface during the anodizing process [57]. The aluminium metal alloy coated with porous ANOX film has usually a low corrosion protection. The corrosive ions penetrate into the pores which enhances the corrosion process. Sealing of the anodized aluminium is needed to close the pores and hinders the effect of the corrosive anions on the aluminium metal sample. [58]

Sealing of anodized aluminium

The pores of the anodized aluminium sample can be sealed by different methods such as sealing in boiling water, sealing in chromate solution and sealing in the sols prepared by sol-gel process. [59; 60]

Through the sealing in boiling water, the original aluminium oxide is partly transformed into a hydrated oxide (Boehmite $Al_2O_3.H_2O$, AlOOH) as equation 12. Boehmite has greater volume than the aluminium oxide which closes the openings of the pores. [61]

$$Al_2O_3 + H_2O \rightarrow 2AlOOH \quad (12)$$

The sealing of the anodized layer in boiling water is controlled by the sealing time and the temperature of the water. The impurities in the water such as phosphate, fluoride and silica can negatively affect the sealing process. [62]

By the sealing of anodized aluminium sample in chromate solution, a layer of aluminium oxydichromate $Al(OH)CrO_4$ is formed in the pores of the anodized layer. The oxydichromate is converted by the heat treatment into trivalent chromium Cr_2O_3 (equation 13). [63; 64]

$$4CrO_4^{2-} + 4H^+ \rightarrow 2Cr_2O_3 + 4O_2 + 2H_2O \quad (13)$$

A barrier layer of the Cr_2O_3 is formed in the pores which hinders the effect of the corrosive anions. The application of this method is restricted because of the toxicity of chromate materials. [65]

The sealing in sol prepared by sol-gel process is based on the formation of silica film in the pores of the ANOX layer to hinder the effect of the corrosive solution. This kind of sealing will be discussed in experimental part.

Plasma electrolytic oxidation

Plasma electrolytic oxidation (PEO) of light-weight metals is widely accepted as an environmental friendly method to form a ceramic coating on different metal alloys such as aluminium and magnesium. The plasma electrolytic oxidation is based on the application of high electric potentials, plasma discharges is formed, and high temperature is produced along the surface of the magnesium or aluminium sample. The hydrogen and oxygen are generated from the dissociation of the electrolyte under high electric potentials. The oxygen reacts with the magnesium or aluminium metal ions at the substrate surface to form the oxide layer. The electrolyte of the PEO process consists of phosphates, silicas, hydroxides, fluorides etc, in variable concentrations. [66; 67; 68]

Cracks are usually formed in PEO layer of magnesium alloy; the cracks are resulted during the PEO process through the quenching of the metal oxide in the PEO electrolyte. However, pores with different shapes are also distributed over the ceramic layer; the corrosion protection provided by PEO layer on magnesium alloy is not good enough to be used as a single layer. Post-treatment is needed to close the pores and the cracks. A number of sealing methods are used for this purpose such as: sealing in organic polymer, chromate conversion coating and sealing in the sols. [69; 70]

2.4.2 Chromate conversion coatings (CCC)

The chromate conversion coating (CCC) for aluminium and magnesium alloys is an electrochemical process involving the oxidation of the metal (equations 14)

and the reduction of Hexavalent chromium into trivalent chromium (equation 15). [71]

$$Me \rightarrow Me^{m+} + me^{-} \quad (14)$$

$$Cr_2O_7^{2-} + 8H^+ + 6e^- \rightarrow 2Cr(OH)_3 \downarrow + H_2O \quad (15)$$

Where Me can be aluminium or magnesium metal, Me^{m+} is the metal ions.

The CCC process is carried out in acid media, the hexavalent chromium Cr^{6+} ions are reduced into trivalent chromium Cr^{3+} [72]. The chromate conversion layer is formed through the adsorption of trivalent chromium hydroxide on the aluminium or magnesium oxide surface. Different compounds can be formed on the substrate surface during the chromate conversion coating such as: Cr_2O_3; $Cr_2O_3.xH_2O$; CrOOH and $Cr(OH)CrO_4$. [73]

The chromate conversion coating provides a barrier layer between the metal and the corrosive media, the barrier properties come from the insoluble trivalent chromium compounds. The growth of the coating during the CCC process can be described by the sol-gel model [74; 75]. In this model, the hexavalent chromium Cr^{6+} is reduced into trivalent chromium Cr^{3+} (equation 15). The hydrolysis and the condensation of the Cr^{3+} ions form monomers, dimers and trimers, these species precipitate at the substrate surface to form the chromate conversion coating. [76; 77]

Advantages of the chromate conversion coatings

Chromate conversion coatings have several advantages such as: [78; 79]

1- Giving an excellent corrosion protection to the aluminium and magnesium alloys,

2- improving the adhesion of the topcoat coating,

3- economically feasible and easy for application,

4- water-based surface treatments without any organic solvent,

5- visibility of the chromate coatings is very good, they can be used as a decorative coatings.

Disadvantages of the chromate conversion coatings

The major disadvantage of chromate process is the toxicity of Cr^{VI}. These compounds have carcinogenic effects and environmentally unsafe, the Hexavalent chromium can be absorbed by the lungs and skin contact [80; 81]. The Cr^{VI} reacts with hydrogen peroxide (H_2O_2), glutathione (GSH) and ascorbic acid in the human body. Reactive intermediates including Cr^{V}, Cr^{IV} and hydroxyl radicals are formed, any of the reactive intermediates could attack DNA, proteins, thus disrupting the functions of the human cells. [82; 83]

2.4.3 Trivalent chromium coatings (TCC)

For safety issues, the application of CCC has been restricted. Studies have been shifted to find alternative safety protective films. Trivalent chromium conversion coatings are accepted as a more environmentally friendly method than Hexavalent chromium conversion coatings. The trivalent chromium coating (TCC) is applied from a Cr^{3+} solution; the solution is free of hexavalent chromium. [84; 85]

An insoluble trivalent chromium hydroxide $Cr(OH)_3$ is formed from the reaction of hydroxide ions OH^- and trivalent chromium ions Cr^{3+} in the TCC bath as in equations 16 and 17. A barrier layer of insoluble trivalent chromium hydroxide precipitates on the substrate surface which hinders the effect of the corrosive solution, TCC can be applied on magnesium and aluminium. [86; 87]

$$Cr(NO_3)_3 + 6H_2O \rightarrow [Cr(OH_2)_6](NO_3)_3 \quad (16)$$

$$Cr^{3+} + 3(OH)^- \Leftrightarrow \underset{\uparrow}{Cr(OH)_3\downarrow} \quad (17)$$

Insoluble trivalent chromium hydroxide

Disadvantage of trivalent chromium coatings

The disadvantage of the trivalent chromium coatings in comparison to chromate conversion coating can be summarized as follow: [88; 89]

- The trivalent chromium coatings need an additional post-treatment to reach an equivalent corrosion protection as the chromate conversion coatings.
- The application time of the trivalent chromium coating is longer than CCC.
- The chemical materials of the TCC bath are more expensive than the CCC chemical materials.
- The activity of the trivalent chromium bath is reduced due to the complexes form in the solution as in equation 17, cleaning of the bath solution from the complexes and may preparing of a new bath is an additional cost of TCC method. [90]

In the recent years, the researches have been actively focused on the silica coatings prepared by sol-gel process. The silica film on aluminium and magnesium metals have several advantages to chromate conversion coating and the trivalent conversion coating such as:

- In contrast to the toxic Cr^{VI}, the use of the silica film is safer for the workers and the environment,
- silica film prepared by sol-gel process gives the same protection performance as the CCC and TCC do, [91]
- the chemical conditions of the sol-gel process are mild, the hydrolysis and the condensation reactions are catalysed by acid or base, extreme pH conditions can easily be avoided, pH sensitive compounds such as dyes, corrosion inhibitors can be entrapped and still retain their functions, [92; 93]
- the hydrophobic property of the silica film prepared by sol-gel process can be varied depending upon the structure of the organo-silica compounds. [94; 95]

2.5 Silica film surface treatment

Silica films prepared by water-based sol-gel process are introduced as non-toxic protective coatings. However, silica films have other attractive properties such as cost-efficient, thin film formability and the capability to coat materials of various shapes; with the easiness to control the composition of the sol. In addition, the silica coating has supplementary pretty features like hydrophobic, self-cleaning, anti-reflection, easy to clean, anti-microbial. Silica films are applied as protective coatings on aluminium and magnesium alloys, and show a great potential in different applications such as aerospace, marine and automotive. [96; 97; 98]

The sol cnosists of organo-silica compounds, catalyst and water [92]. The organo-silica compounds are immiscible with water in all proportions. Thus, organic solvents are needed to achieve the dispersion of water with the organo-silica compounds. The using of the organic solvent or volatile organic compounds (VOC) showed several problems in the applications such as the flammability, evaporation and human safety issues. [99]

The recent studies have been focused on the water-based sol-gel process to reduce the amount of VOC for safety issues and to obtain a cost-efficiency sol. The organo-silica compounds of the water-based sol have low hydrophobic properties; the homogeneity of the water-based sol can be achieved by mechanical stirring without using the VOC. Therefore, the choice of the organo-silica compounds is an important aspect to prepare the water-based sol.

Organo-silica materials have the general formula $Si(OR)_4$, where OR is the alkoxy such as (OCH_3) or (OC_4H_9). For the water-based sol-gel system, OR groups in the organo-silica materials should have a short structure (low hydrophobic) to achieve the sol homogeneity without using VOC. For alcohol-based sol-gel system, alcohols are added to the sol as a solvent, OR groups with long structure can be used. [100]

A various number of organo-silica materials can be used to prepare the water-based sols [101]. Table 1 presents some of the organo-silica materials, (3-Glycidoxypropyl)methyldiethoxysilane has short organic groups, it is able to be dispersed in the water-based sol without the need of the organic solvent.

However, N-Octyltriethoxysilane has a long organic group and need an organic solvent to achieve the dispersion with the sol. Therefore, the structure of the organo-silica material controls the type of the sol, alcohol-based or water-based. [102; 103]

Table 1: The structure of organo-silica materials

N,N-Dimethylaminopropyl-trimethoxysilan	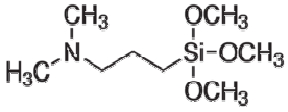
N-Octyltriethoxysilane	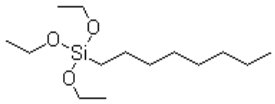
(3-Glycidoxypropyl)methyldiethoxysilane	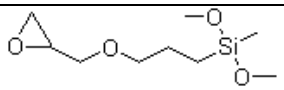
(3-Trimethoxysilylpropyl)diethylenetriamine	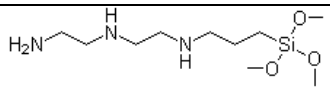
Bis[3-(triethoxysilyl)propyl]-tetrasulfide	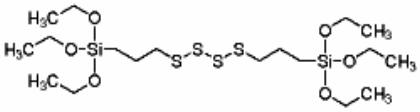

2.5.1 The chemistry of the sol

Hydrolysis and condensation of the sol

The sols are often synthesised by hydrolysing of the monomers, the alkoxy groups (–OR) are converted into (–OH) in the presence of acid e.g. HCl or base e.g. NaOH as a catalyst. R-Si$(OR)_3$ is hydrolysed to form R-Si$(OR)_2OH$, alcohol ROH is generated as seen in equation 18. The hydrolysis process is continued to form R-Si$(OH)_3$ as in equations 19 and 20. [104; 105]

$$R - Si(OR)_3 + H_2O \Leftrightarrow R - Si(OR)_2OH + ROH \quad (18)$$

$$R - Si(OR)_2OH + H_2O \Leftrightarrow R - Si(OR)(OH)_2 + ROH \quad (19)$$

$$R - Si(OR)(OH)_2 + H_2O \Leftrightarrow R - Si(OH)_3 + ROH \quad (20)$$

The kind and the concentration of the catalyst have an important effect on the hydrolysis mechanism and the rate of the hydrolysis reaction.

Acid-Catalysed Mechanism

Under acidic catalysis condition of the alkoxide group, the -OR is first protonated, and then hydrolysed into hydroxyl group as in Figure 2.8 [106]. The condensation process between the –OH groups and the alkoxide group have an important role in the sol chemistry as in Figure 2.9. An open network structure results initially (Figure 2.12-a), followed by further hydrolysis and condensation reactions. Relative dense silica film is obtained by using acid as a catalyst. [107; 108]

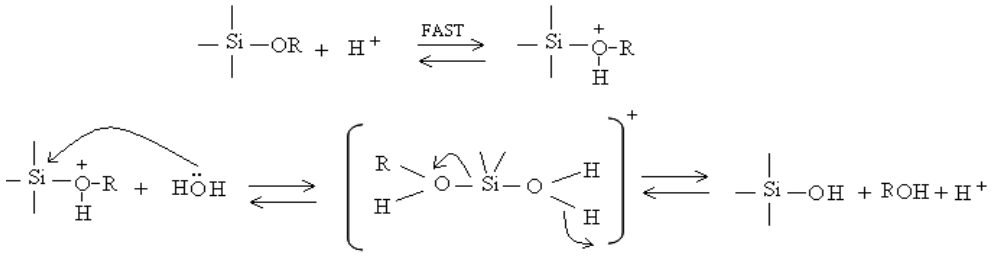

Figure 2.8: Hydrolysis process using acid as a catalyst [106]

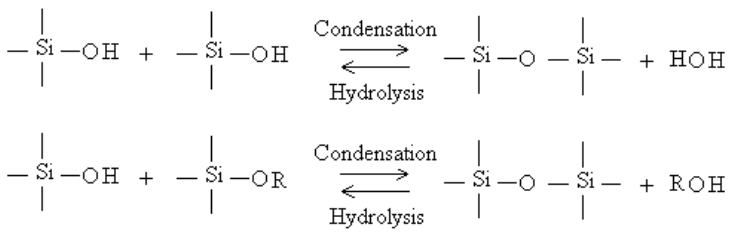

Figure 2.9: Condensation reactions of the silica compounds [106]

Based-Catalysed Mechanism

Under base catalysis condition of alkoxy group, the silicon atom is attacked by the hydroxyl group from the solution as in Figure 2.10. The completely hydrolysed alkoxy groups are condensed to form the silica film structure. [109]

The high crosslinked species are formed in the sol-gel structure because of the high condensation rate of the silica molecules under the base catalyst conditions (see Figure 2.11), and porous gel is formed as in Figure (2.12-b). [110]

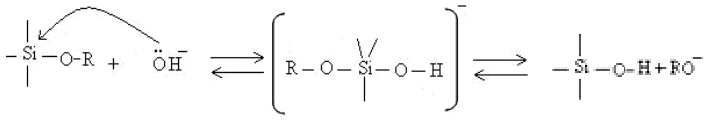

Figure 2.10: Hydrolysis process of alkoxy groups using base as a catalyst [106]

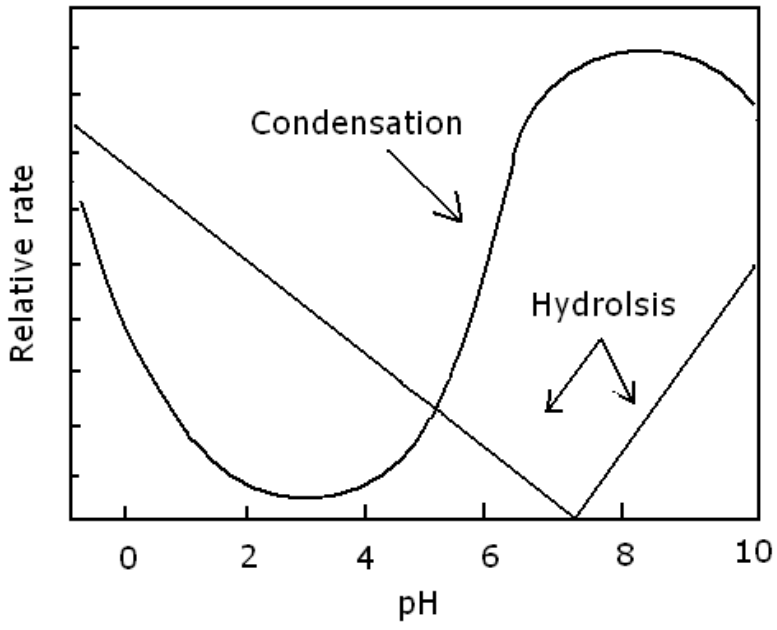

Figure 2.11: The effect of pH value on hydrolysis and condensation of the sol [105]

Acid-catalysed, linear branched polymer

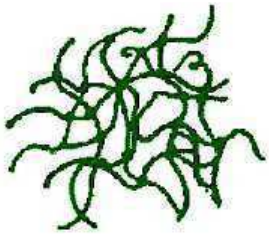

Base-catalysed, high crosslinked spieces

Figure 2.12: Effect of the catalyst on the structure of the monomer [104]

Cesar tested the effect of the catalyst on the hydrolysis of the organo-silica molecules and the structure of the silica material [111]. Ammonium hydroxide and hydrochloric acid are used as a base catalyst and as an acid catalyst respectively. The study showed that the surface area and the structure of the silica are modified by the different in the type of the catalyst (acid or base); this behaviour can be attributed to the different in the kinetic of the hydrolysis/ condensation process.

The steps involve synthesis of the silica film can be seen in Figure 2.13, the steps are: [112]

a) the sol procurer is aged to obtain the workable sol,

b) the wet silica film is applied on magnesium and aluminium substrates, it can be applied by different methods such as dip-coating, spin coating and spray,

c) the heat treatment of the wet silica film is an important step to obtain a cross-linked protective silica film.

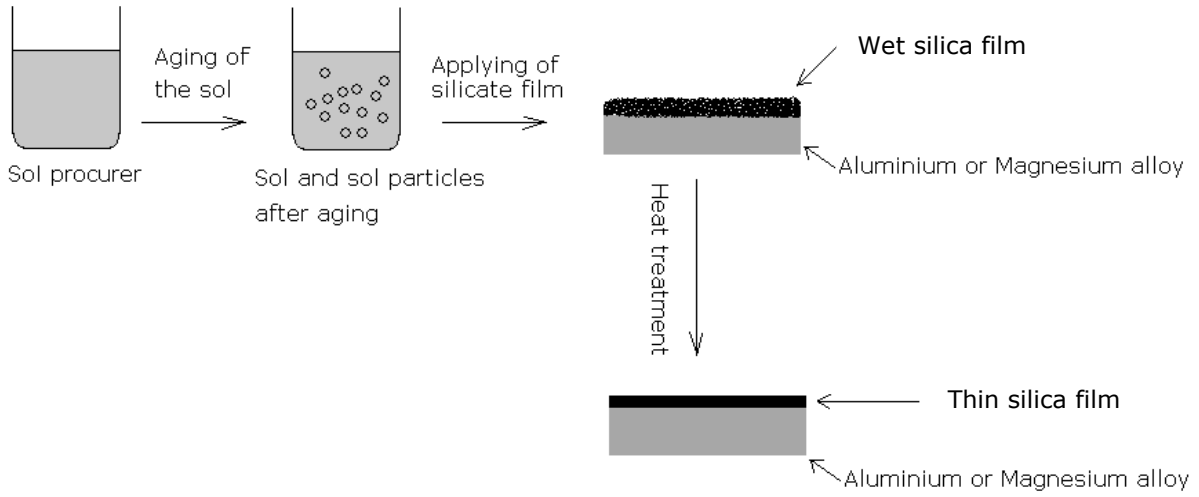

Figure 2.13: The steps involved in the sol-gel processing to obtain the silica film [113]

According to the chemistry of the sol-gel process, the workable sol has to have sufficient numbers of Si-OH which results from the hydrolysis of Si-OR groups. An oily film with low corrosion protection is formed from the sol with unhydrolysed or low hydrolysed alkoxy groups. The chemistry of the sol is a time-dependent process. Consequently, the aging period of the sol has a key role effect on the features of the silica film.

2.5.2 Aging of the sol

The aging process is an important step to obtain a workable water-based sol. Through the aging period, the hydrolysis and the condensation reactions of alkoxy groups happen simultaneously [114]. The organo-silica compounds in the sol are linked together through the condensation reactions of OH and OR groups, the size of the linked molecules increases, and colloidal sol is obtained. The particles in the sol so called sol-particles (see figure 2.14). [115; 116]

After the aging period, the silica molecules in the sol are progressively connected to the network and the viscosity of the sol increases. Aging process usually carried out at an ambient temperature in controlled water content and pH values. [117]

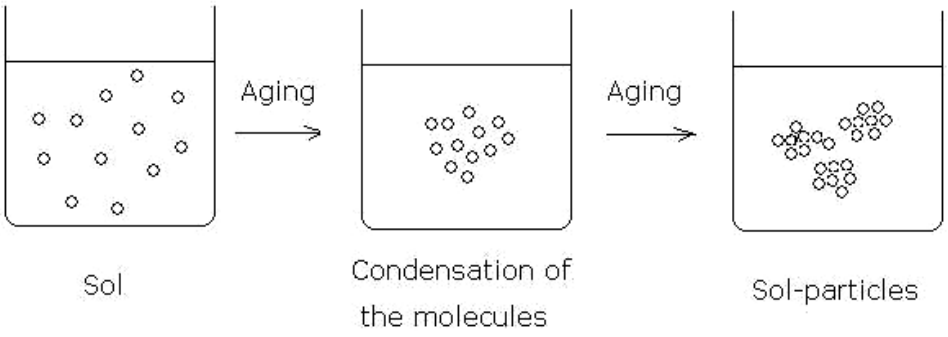

Figure 2.14: The formation of sol-particles in the sol during the aging period [115]

2.5.3 Effect of the solvent on the sol-gel process

Organo-silica compounds are immiscible with water in all proportions, it is necessary to add an organic solvent to achieve the miscibility and to facilitate the hydrolysis. Alcohol is a product of the hydrolysis reaction of the sol. When the organo-silica compounds and water can be mechanically mixed and induced to react eventually, a single phase mixture can be obtained due to the hydrolysis reaction, the process so called "water-based sol-gel". This can be achieved for organo-silica compounds with short organic group. [118]

When organo-silica compounds with long organic group are used, the miscibility of these materials with water is low which leads to phase separation in the sol. The organic solvents are then needed to achieve the homogeneity of the sol. The organic solvents are usually alcohol compounds, the process so called "alcohol-based sol-gel". [119]

Alcohol-based sol-gel process

Alcohol-based sol-gel process is based on the dispersion of organo-silica compounds and water in a solution of an organic solvent. Different organic solvents can be used such as ethanol and methanol. When alcohol as a solvent of the sol and alcohol generated by the hydrolysis reactions have the same chemical structure, a competition between the hydrolysis and the alcoholysis reactions takes place. Equation 21 shows the hydrolysis reaction of organo-silica

compounds in alcohol-based sol, the high concentration of ROH in the sol shifts the reaction to the alcoholysis direction. Therefore, the hydrolysis of OR groups in the alcohol-based sol is not complete. [120; 121]

$$R-Si(OR)_3 + H_2O \underset{Alcoholysis}{\overset{Hydrolysis}{\rightleftarrows}} R-Si(OR)_2OH + ROH \qquad (21)$$

Several studies investigated the effect of the organic solvent on the silica coating. For example, Metroke found that the structure and the concentration of the alcohols control the properties of the silica film on aluminium substrate [121]. The best corrosion protection is obtained at the low concentrations of the small alcohols. In contrast, the depolymerisation of the hydrolysed species is observed for sols with high concentrations of alcohols.

It can be concluded that the correct choice of the organic solvent allows tailoring of the film thickness, the coating structure and providing appropriate film hydrophobicity.

Water-based system

Using of alcohols poses the major obstacle in the transfer of the silica films prepared by sol-gel process into existing industrial systems. This difficulty is due to the flammability of the volatile organic compounds (VOC), concerns regarding health, safety issues and the cost. Thus, researches have focused on the water-based sol-gel process. The main advantages of the water-based over the alcohol-based sol systems can be summarized as follow: [122; 123]

1. Hydrolysis reaction of water-based process is close to the completion. While the hydrolysis of alcohol-based sols reach the equilibrium because of the competition between the hydrolysis and the alcoholysis as discussed before in equation 21.
2. water-based sols are environmental friendly and non-flammable. while the alcohol-based sols are flammable,

3. evaporation of alcohols from alcohol-based sol leads to a different in the concentration of the sol and also different in the thickness of the silica film, this problem is not of concern for the water-based sols.
4. the water-based system is cost-efficient; the materials used in the water-based sols are cheaper than the materials in alcohol-based sols such as organo-silica materials.

Table 2 shows the prices of some organo-silica materials. It is clear that the materials used to prepare water-based sols are cheaper than the materials for alcohol-based sols. Some of the organo-silica materials which can be used for water-based sols are expensive; the cost-efficient water-based sol can be achieved through the right choice of the chemicals according to the prices and the protection efficiency. The prices of the materials are from Sigma-Aldrich Company /13-11-2011/.

Table 2: The prices of the organo-silica materials, Sigma-Aldrich GmbH

Name of organo-silica	Sol type	Cost of 100 ml organo-silica (Euro)
(3-Glycidoxypropyl)methyldiethoxysilane *	Water-based	44.00
Tetraethyl orthosilica *	Water-based	8.12
Triethoxysilane	Water-based	292
N-Octyltriethoxysilane	Alcohol-based	56.00
(3-Trimethoxysilylpropyl)diethylenetri-amine	Alcohol-based	56.30
Bis[3-(triethoxysilyl)propyl]-tetrasulfide	Alcohol-based	198.40
N,N-Dimethylaminopropyl-trimethoxysilan	Alcohol-based	524.00
In addition, alcohol (VOC) as a solvent raises the cost of the alcohol-based sols.		

* The chemical materials used in this work to prepare the sol, they are chosen according to prices and the effectiveness on the corrosion protection.

2.5.4 Processing of the silica film

The deposition of the silica film on aluminium and magnesium substrates is performed in this work by dip-coating method. The process is schematically described in figure 2.15. The pre-treatment, the viscosity of the sol and the temperature of the sol have an important effect on the thickness of the silica film [124]. The film is deposited on the substrate surface during the withdraw from the water-based sol.

Figure 2.16 presents the changes occurring at substrate surface during the withdraw of from the water-based sol, the following observations can be pointed:

a) The surface tension of the aluminium or magnesium substrate hinders the formation of the silica film, b) the desposition of thin silica film on the substrate, and c) evaporation of the water. [125]

In this work, the physical properties of the water-based sol are maintained always constant by using the same: sol composition and the sol temperature. Silica film with the same thickness can be obtained by controlling these parameters. The pre-treatment of the aluminium or magnesium substrate is carried out at same parameters to obtain the same surface tension of all substrates, where the surface tension resists the film deposition [126].

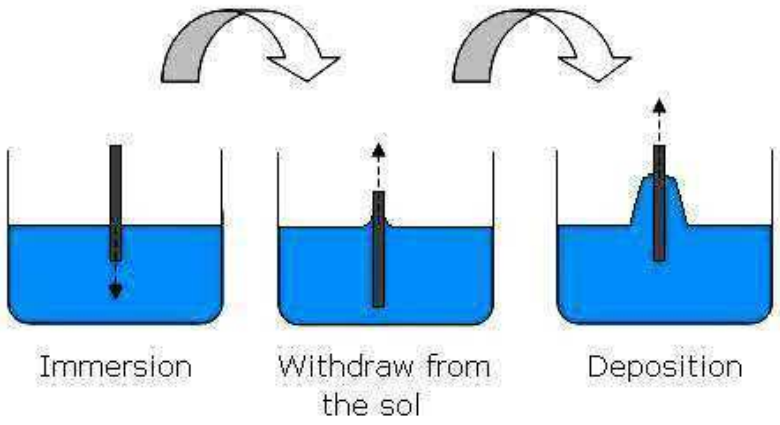

Figure 2.15: The dip-coating process [124]

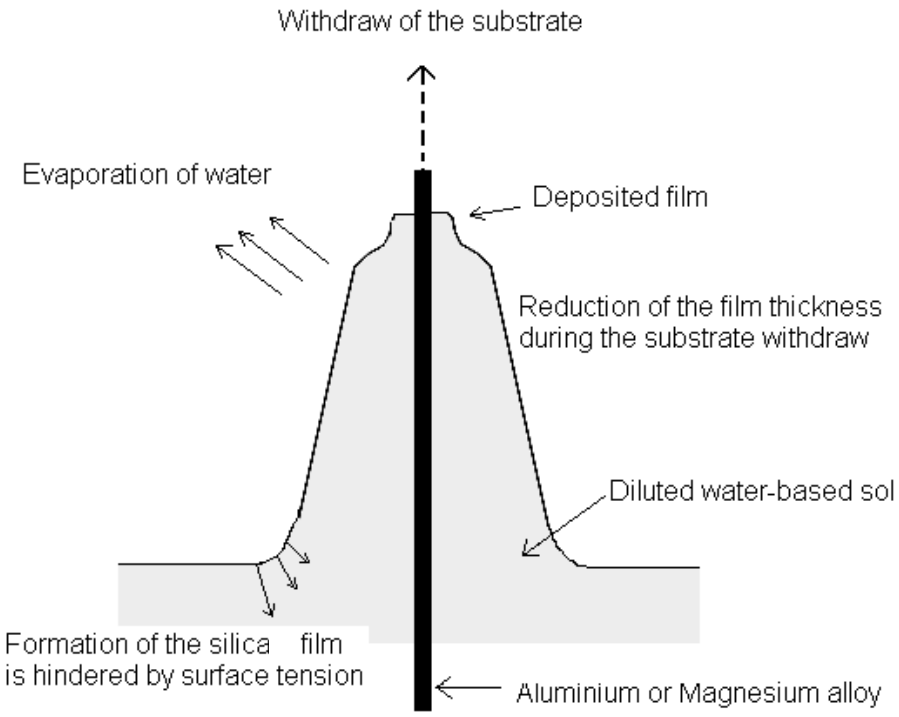

Figure 2.16: Schematic of the substrate during the withdraw from the water-based sol [125]

2.5.5 Cross-linking of the silica film

The cross-linking of the silica film is needed to obtain a dense protective film, which can be achieved through the heat treatment. The heat treatment process can be divided into two steps: drying and densification

Drying

When the silica film from water-based sol is applied on the aluminium or magnesium samples, hydrogen bonds are formed between –OH from the sol and –OH from the oxide layer on the substrate surface (Figure 2.17). The water is evaporated through the drying step of the silica film; this step is usually implemented carefully. Cracks can be formed through the high evaporation rate of the water. [127; 128]

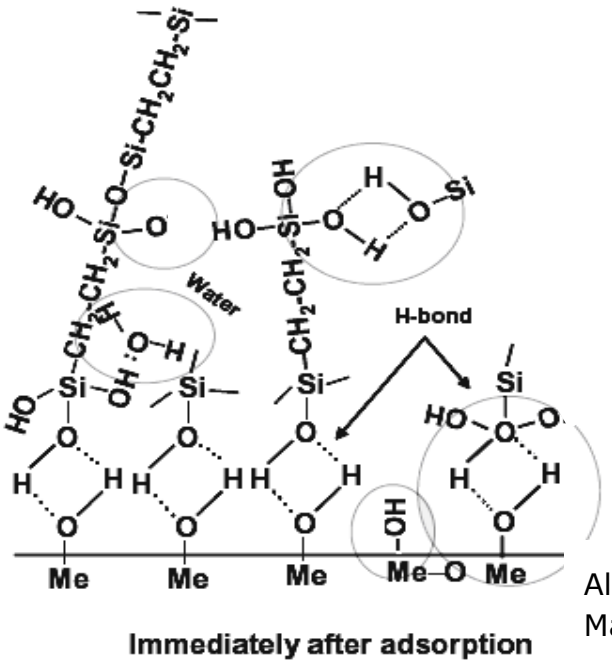

Figure 2.17: Silica film on the aluminum or magnesium substrate before heat treatment [128]

Densification

After the drying step, the heat treatment is needed to obtain a cross-linked protective silica film. The cross-linked silica film structure on the aluminium or magnesium substrates is obtained through the polycondensation of OH and OR groups. The silica film is also bonded to the substrate through the condensation reaction between the OH groups from the sol and the OH on the metal oxide. [129]

Figure 2.18 shows aluminium or magnesium substrate coated with silica film during the densification process, several Hydroxyls (-OH) are condensed to form the structure of the silica film.

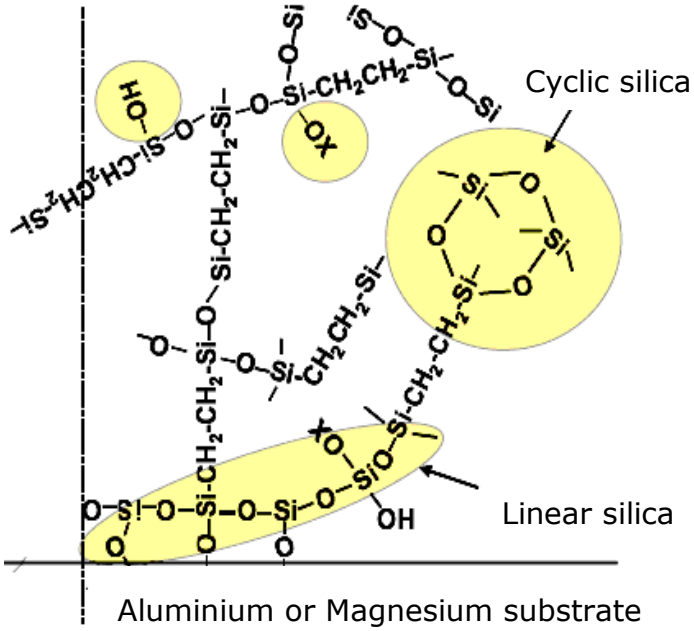

Figure 2.18: Silica film on the aluminium or magnesium metal surface during the heat treatment [128]

A rigid structure and a fully cross-linked film is formed after the heat treatment (Figure 2.19). The dense silica film prevents the penetration of the moisture and the corrosive electrolyte to the aluminium or magnesium metal substrate.

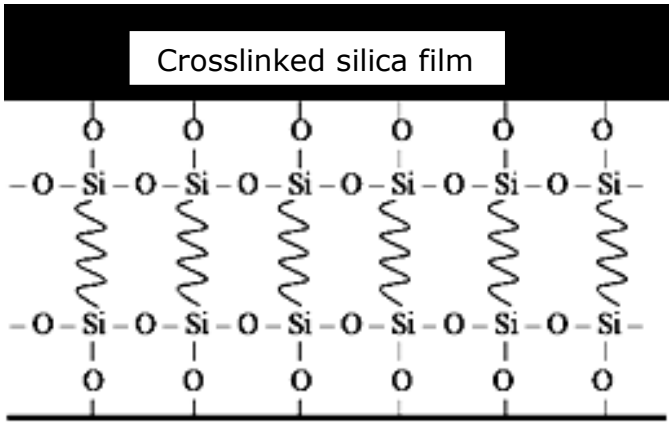

Figure 2.19: Fully cross-linked silica film [128]

2.5.6 Bonding of silica film to the inorganic substrate

The bonding of the silica film to aluminium and magnesium substrate is based on the condensation reaction between the –Si-OH from the sol and Me-OH on the substrate surface which ensures the excellent film adhesion. Therefore, non-protective film is formed when OH groups at the metal surface are not existed. Figure 2.20 demonstrates the bonding mechanism of silica film to the aluminium and magnesium metal alloy. It is clear that the pre-treatment of metal substrate surface and the chemistry of the sol are essential to obtain protective silica film. [130; 131]

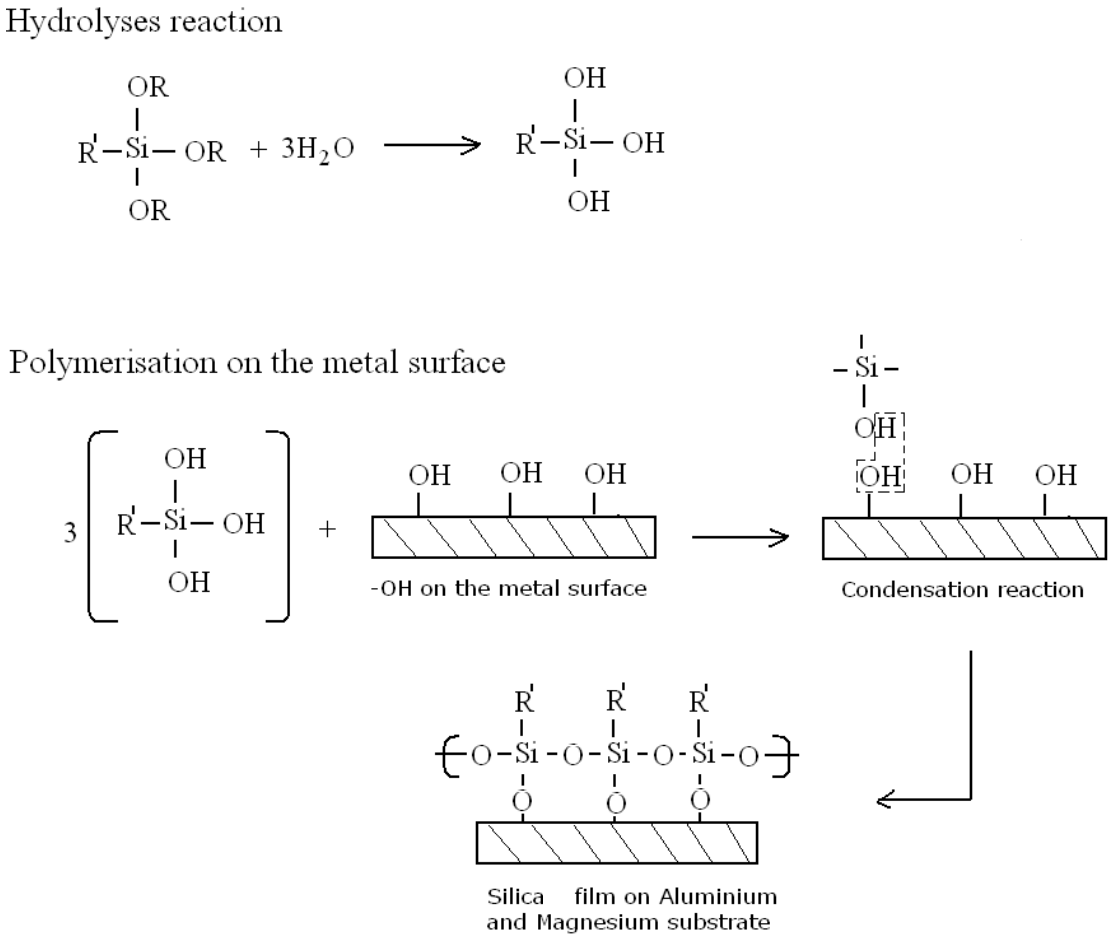

Figure 2.20: Bonding of silica film to the aluminum and magnesium metal alloy [131]

2.5.7 Silica film cracking

Cracking is one of the major drawbacks of the silica film. Cracks occur when the critical film thickness of 300 nanometre is exceeded [132]. The cracking is accompanied with film delamination. The crack of the silica film happens during heat treatment step. The heat treatment of the silica film prepared by water-based sol-gel process consists of three stages:

1) heating-up,

2) isothermal heating,

3) cooling-down stages

At the stages 1 and 2, changes occur in the chemistry and the structure of the silica film which accompanies with the decreasing in the volume of the film due to a) evaporation of the water and b) polycondensation reactions of the OH and OR of the organo-silica compounds. [133]

Figure 2.21 demonstrates the silica film during the heat treatment, the silica film is constrained on the aluminium or magnesium metal substrate surface through the covalent bond, the decreasing in the volume of the silica film during the shrinkage (cross-linking) increases the stress in the film, and cracks are generated. The cracks of the silica film can be also generated at the cooling down stage, when the aluminium or magnesium substrate and the silica film have different thermal expansion coefficient. [134; 135]

Different methods can be used to obtain crack-free silica films such as:

- Modifying the composition of the sol to reduce the stress in the film, this point will be discussed by details in this work,
- Applying multi-thin silica films.

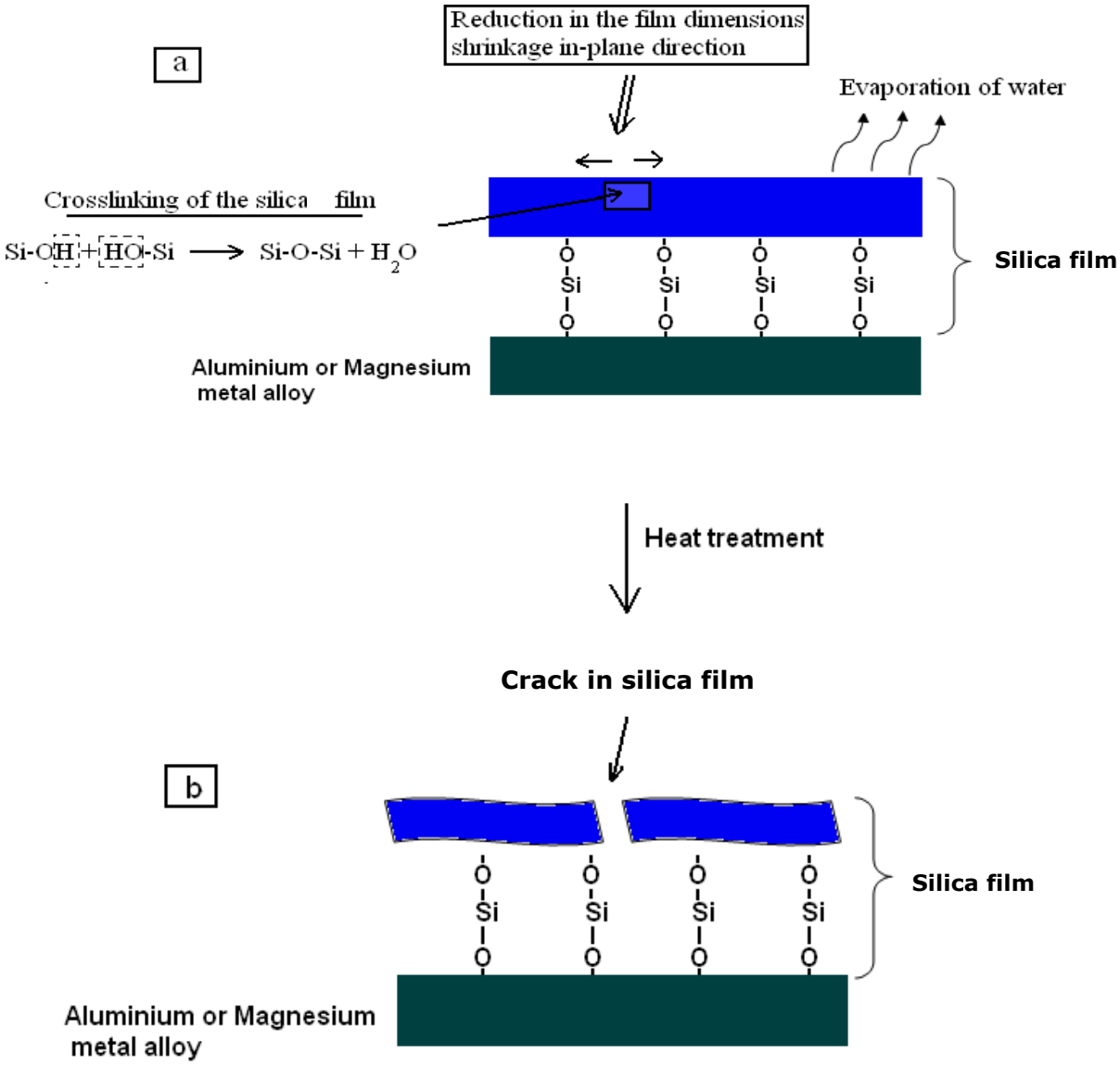

Figure 2.21: Silica film during the heat treatment, a) the dimensions of the film decreases, in-plane tensile stress raises, b) silica film-crack [134]

2.5.8 Self-Healing

Silica films prepared by sol-gel process can be doped by different kinds of corrosion inhibitors. The dopants in the sol become entangled in the network of the silica film. The structure of the silica film network has an important effect on the effectiveness of the corrosion inhibitors such as the pores size of the silica film, the distribution of the pores in the film and the stability of the coating network in the surrounding media. [136; 137]

The corrosion inhibitors-doped silica film has several advantages such as: [138]

1- The silica films are stable chemically and photochemically, especially when compared to plastic materials.

2- The chemistry of the sol can be modified to fit the chemical property and the reactivity of the dopant.

3- The dopants in the silica film are well protected from the surrounding environment.

4- The trapped molecules in the silica film are leachable, which is an important feature for the self-healing of the aluminium or magnesium metal alloys coated with silica film.

The long-term corrosion protection of aluminium and magnesium metal alloys coated by silica films can be achieved by two approaches. First, the deposition of the silica barrier layer on the alloy surface is to prevent the contact with the corrosive media. Second, introducing of the effective corrosion inhibitors to the coating system is for self-healing effect. [139]

The easiest way to generate the self-healing of the aluminium and magnesium metal substrate coated with silica film is the simple mixing of the corrosion inhibitors with the water-based sol. the corrosion inhibitors should be completely soluble in the water-based sol and in the corrosive aqueous media. [140]

Figure 2.22 demonstrates schematic for the self-healing at the defect of aluminium or magnesium sample coated with corrosion inhibitors-doped silica

film. When a defect occurs in the silica film, the corrosive electrolyte reaches the metal surface in the defect area, the corrosion starts. The corrosive solution also penetrates in the structure of the silica film, the soluble corrosion inhibitors leach out of the coating under the capillary forces to the defect area, where the capillary is the ability of a liquid to flow in a narrow space like pores or small defects in the silica film [141]. A layer of corrosion inhibitors precipitates on the corroded metal surface in the defect which reduces the effect of the corrosive solution.

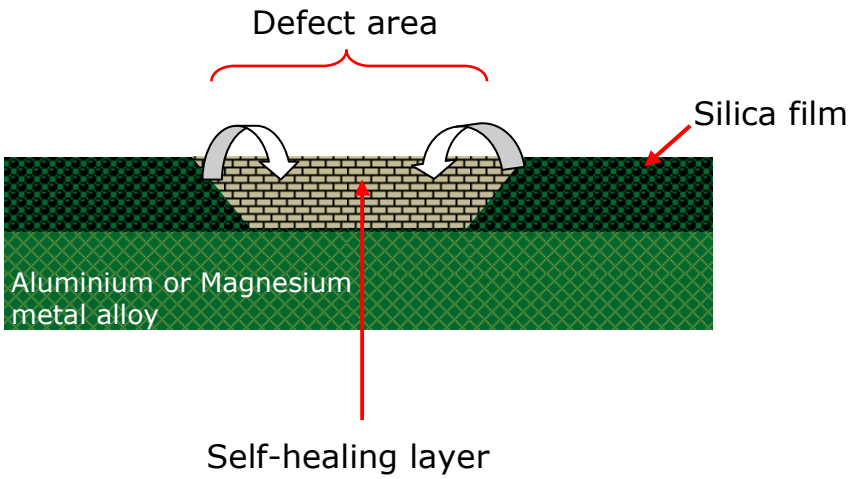

Figure 2.22: Schematic for self-healing at the defect area of aluminium or magnesium sample coated with corrosion inhibitors-doped silica film [141]

The long-term corrosion protection effect is an important aspect to ensure the stability of the coated aluminium and magnesium metal substrate in the corrosive environment [142]. The concentration of the corrosion inhibitors, the structure of the silica film and the barrier property of the self-healing layer formed in the defect area are important factors for long-term corrosion protection.

Other factors can affect the self-healing such as the solubility of the corrosion inhibitors in the corrosive media. Low solubility of the corrosion inhibitors leads to a lack of the active agent at the damaged area of the coating. While, high solubility of the corrosion inhibitors results in a quick leach out of the active

compounds from the coating, and short-term of protection is then obtained. [143; 144]

Another important problem appears in the silica films when the corrosion inhibitors are chemically reacted with the components of the silica coating which destroys the barrier properties of the silica film. [136].

D. Raps investigated the effect of benzotriazole on the properties of the silica film [140]. The study demonstrated that benzotriazole reduces the barrier properties of the silica film. This can be explained in the term of the strong influence of benzotriazole on the hydrolysis/polymerization processes during the coating preparation. The negative effect of benzotriazole on the barrier property of the silica film is reported also by D. Shchukin [141], Shchukin proposed in his work the using of capsules containing benzotriazole-doped silica film to reduce the interaction between benzotriazole and the silica film compounds. Lamaka studied the effect of benzotriazole on the corrosion protection of aluminium substrate coated with multi-layer films prepared by sol-gel process [142]. The study showed that benzotriazole has no negative effects on the barrier properties of the studied coating.

The conclusion can be drawn that the (negative or positive) effects of benzotriazole on the barrier property of the coating prepared by sol-gel process depends on factors such as the composition of the sol, the application parameters and the concentration of the benzotriazole in the sol.

A cerium salts-doped silica film is synthesised by Shi [143]. The study examined the effect of different cerium salts on the self-healing of the aluminium sample coated with silica film. As a result, cerium nitrate showed a positive effect on the self-healing. While, limited protection performance is measured for cerium chloride; pitting corrosion beneath the silica film is observed, which is caused by chloride ions from cerium chloride.

It can be concluded that the anions of the cerium salt (chloride or nitrate) have an effect on the effectiveness of cerium salt as a corrosion inhibitor.

EADS GmbH has been worked on the silica film as a protective layer for aluminium and magnesium metal alloys, the company hold the patent "Anti-corrosion layer for aluminium and magnesium alloys" [144]. A

Phosphonatoethyltriethoxysilan is added to the sol to improve the adhesion of the silica film on magnesium alloy. The silica film showed better barrier properties and better adhesion on the substrate when Phosphonatoethyl-triethoxysilan is added to the sol. It is important to indicate that the sol should be alcohol-based to achieve the homogeneity of the solution; Phosphonatoethyl-triethoxysilan has high hydrophobicity and need VOC to realize the dispersion with water.

It can be concluded that the corrosion protection of the alcohol-based silica film can be enhanced by using high hydrophobic organo-silica compounds; these materials are immiscible with the water–based sol. Therefore, the corrosion protection of the water-based silica film has to be developed by other methods such as doping of nanoparticles, corrosion inhibitors and others which will be discussed in this work.

2.6 Conclusion of the recent literature publications

Silica films prepared by sol-gel process are widely accepted in recent years as protective safety coatings for aluminium and magnesium alloys. The sol consists of organo-silica materials, water and acid as a catalyst. Volatile organic compounds (VOC) are added to the sol as a solvent to achieve the dispersion of organo-silica materials with water.

The using of VOC shows obstacles in the applications such as the flammability, evaporation and some of VOCs are toxic like methanol. These reasons have shifted studies to develop the water-based sols. No VOCs are added to the water-based sols, the organo-silica materials and water are dispersed by mechanical stirring to achieve the homogeneity of the sol; this can be attained when the organo-silica materials have low hydrophobic property (short organic group).

The long-term corrosion protection of aluminium or magnesium alloys coated with silica film is based on two approaches: 1) the barrier property of the silica film prevents the contact between the substrate and the corrosive environment,

2) self-healing feature of the silica film, which is realized by corrosion inhibitors as dopants in the water-based sol.

The solubility of the corrosion inhibitors in aqueous media has an important effect on the self-healing of the coated aluminium and magnesium sample. Low solubility of the corrosion inhibitors leads to a lack of the active agent at the damaged area of the coating. While, high solubility of the corrosion inhibitors results in a quick leach out of the active compounds from the coating, short-term of corrosion protection is then obtained.

2.7 Missing points in the recent studies

Several points are missing in the recent literature reviews which can be described as follow:

- Studies investigated the effect of the corrosion inhibitors on the self-healing of the sample, the following points are missing:
    - Studies reported that the benzotriazole lead to degradation in the stability of the silica film [140; 141]. Other researches found that the benzotriazole have no negative effects on the stability of the multi-films prepared by sol-gel process [142]. In this work the impact of the benzotriazole on the stability of the silica film will be clarified,
    - the appropriate concentration of the corrosion inhibitor-doped film is missing, which is needed to obtain the best corrosion protection. A range of corrosion inhibitor concentrations has to be used to reach the best protection effectiveness.
    - the long-term corrosion protection of the aluminium or magnesium sample coated with corrosion inhibitors containing silica film will be tested. A mixture of corrosion inhibitors is used to ensure better self-healing ability of the coated samples,
    - the fitting of the impedance spectra with the suitable electrical equivalent circuit is essential for better understanding of the self-

healing process. Especially for multi-layers coating. Also fitting is needed for better characterization of the self-healing process and the long-term corrosion protection.

- Studies focused on the effect of the nanoparticles on the corrosion protection of the substrate coated with the silica film. The following points are missing:
  - evaluation of the effect of different nanoparticles at varying concentrations on the corrosion protection is missing,
  - identification of the kind of the nanoparticles-doped silica film which provides better corrosion protection,

- Improving the stability of the sol without the chemical stabilizer additives.

2.8 The work schedule

In an attempt to obtain crack-free silica film with self-healing features, the subsequent points are of interest:

- preparation of the water-based sol, using DI water and acid as a catalyst instead of volatile organic compounds (VOC), that will render the silica film more applicable,
- optimisation of the aging period of the sol and the heat treatment parameters of silica film for better corrosion protection,
- application of the silica film in dependence on the proper viscosity of the sol in order to achieve crack-free films with excellent corrosion protection,
- investigation of the pitting corrosion and the protection effectiveness of the aluminium sample coated with silica film,
- evaluation of the proper concentration of the nanoparticles containing silica film for better film thickness and enhanced corrosion protection,

- incorporation of the corrosion inhibitors at different concentrations in the sol to generate the self-healing feature, the doped corrosion inhibitors should have good solubility in the water-based sol,
- Estimation of the long-term corrosion protection of the aluminium or magnesium sample coated with corrosion inhibitors-doped film,
- Characterization of the nanoparticles and corrosion inhibitors-doped silica film by scanning electron microscope (SEM), electrochemical technique and contact stylus instrument,
- modification of the composition of the water-based sol for better solution stability,
- comparison of this work with other up to-date work on silica films for corrosion protection,
- the achievement of this work.

3 Objectives of the work

The silica films prepared by sol-gel process have been widely accepted as environmentally friendly protective coatings for aluminium and magnesium alloys. The sol consists of organo-silica compounds, catalyst and water. The organo-silica compounds are immiscible with water in all proportions. Thus, Volatile Organic Compounds (VOCs) are needed to achieve the homogeneity of the sol. VOCs showed problems in the applications such as flammability and evaporation. This has shifted studies to develop the water-based sols; the water-based sol is prepared without the VOC which is demanded for applications. **The first aim of this work** is to prepare cost-efficient, protective water-based silica films. The composition of the sol, the application parameters, the cost and the stability of the sol will be studied.

Cracking is one of the major drawbacks of the silica film. The cracks occur during the cross-linking of the silica film by heat treatment, the in-plane tensile stress is increased during the shrinkage of the silica film which leads to cracks. **The second aim of this work** is to prepare crack-free silica film. The effect of the nanoparticles-doped silica film to reduce the shrinkage of the film will be tested. The structure and the corrosion protection of aluminium and magnesium samples coated with nanoparticles-doped silica film will be characterized by electrochemical technique and SEM.

Self-healing is an important aspect to improve the stability of aluminium and magnesium samples in corrosive solution. When a defect occurs in the corrosion inhibitors-doped silica film, the corrosion inhibitors leach out of the film to the defect area, a layer of corrosion inhibitors is formed in the defect which reduces the corrosion process. **The third aim of this work** is to develop the self-healing ability of the coated samples in order to reach the long-term corrosion protection. To achieve this aim, the following points will be discussed: The effect of the corrosion inhibitors on the stability of the silica film, the size of the defect in the silica film to generate the self-healing and reducing the lack of the corrosion inhibitors from the silica film.

4 Experiments and results

4.1 Experiments and methods

4.1.1 The chemical materials

The chemical materials are chosen in this work according to the following principles: 1) the cost-efficiency of the chemical materials, 2) the protection efficiency of the silica film which prepared from these chemicals. The prices of the chosen organo-silica compounds is mentioned already in table 2, it is clear that Glycidoxypropyltrimethoxysilane (GPTM) and Tetraethylorthosilane (TEOS) have the lowest prices; these chemical materials have low hydrophobic properties in comparison to other compounds in the table 2, and can be used to prepare the water-based sol. No volatile organic compounds (VOC) are needed to prepare the water-based sol which reduces also the cost.

The water-based sol precursor was prepared from 3-glycidoxypropyltrimethoxy-silane (GPTM), tetraethylorthosilane (TEOS), DI water and HCl. The pH value of the solution was 4.5 in order to facilitate the hydrolysis reaction of the alkoxy groups in the organo-silica compounds, the water-based sol was mixed by magnetic stirring and induced to react eventually. Tables 3 displays the chemical materials used to prepare the water-based sol. All the chemicals were provided by Sigma-Aldrich Company.

Table 3: The chemical materials used to prepare the sol

Glycidoxypropyltrimethoxysilane (GPTMS) Purity: 98 %	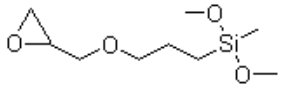
Tetraethylorthosilane (TEOS) Purity: 98 %	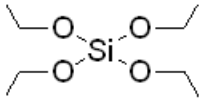
Sodium hydroxide	NaOH
Hydrochloric acid	HCl
Silicon Dioxide SiO_2	nanopowder Ø 40nm
Zercunium oxide ZrO_2	nanopowder Ø 30nm
Silicon carbide SiC	nanopowder <100 nm

The corrosion inhibitors are selected in this work according to following aspects:

1- The corrosion inhibitors act as anodic and cathodic corrosion inhibitors, the aim is to block the anodic and the cathodic corrosion reactions for better corrosion protection.

2- The solubility of the corrosion inhibitor, the solubility of the inorganic corrosion inhibitors such as cerium nitrate in aqueous media is higher than the solubility of the organic inhibitors such as benzotriazole. When a defect occur in the corrosion inhibitors-doped silica film, cerium ions leach out of the silica film to heal the defect area due to high solubility of the cerium nitrate. Benzotriazole leach out of the silica film in low concentrations which insures a long-term source of the corrosion inhibitors (in low concentration) and reduces the quick lack of the corrosion inhibitor (Benzotriazole) from the silica film. Table 4 demonstrates the corrosion inhibitors used in this work.

Table 4: The corrosion inhibitors used in this work

Name	Structure	Effect on corrosion
Zinc phosphate	$Zn_3(PO_4)_2$	+
Cerium nitrate	$Ce(NO_3)_3$	+
Sodium orthosilica	Na_2SiO_3	-
Sodium molybdat	$Na_2MoO_4 \cdot 2H_2O$	-
Sodium tungstate	Na_2WO_4	-
1.2.3 Benzotriazole	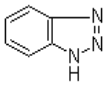	+
Thiourea	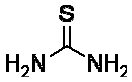	-
Aconitic acid	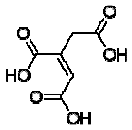	-

+ Improvement in the corrosion protection, - No improvement in the corrosion protection

4.1.2 The sol precursor

Different concentrations of the water-based sols were tested 6 and 50 % sol. The sol 6 % was used for the sealing of anodized aluminium and plasma oxidized of magnesium samples. The viscosity of the sol 6 % is low which allows the sol to penetrate into the pores and the defect of the ceramic coatings. 6 % sol was synthesised from the organo-silica compounds GPTM: TEOS (1:1), deionized (DI) water and HCl as a catalyst. The volume ratio of the sol was GPTM/ TEOS/ DI water (3/3/94) to prepare 100 ml sol. The pH value of the sol was adjusted by the catalyst to 4.5 to ensure the stability of the sol. The sol at pH values less than 4.5 demonstrates stability for 2 months, but low barrier property is observed for the silica films deposit from this sol, this can be explained in terms of the dissolution of the metal oxide at the surface of

aluminium or magnesium substrate in the acid sol. The neutral and slight alkaline water-based sols show low stability due to the attraction between different charged molecules in the sol, this point will be discussed later in the stability of the water-based sol.

The ratio 25/25/50 GPTM/ TEOS/ DI water was set up the 50 % sol. Cracks are observed in the silica film from this sol. The aim from using this sol is to study the effect of the nanoparticles on the silica film, in order to obtain crack-free silica film.

The GPTM is added to the sol to enhance the corrosion protection of the coated sample, GPTM has an organic part which improves the hydrophobic property of the silica film, also GPTM link to the structure of the silica film through Si-OH which generated by the hydrolysis of Si-OR, as discussed before in the hydrolysis and condensation of the sol. The TEOS is cost-efficient material (see table 2), it is added to the water-based sol to lower the cost. TEOS has Si-OR groups which hydrolysed to Si-OH to form the structure of the silica film through the cross-linking. Low corrosion protection was measured for the silica film prepared from TEOS. The silica film is non-dense and has low hydrophobic properties. Figure 4.1 demonstrates silica film prepared from TEOS at concentration of 6 %, it is clear that non-protective silica film is formed on the aluminium substrate surface. Therefore, GPTM is added to the sol for better corrosion protection.

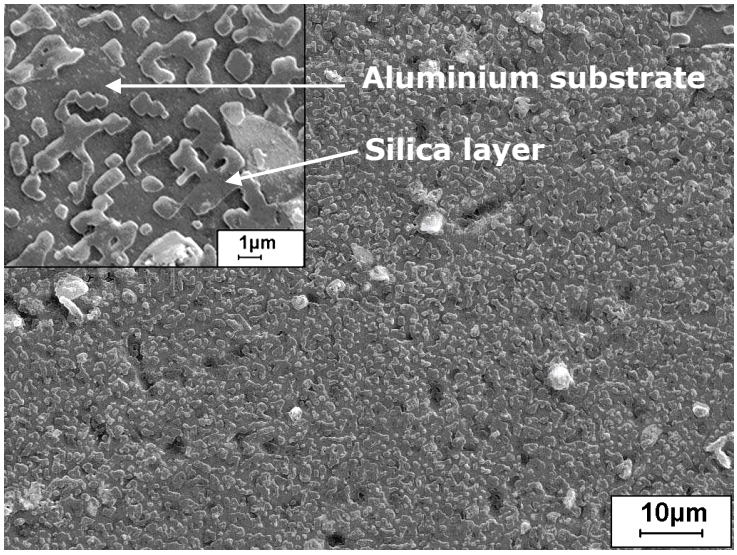

Figure 4.1: Aluminium substrate coated with silica film 6 % TEOS sol

The sols were aged at ambient circumstances with magnetic stirring, the aging of the sol is essential to obtain "workable" solution and forms solid protective silica coating rather than an oily film.

4.1.3 Metal substrates

The aluminium alloy 6082-T6 and magnesium AZ31 alloys were used in this work as metal samples; both metal alloys have low corrosion protection in corrosive media. The aluminium alloy 6082-T6 is widely used in commercial vehicles, railcars, shipbuilding, mechanics industry and machining applications. This alloy offers good finishing characteristic and responds well for anodizing. The chemical composition of 6082-T6 alloy is shown in Table 5. [8]

Table 5: The chemical composition of the aluminium alloy 6082-T6

Wt-%	Si	Mg	Mn	Fe	Zn	Cu	Ti	Cr	Al
6082	0.98	0.70	0.58	0.21	0.014	0.015	0.02	0.01	Rest

The light-weight of the magnesium alloy AZ31 attracts aerospace and vehicle industries where the weight reduction is needed. Magnesium alloy AZ31 has also applications in electronic industries. The chemical composition of the magnesium alloy AZ31 is seen in table 6. [12]

Table 6: The chemical composition of magnesium alloy AZ31

Wt-%	Al	Zn	Mn	Fe	Cu	Mg
Mg AZ31	2.5 – 3.5	0.6 – 1.4	0.2	0.005	0.05	Rest

The metal substrates were a sheet of aluminium or magnesium metal alloys, the samples were cut into dimensions 20X20 mm, the metal samples were grounded to grade 2500 by means of SiC emery paper, washed with water and ethanol, and then air-dried. The cleaned samples have to be completely wettable by water. The silica films were applied on the magnesium and aluminium metal substrates to improve the corrosion resistance. The ANOX of aluminium and PEO of magnesium were sealed in the water-based sol to hinder the penetration of

the corrosive solution in the defects of the ceramic layer for better corrosion protection in corrosive solutions.

4.1.4 Silica film surface treatment

The following steps were determined in this work to apply the silica coating: Grinding of the metal sample to 2500 SiC → tap water rinsing → alcohol washing → air drying → immersion of the aluminium or magnesium substrate in the sol for 30 second → drying for 30 min at room temperature and then curing at 150 °C for 3 hours.

When the aluminium or magnesium substrate is immersed in the sol, hydrogen bonds are formed between Si-OH from the solution and Me-OH on the metal surface. The uncrosslinked film is non-protective and easily dissolved in water. Therefore, heat treatment is needed to form the covalent bonds between the film and the metal surface. [115; 126]

The immersion period of the aluminium or magnesium substrate in the sol has no effect on the film thickness. Therefore, thirty seconds immersion period was determined in this work for the treating of the metal samples in the sol.

4.1.5 Characterisation techniques

The electrochemical impedance spectroscopy (EIS) is well known as a useful technique to characterise different coating systems. The EIS was used in this work to evaluate the performance of the silica film, the cyclic voltammetry (CV) was employed to study the pitting corrosion of the aluminium samples coated with silica film. The surface morphologies of the treated samples were investigated by scanning electron microscope (SEM).

4.1.5.1 Cyclic Voltammetric test

The Cyclic Voltammetric is commonly used to evaluate the pitting corrosion of the aluminium substrate coated with silica film. When the potential applied or the electrode polarised, it can promote the current to flow through the electrochemical reaction that happens at the studied aluminium or magnesium metal surface, the current is controlled by the kinetics of the electrochemical

reactions and the diffusion of the reactants both towards and away from the electrode surface. [145]

When the electrode undergoes uniform corrosion at open circuit, the Open Circuit Potential (OCP) value is controlled by the equilibrium between two reactions; one of the reactions is the anodic reaction where the metal oxide is formed as in the equation 22, the current is called anodic current.

$$Me \rightarrow Me^{2+} + 2e^{-} \qquad (22)$$

The second reaction is the cathodic reaction where OH ions are generated in neutral media as in the equation 23; the current is then called cathodic current.

$$O_2 + 2H_2O + 4e^{-} \rightarrow 4OH^{-} \qquad (23)$$

Once the cathodic and anodic currents are equal, the OCP occurs or the system is in the equilibrium state; it is referred to as the E_{corr} or the corrosion potential. When the cyclic voltammetry measurement plotted on the log i_{corr} versus the potential, the diagram then called Tafel diagram and the corrosion current can be obtained by analysing the data as in the Figure 4.2. [145]

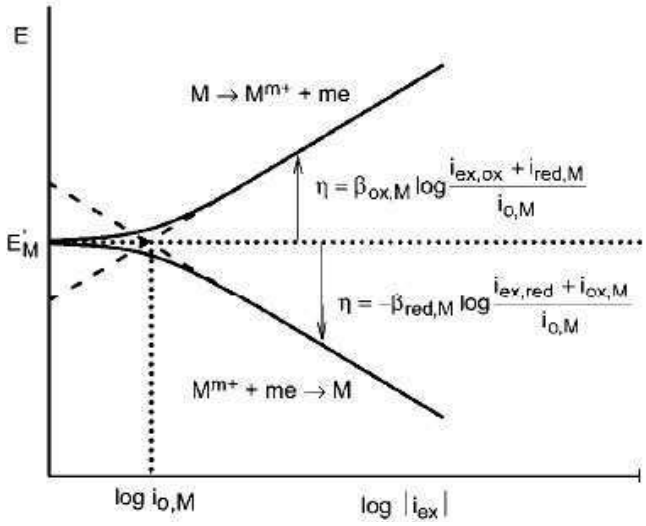

Figure 4.2 : Tafel diagram with the slops for measuring the E_{corr} and I_{corr} [145]

In this work, the cyclic voltammetric (CV) tests were applied under the potentiostatic mode. The polarisation plots were generated by applying a potential of 250 mV (-250 mV to +250 mV) in both positive and negative

directions from the open circuit potential. Series of CV cycles were used to evaluate the pitting corrosion and the effect of the corrosion products on the corrosion process, the data obtained from Tafel diagrams (E_{corr}, I_{corr}) were used to estimate the protection efficiency of the coating.

4.1.5.2 Electrochemical Impedance Spectroscopy (EIS)

The electrochemical Impedance Spectroscopy EIS has been used as an effective technique for characterisation of the coating systems. The impedance Z(f) is a frequency depended value, the impedance data are obtained by applying small signals to perturb the electrode surface (such as silica film or epoxy) in a range of frequencies. The sinusoidal voltage signal of 10 mV is usually applied by the impedance instrument, and the current signal is measured at the same frequency. [146]

The impedance spectra of the sample are measured for a range of frequencies. The result is a complex number which comprises of two quantities, the real and the imaginary components of the electrical impedance. The impedance value can be calculated by Ohm`s law (equation 24). [146]

$$Z = \frac{E_t}{I_t} \qquad (24)$$

Where the potential is expressed as equation 25,

$$E_t = E_0 \exp(j\omega t) \qquad (25)$$

The associated current response is shown in equation 26,

$$I_t = I_0 \exp(j\omega t - \phi) \qquad (26)$$

the impedance is then described as equation 27,

$$Z = \frac{E}{I} = Z_0 \exp(j\phi) = Z_0(\cos\phi + j\sin\phi) \qquad (27)$$

$j = \sqrt{-1}$ the imaginary part.

$\omega = 2\pi f$ the radial frequency in radian per second

f the frequency in Hertz.

ϕ the phase shift is the difference in the phase of the current and the voltage (Figure 4.3).

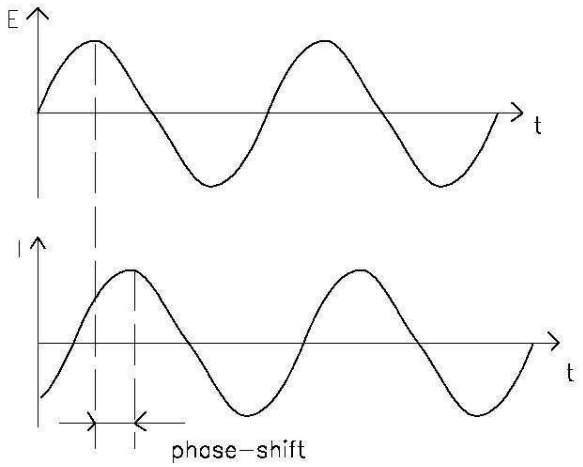

Figure 4.3: The phase shift between the current and the voltage [146]

The complex impedance data can be plotted by two different methods as Nyquist plot or Bode plot. When the real part and the imaginary part of the EIS data are plotted on the X axis and the Y axis respectively, the EIS spectra is called Nyquist plots (Figure 4.4). [147]

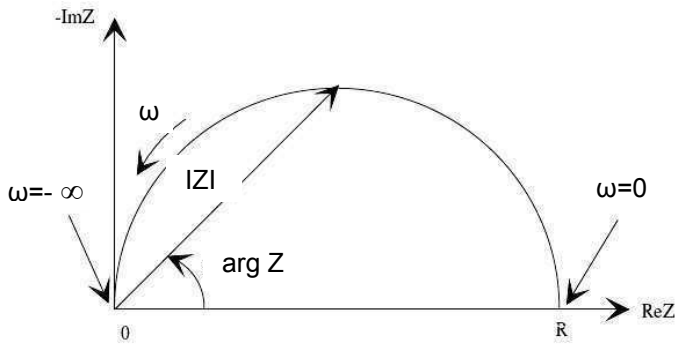

Figure 4.4: Nyquist plot with one time constant [147] ∞

When the log frequency plots on the X axis and the both $|Z|$ and phase shift are on the Y axis, the EIS spectra presents Bode plot (Figure 4.5-a) [107]. The EIS data analysis is commonly carried out by fitting it to an equivalent circuit model.

The equivalent circuit model is a combination of resistance, capacitance and other electrochemical elements which depend on the studied system. The simplest and the most common equivalent circuit model is Randel Circuit (Figure 4.5-b), Randel model is used for fitting of the uncoated aluminium and magnesium substrates, or for substrates coated with high protective coatings. [147]

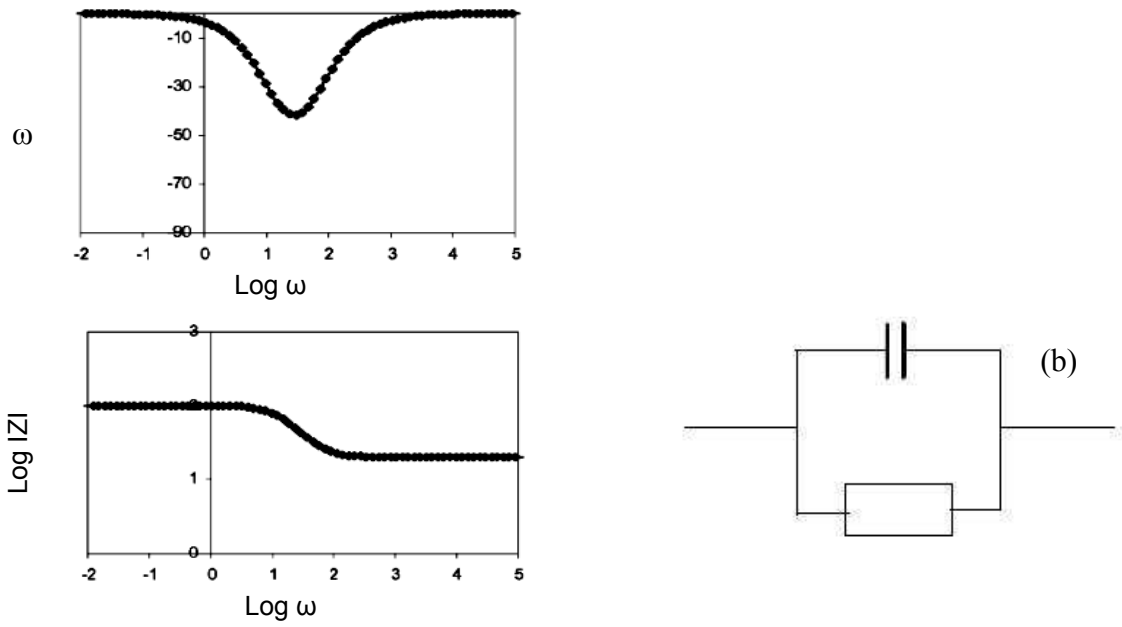

Figure 4.5: Bode plot with one time constant [147]

Figure 4.6-a shows Bode plot of metal sample coated with organic coating, two time constants are observed in the phase shift and the impedance plots. The time constant at high frequency refers to the coating where C_c and R_p are the coating capacitance and the pore resistance respectively. The second time constant at low frequency indicates to the double layer at the metal surface or the corrosion beneath the coating, the double layer capacitance C_{dl} and double layer resistance R_{dl} are shown in Figure 4.6-b. The solution resistance (R_s) value depends on the concentration and the temperature of the surrounding media. [148; 149]

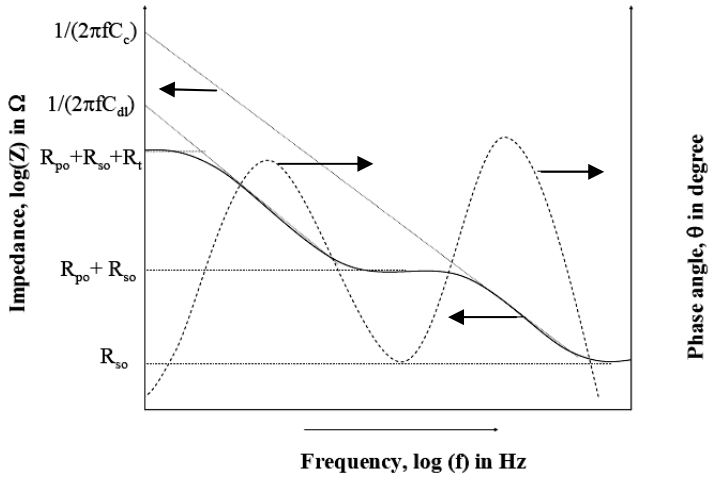

(a)

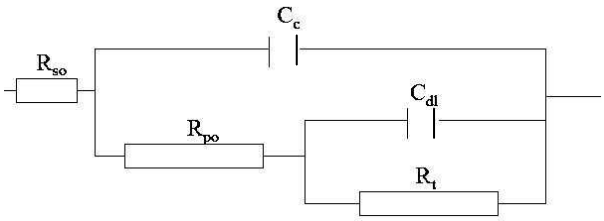

(b)

Figure 4.6: Impedance spectra as a Bode plot for aluminium or magnesium samples coated with organic coating (a), and (b) the equivalent electric circuit for the fitting the EIS spectra [148]

4.1.5.3 Salt spray test (SST)

Salt spray test was used to evaluate the corrosion protection of the aluminium alloy 6082 coated with silica film and PEO of magnesium substrate MgAZ31 sealed in the sol. The salt spray test was not employed for the magnesium alloy coated with silica film due to the low corrosion protection of these samples, as noticed also by the electrochemical measurements. The ANOX samples were sealed in the sol to improve the stability of the samples in the base solutions (such as NaOH). Therefore SST did not apply for the sealed ANOX samples. The tests were done according to the (DIN EN ISO 9227). The salt spray tests were stopped when traces of corrosion appeared on the samples.

4.1.5.4 The scratch test

The scratch test instrument CSM Revetest®27-445 (Figure 4.7) is used in this work to defect the aluminium or magnesium substrate coated with corrosion inhibitors-doped silica films in order to generate the self-healing. The instrument consists of a diamond indenter connected to a load cell and acoustic emission detector (AE), the indenter is situated above a motor driven sample table where the sample is fixed.

A steady load of 10 N was applied for scratch length 10 mm, this parameter was used to defect the samples "to evaluate the self-healing" in order to obtain the same defect dimensions for all samples.

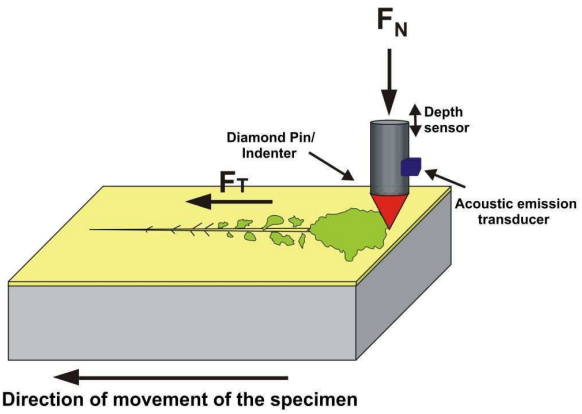

Figure 4.7: Scratch Testing Instrument CSM Revetest®27-445

4.2 Aluminium alloy 6082-T6 coated with silica film

Prior to study the corrosion protection of the aluminium alloy 6082-T6 coated with the silica film, the impedance (EIS) data were recorded for the uncoated substrate in 0.5M NaCl. The aim of this experiment is to evaluate the effect of the heat treatment on the protection performance of the natural aluminium oxide.

One time constant is observed in the EIS spectra of the uncoated aluminium alloy as in Figure 4.8, no differences were seen on the electrochemical behaviour of the aluminium substrate after the heat treatment for 3h at 150°C. The conclusion can be drawn that the electrochemical behavior of the natural aluminum oxide on the aluminum alloy did not change through the heat treatment. Any development in the corrosion protection of the aluminum alloy coated with silica film is related to the interaction between the aluminium surface and the silica film.

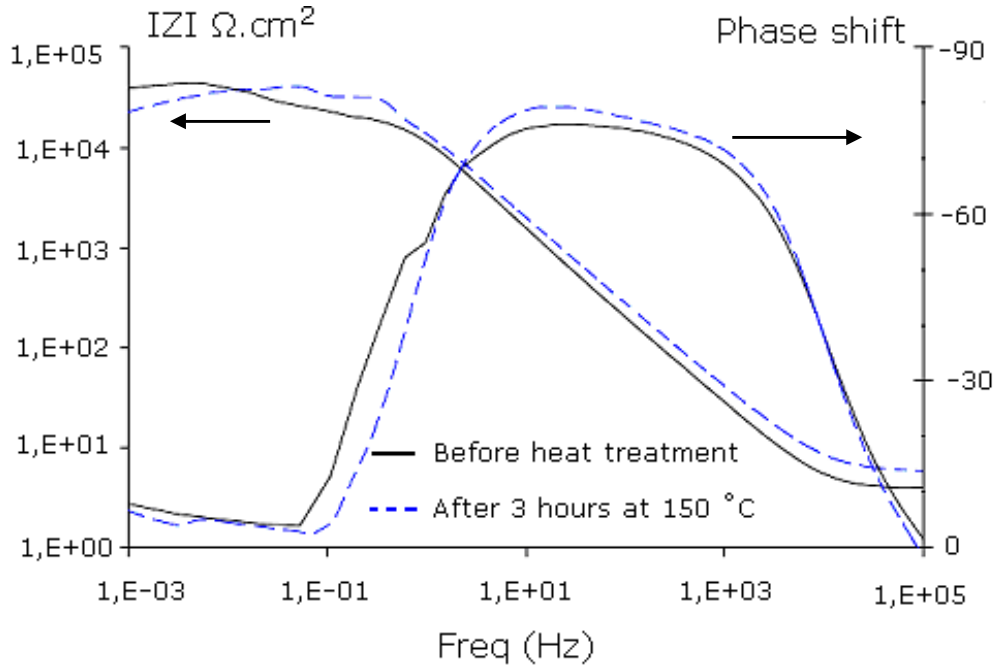

Figure 4.8: Bode plots for Aluminium 6082-T6 after heat treatment

4.2.1 Application parameters of the silica film

4.2.1.1 Effect of aging period of the sol

The aging process is aimed to obtain a workable sol, alkoxide group (OR) of the silanes is converted into (OH). The water-based sol was prepared by mixing the silanes with water and acid as a catalyst, the mixture was aged at room temperature for different periods. Figure 4.9 shows the effect of the aging periods of the sol on the impedance spectra of the aluminium sample coated with silica film. One time constant (TC1) appears after aging the sol for 1 day (Figure 4.9), this indicates that the amount of the hydrolysed alkoxy groups in the sol is not sufficient to obtain cross-linked silica film. The second time constant (TC2) is distinguished after the aging period of 3 days; this can be explained in terms of the amount of the -OR groups hydrolysed to -OH are sufficient to obtain cross-linked silica film. Moreover, the structure Al-O-Si is formed at the interfacial layer of the aluminium substrate which ensures the adhesion of the silica film on the aluminium substrate.

No further improvement of the corrosion protection of the aluminium sample coated with silica film was measured for the aging period more than 3 days. This indicates that most of the alkoxy groups in the water-based sol are hydrolysed during the aging period of 3 days.

It can be concluded that the aging of the water-based sol for 3 days is sufficient to obtain a dense cross-linked silica film. This result is determined in this work to prepare the sol.

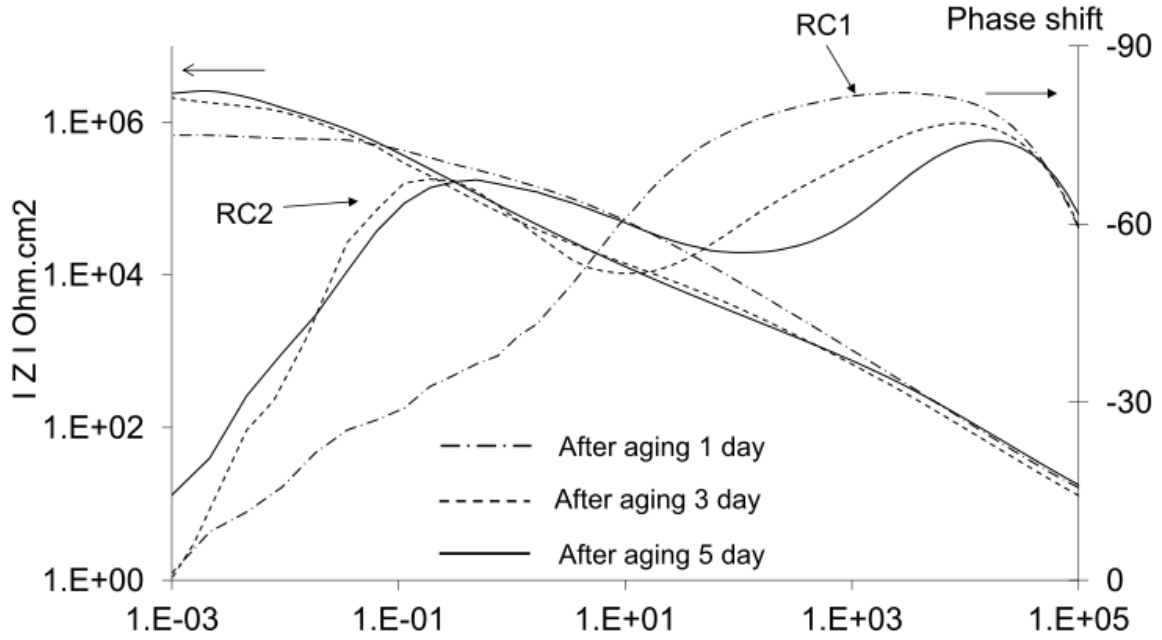

Figure 4.9: EIS spectra shows effect of aging period of sol on corrosion protection

4.2.1.2 Effect of the heat treatment parameters

The heat treatment process is carried out for crosslinking of the silica film. D. Zhu studied the effect of the heat treatment parameter on the crosslinking of silica film [26]. The corrosion protection of the aluminium sample coated with silica film is enhanced when the heat treatment temperature rises from 80 to 100 °C. Zhu determined the heat treatment for 4 hours at 100 °C to obtain crosslinked silica film.

The fully croslinked silica film can be reached by the heat treatment at temperature of 300 °C for 1.5 hours [150]. The heat treatment at temperature of 300 °C leads to changes in the microstructure of the aluminium and magnesium alloys which results in different metal alloy properties.

In this work, the heat treatment of the aluminium and magnesium samples coated with silica film was carried out at 150 °C; the heat treatment period is estimated to identify the best curing time for better corrosion protection.

Figure 4.10 shows bode plot for aluminium substrate coated with water-based silica film after different heat treatment periods 1; 3 and 5 hours at 150 °C. The experiments demonstrated that the corrosion protection and the barrier property of the sample were improved after the heat treatment period of 3h. The time constant TC2 was shifted to lower frequencies, this behaviour is attributed to the crosslinking between the –OH from the metal surface and the –OH from the silica film. Heat treatment period more than 3 hours did not show further improvement in the corrosion protection, this can be explained in terms of the most of the OH and OR groups in the silica film are condensed after the heat treatment period of 3 hours at 150 °C.

It can be concluded that the heat treatment of the sample for 3 hours at 150 °C is sufficient to obtain a protective dense silica film, this result is determined for the crosslinking of the silica films in this work.

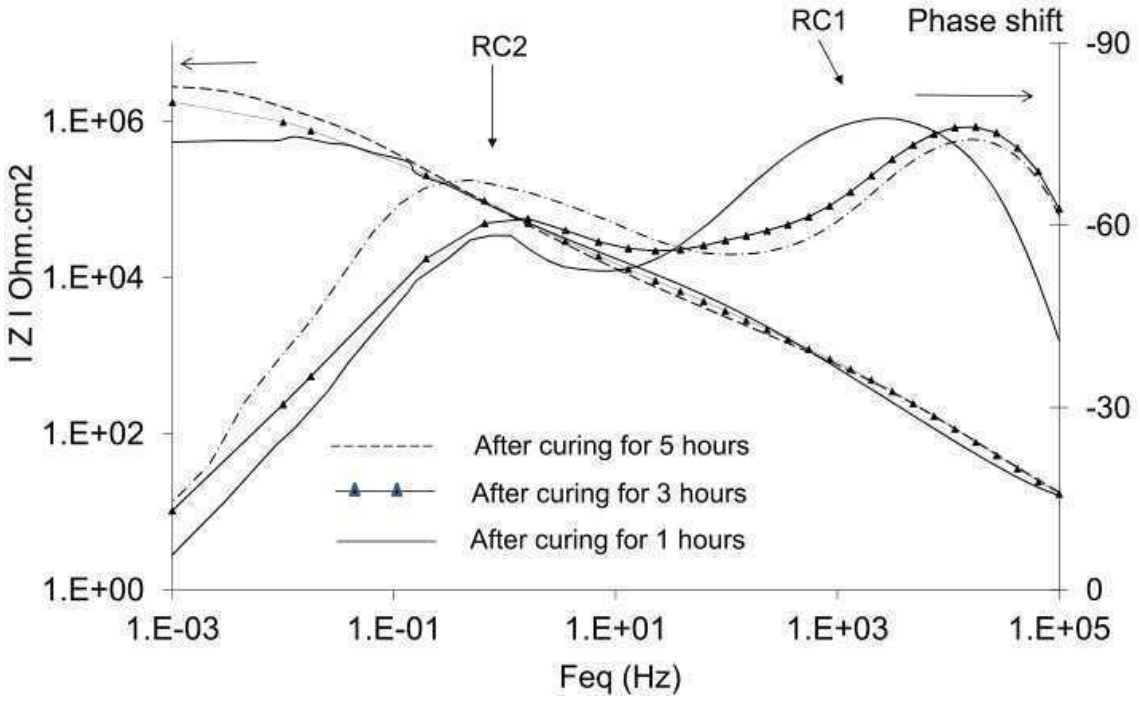

Figure 4.10: EIS spectra shows effect of heat treatment of silica film on the corrosion protection

The development in the impedance of the aluminium sample coated with silica film indicates that a barrier silica film structure is formed. Better understanding of this observation can be reached through the mechanism of the silica film formation on aluminium substrate.

4.2.1.3 The formation of crosslinked silica film

The crosslinked silica film is a result of the condensation of SiOH groups which are formed by the hydrolysis reaction of silane molecules. The hydrolysis of silanes in water-based sol tends to be complete rather than reversible reaction. Alcohols are generated through the hydrolysis reaction of the water-based sol as in equation 28; the aeration of the water-based sol during the aging period is needed to evaporate the alcohols and to shift the hydrolysis reaction to the right direction.

$$Si-OR+H_2O \Leftrightarrow Si-OH+R-OH \tag{28}$$

The development in the EIS spectra is mainly caused by the crosslinking of the silica film through the heat treatment process. No further hydrolysis, condensation or reversible reactions are expected after the crosslinking of the water-based silica film. Another contribution to the improvement in the impedance of the sample is made by the silica film / metal surface interface. A strong covalent bond is formed in the structure Al-O-Si which enhances the adhesion of the silica film to aluminium and magnesium substrates (equation 29). [26]

$$Me-OH+Si-OH \rightarrow Me-O-Si+H_2O \tag{29}$$

Me is the metal substrate which can be aluminium or magnesium

4.2.1.4 Pitting corrosion of aluminium alloy 6082-T6 coated with silica film

Open circuit potential (OCP) measurements were carried out for two hours before any electrochemical measurements to ensure that the system is in equilibrium state. Cyclic voltammetric measurements (CVs) were carried out to study the pitting corrosion of the aluminium substrates 6082-T6 in 0.5 M chloride solution.

Three CV measurements were implemented on the aluminium substrate to evaluate the effect of the corrosion products on the corrosion process. The polarisation plots were generated by applying a potential of 250 mV (-250 mV to

+250 mV) in both positive and negative directions from the open circuit potential.

Figure 4.11 exhibits the polarisation curves of the uncoated aluminium substrate. The anodic current density is increased rapidly to a value of 8 mA/cm^2. This indicates the high anodic corrosion of the uncoated aluminium substrate. The E_{corr} of the sample is -750 mV. The repassivation of the pitting corrosion is observed at potential of -860 mV. The shift in the potential of the sample from (-750 to -860) mV indicates the degradation in the corrosion protection of the aluminium sample.

The third voltammetric cycle is shifted from -860 mV to higher potential value of -900 mV, which indicates that a high corrosion process occurs at the aluminium substrate. The corrosion products at the aluminium substrate surface did not show any development in the protection of the sample, this can be explained by the migration of the corrosion products to the solution, also it can be related to the non-dense layer of corrosion products at the substrate surface. Signs of pitting corrosion are observed on the uncoated aluminium sample after the cyclic voltammetric measurements.

Figure 4.12 demonstrates the aluminium substrate 6082-T6 coated with silica film. The anodic current density of the sample is increased to an anodic current value of 10 μA/cm^2. The E_{corr} of the sample was -680 mV, the re-passivation of the pitting corrosion is observed at potential of -800 mV. A region of "Zig-Zag" is observed in the CV spectra at high potential as in Figure 4.12; The "Zig-Zag" can be attributed to the breakdown of the silica film which reduces the corrosion protection of the coated aluminium sample, the corrosive solution penetrates through the cracks of the film to reach the metal surface, the corrosion process occurs in the cracks and beneath the silica film.

The breakdown of the silica film can be explained as follows

Defects are usually formed in the silica film during the application process; the corrosive solution penetrates through these defects which open pathways for the corrosive solution toward the aluminium surface, and active corrosion process occurs. The corrosion products are difficult to diffuse away from their original corrosion sites, the accumulation of the corrosion products beneath the silica film forces the film to diverge from the aluminium substrate surface, which leads to cracks in the film, this phenomenon is seen as a "Zig-Zag" in the Cyclic

voltammetric measurements. However, no signs of pitting corrosion are observed on the aluminium sample coated with silica film after the CVs measurements.

The conclusion can be drawn that the barrier property of the silica film reduces the effect of the chloride solution on the aluminium substrate. The breakdown in the silica film is observed in the CV spectra as a Zig-Zag at the region of high potential. The breakdown in the film can be attributed to the corrosion at the original defects of the silica film; the accumulation of the corrosion products beneath the silica film leads to the cracks. The corrosion products did not show any effect on the corrosion protection of the sample.

To prevent the breakdown of the silica film, the barrier property of the silica film has to be improved; this can be achieved through the use nanoparticles to obtain crack-free silica film.

The corrosion current density of the samples are evaluated by tafel diagram (as in table 7)

Table 7: Corrosion current density obtained from the analysis of Tafel curves

	Uncoated aluminium sample	Aluminium sample coated with silica film
Corrosion current density $\mu A/cm^2$	3.96	0.052

The protection efficiency of the aluminium sample coated with silica film can be calculated from the equation 30.

$$protection\ \ Effeciency\ \ (\%) = \frac{icorr_{uncoated} - icorr_{coated}}{icorr_{uncoated}} * 100 = \underline{\underline{98.68\ \%}} \qquad (30)$$

$Icorr_{coated}$ is the corrosion current density for the aluminium sample coated with silica film

$Icorr_{uncoated}$ is the corrosion current density for the aluminium sample

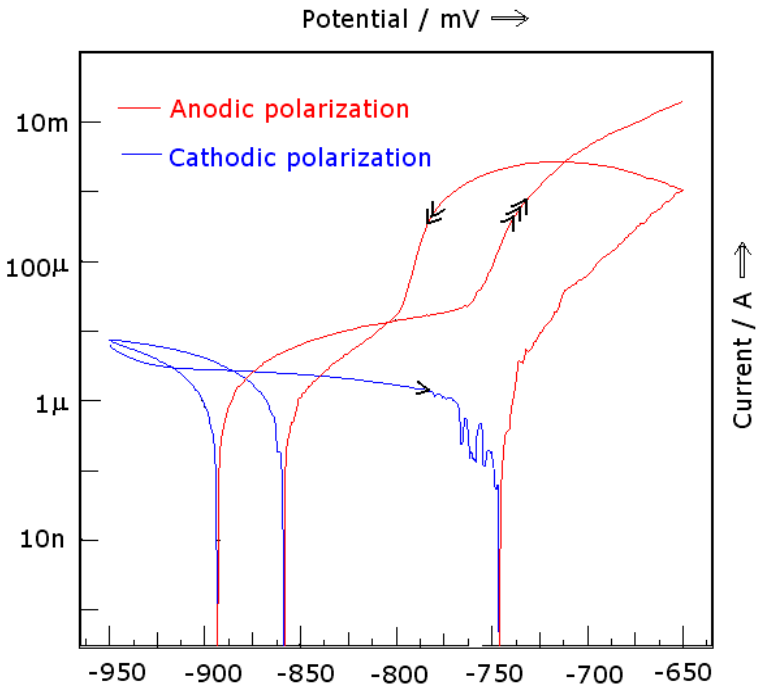

Figure 4.11: Cyclic voltammetric measurement for uncoated aluminium substrate

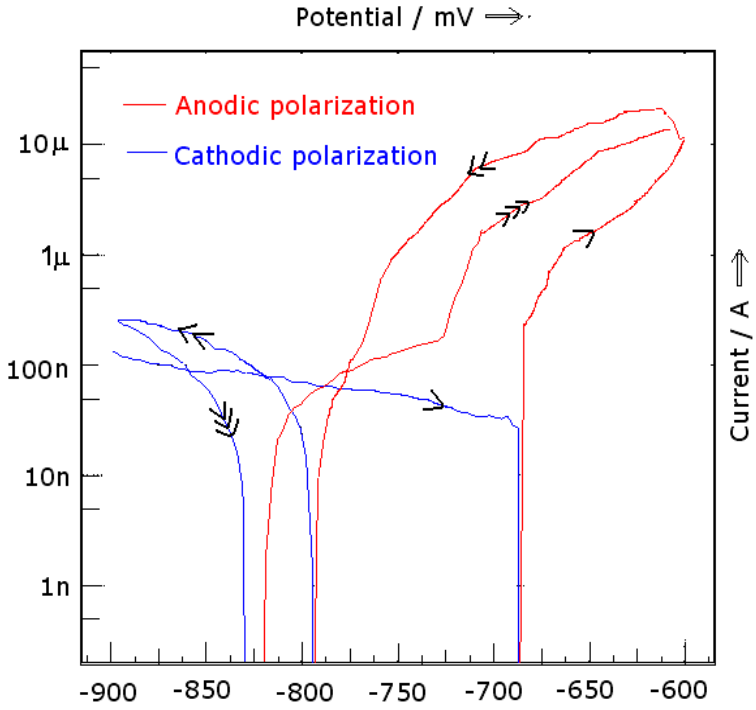

Figure 4.12: Cyclic voltammetric measurement for aluminium substrate coated with silica film

4.2.2 Nanoparticle-doped silica film

Cracking is one of the major drawbacks of the silica film. The cracks occur when the critical film thickness of 300 nanometres is exceeded [127]. The cracks are generated during the crosslinking of the water-based silica film by the heat treatment. The volume of the silica film is reduced during the heat treatment due to a) evaporation of the water, b) shrinkage of the silica film through the polycondensation reactions of OH and OR groups of the organo-silica compounds. The decreasing in the volume of the silica film raises the in-plane tensile stress in the silica film and cracks are formed. [128]
Crack-free film can be deposited by multi-layers of thin silica films [130], multi-layers method is not economic feasible. Crack-free silica film can be prepared through organic polymer-doped alcohol-based sol. The organic polymers are added to the sols to recover the cracks may occur in the silica film [151]. The organic polymers are immiscible with water; they can not be used as dopants for the water-based sols.

In this chapter, the effect of different kinds of nanoparticles at varying concentrations on the property of the silica film was tested. The aim is to prepare crack-free water-based silica film. The nanoparticles-doped water-based sol is treated by ultrasonic for 30 minutes to reduce the particles agglomeration. The electrochemical impedance spectroscopy (EIS) was used to evaluate the protection performance and to characterise the nanoparticles-doped silica film. The scanning electron microscope (SEM) LEO 1455VP was employed to characterise the silica films.

4.2.2.1 Encapsulation of silicon carbide nanoparticles

Silicon carbide nanoparticles at different concentrations were added to the sol. Figure 4.13 illustrates the impedance spectra for aluminium 6082-T6 alloy coated with SiC nanoparticle-doped silica film. The impedance spectra show a plateau at intermediate frequencies, which is formed because the number of the defects in

the film is constant with time [148]. The impedance value of the plateau is increased with higher concentrations of SiC nanoparticles in the silica film. The polarization resistance R_p of the sample with 1 % SiC nanoparticle is 1.E7 Ω.cm^2, which increases to 1.62E7 Ω.cm^2 for the samples with 6 % SiC nanoparticle (as seen in Table 9).

The development in the coating resistance indicates that the cracks and the defects of the silica film are reduced by higher concentrations of SiC nanoparticles.

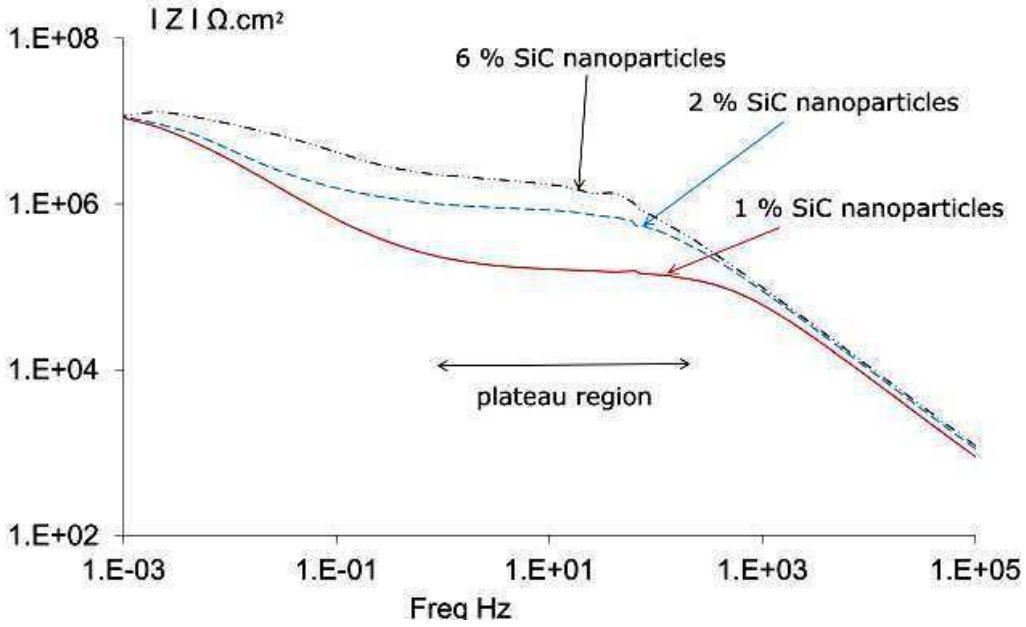

Figure 4.13: Impedance spectra of aluminium substrate coated with SiC-nanoparticle-doped silica films

The silica film doped with SiC nanoparticles is made up of three different regions. They are from outside to inside, the cross-linked silica film with the Si-O-Si bonds, cross-linked silica interfacial layer dominant with Si-O-Al and Si-O-Si bonds, inner layer of Al oxide on the aluminium alloy substrate as in Figure 4.14.

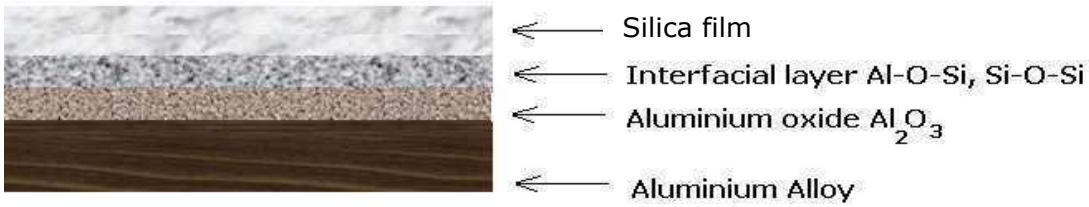

Figure 4.14: Schematic describes the regions of the silica film

According to this structure, the time constant (TC1) at high frequency refers to the silica film. The response of the interfacial layer (TC2) is seen at frequencies less than 10 Hz, The time constant of the aluminium oxide film is not seen in Figure 4.15, it can be studied at frequencies less than 10^{3-} Hz.
Figure 4.15 describes the spectra phase shift versus frequency. The spectra show that the phase shift at high frequencies is increased with higher concentrations of SiC nanoparticles in the silica film; this indicates the development of the barrier property of the silica film.

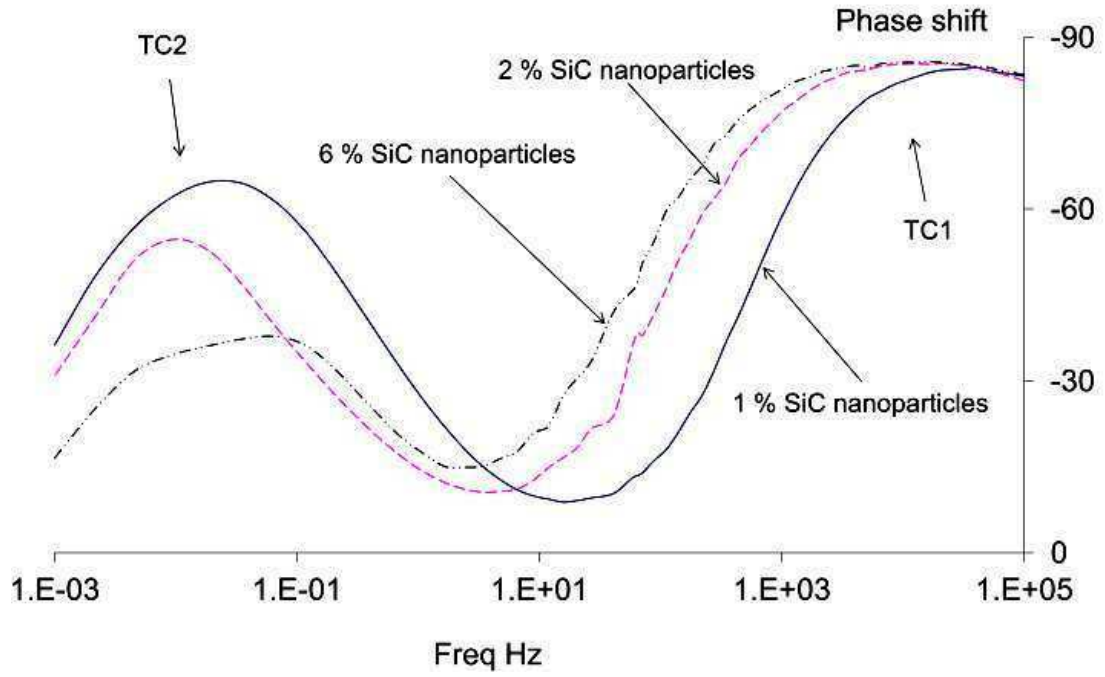

Figure 4.15: Spectra phase shift versus frequency of aluminium substrate coated with SiC nanoparticle-doped silica films

The conclusion can be drawn that the corrosion protection of the aluminium samples coated with SiC nanoparticles-doped silica film is enhanced by higher

concentrations of the SiC nanoparticles. This can be explained in terms of the decreasing in the cracks of the SiC nanoparticles-doped silica film.

4.2.2.2 Encapsulation of zirconium oxide nanoparticles

Figure 4.16 shows impedance spectra of the aluminium samples coated with a zirconium oxide nanoparticle-doped silica film. A plateau region is observed at the intermediate frequencies of EIS spectra. The impedance value at the plateau is increased with concentrations higher than 1 % ZrO_2 nanoparticles, this indicates the development in the barrier property of the silica film at higher concentrations of the ZrO_2 nanoparticles.

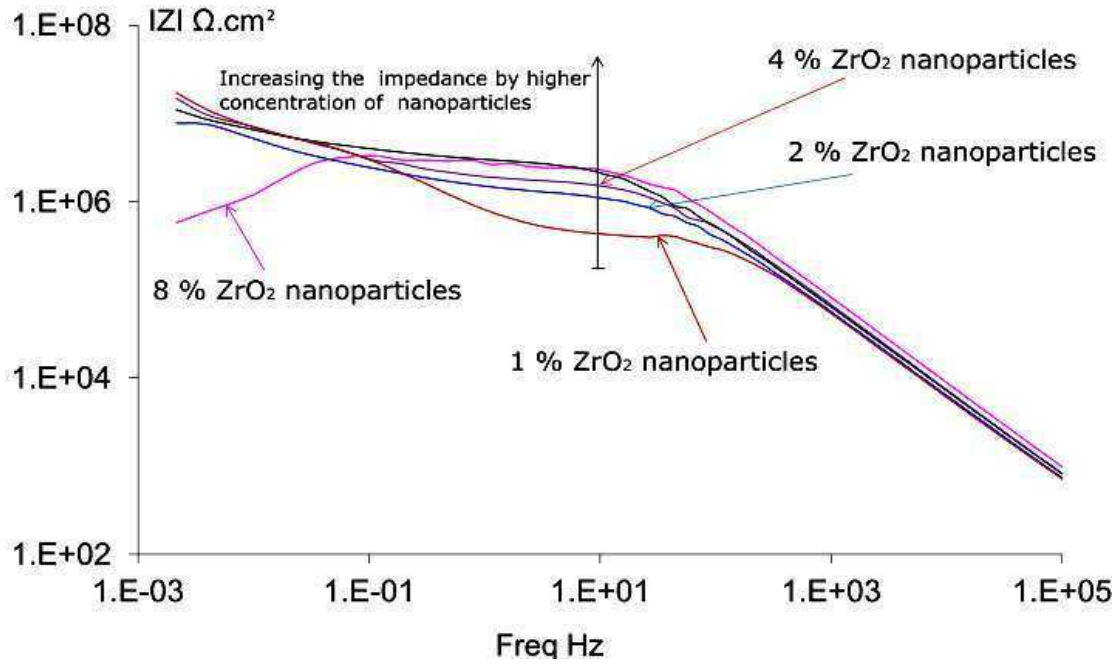

Figure 4.16: Impedance spectra of aluminium samples coated with ZrO_2 nanoparticle-doped silica films

At concentrations higher than 8 % of ZrO_2 nanoparticles, the ultrasonic treatment is not sufficient to achieve the dispersion of the nanoparticles in the water-based sol. The agglomeration of ZrO_2 nanoparticles reduces the homogeneity of the silica film as seen in Figure 4.17.

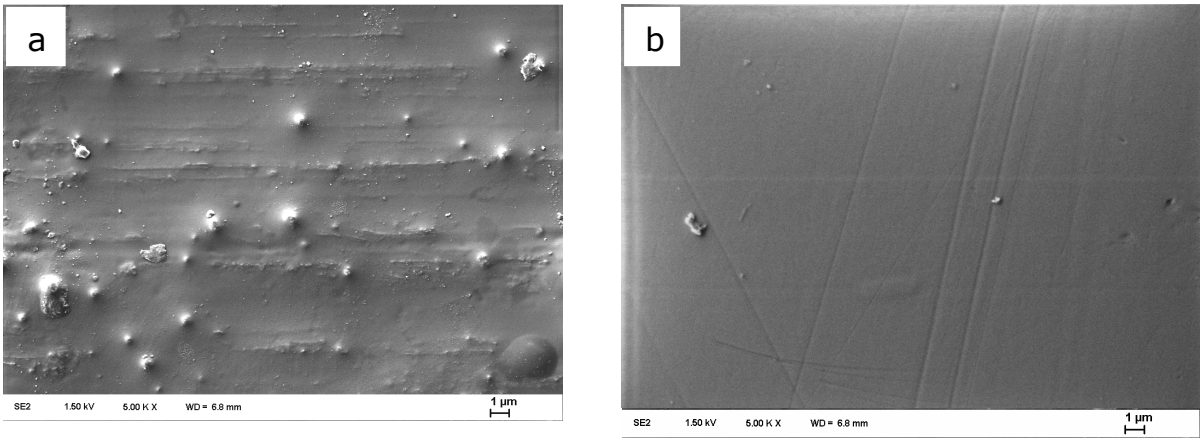

Figure 4.17: Silica film doped with ZrO_2 nanoparticles a) 8 % ZrO_2 and b) 1 % ZrO_2

The film delamination is observed for the silica films with concentrations higher than 8 % of ZrO_2 nanoparticles, the high concentrations of the nanoparticles reduce the surface of the aluminium substrate that bonds to silica film as in Figure 4.18-a. Thus, the adhesion of the silica film on the substrate is low.

Concentrations less than 8% of ZrO_2 nanoparticles are dispersed in the silica film and homogenous film is obtained as Figure 4.18-b, No coating delamination is observed.

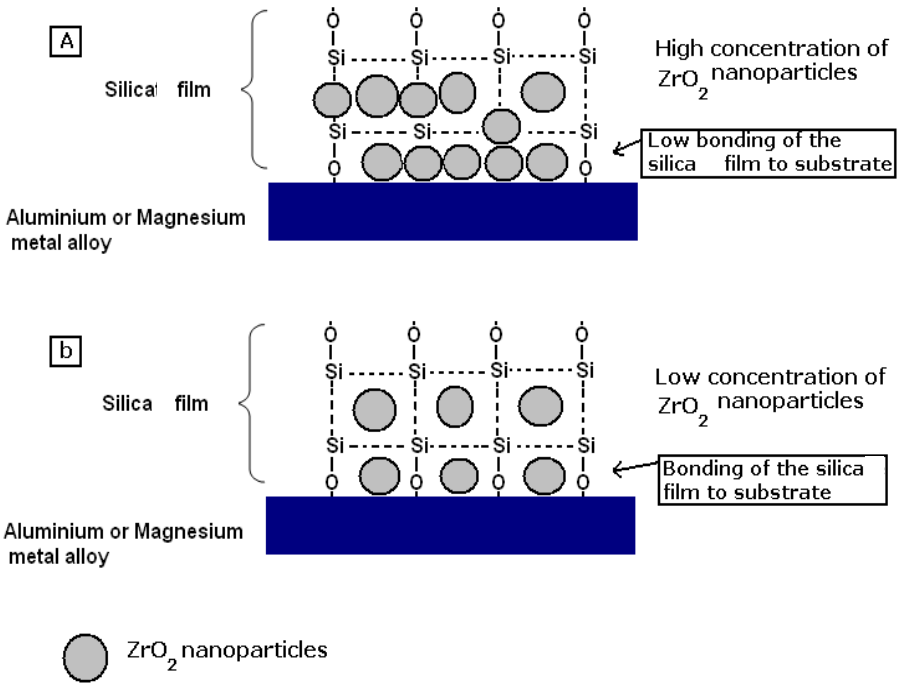

Figure 4.18: Effect of the ZrO_2 nanoparticles on the silica film, a) low concentrations of ZrO_2 nanoparticles, b) high concentrations ZrO_2 nanoparticles

It is important to indicate that the phase shift at low frequencies is reduced by higher concentrations of ZrO_2 nanoparticles (Figure 4.19). The fitting of the impedance spectra at low frequencies shows that the corrosion resistance of the double layer (R_{dl}) is increased by higher concentrations of ZrO_2 nanoparticles as in table 9. The development in the R_{dl} value can be described in the term of the accumulation of the corrosion products at the defects of the silica film, which reduces the corrosion process.

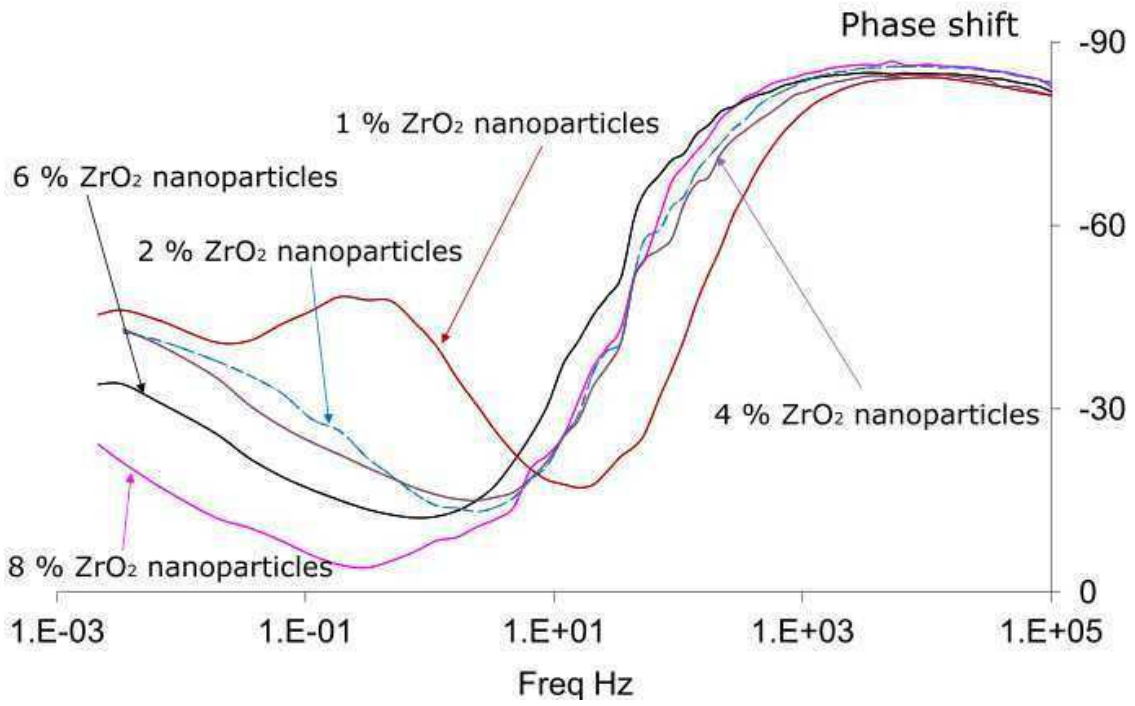

Figure 4.19: The spectra phase shift versus frequency of aluminium substrate coated with ZrO_2 nanoparticle-doped films

The conclusion can be drawn that the barrier property of the silica film is increased by higher concentrations of the ZrO_2 nanoparticles. The coating delamination is observed at concentrations higher than 8 % ZrO_2 nanoparticles. This behaviour can be explained in terms of the nanoparticles at concentrations higher than 8% reduce the surface of the aluminium substrate that bonds to silica film. Therefore, the adhesion of the silica film on the substrate is low.

4.2.2.3 Encapsulation of silicon dioxide nanoparticles

Figure 4.20 shows impedance spectra of the aluminium samples coated with SiO_2 nanoparticle-doped silica film. The phase shift of the sample with 6 % SiO_2 nanoparticles is reduced at low frequencies; this can be attributed to the accumulation of the corrosion products at the defects of the silica film.

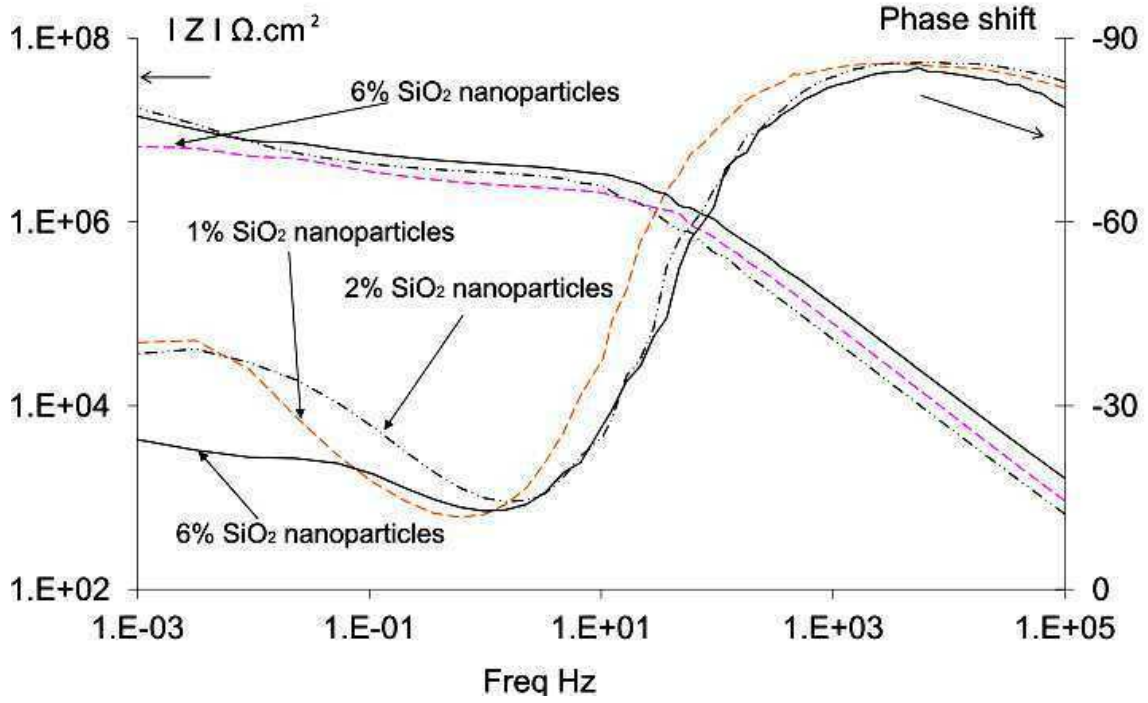

Figure 4.20: Impedance spectra of aluminium samples coated with SiO_2 nanoparticle-doped silica films

It is important to indicate that the corrosion resistance of the samples with SiO_2 nanoparticles is higher than the corrosion resistance of the samples with ZrO_2 or SiC nanoparticles. The fitting of the EIS spectra showed that the corrosion resistance of the samples with 6 % SiC nanoparticles is 8.5E5 $\Omega.cm^2$, the corrosion resistance increases 7 times to reach 2.8E6 $\Omega.cm^2$ for the samples with SiO_2 nanoparticles as in Figure 4.21. This behaviour can be explained in the term of the formation of aluminium silica passive layer at the aluminium substrate surface. This layer is attributed to the reaction of SiO_2 nanoparticles with hydroxide ions generated by the cathodic corrosion reaction to form (SiO_3^{2-}) ions as in Equation 31. [152]

$$SiO_2 + 2OH^- \rightarrow SiO_3^{2-} + H_2O \quad (31)$$

Aluminium ions at the anodic sites react with the SiO_3^{2-} to form a passive Al-silica layer at the aluminium metal surface (Equation 32) [152; 153].

$$SiO_3^{2-} + Al^{3+} \rightarrow \textit{Passive aluminium silica layer} \quad (32)$$

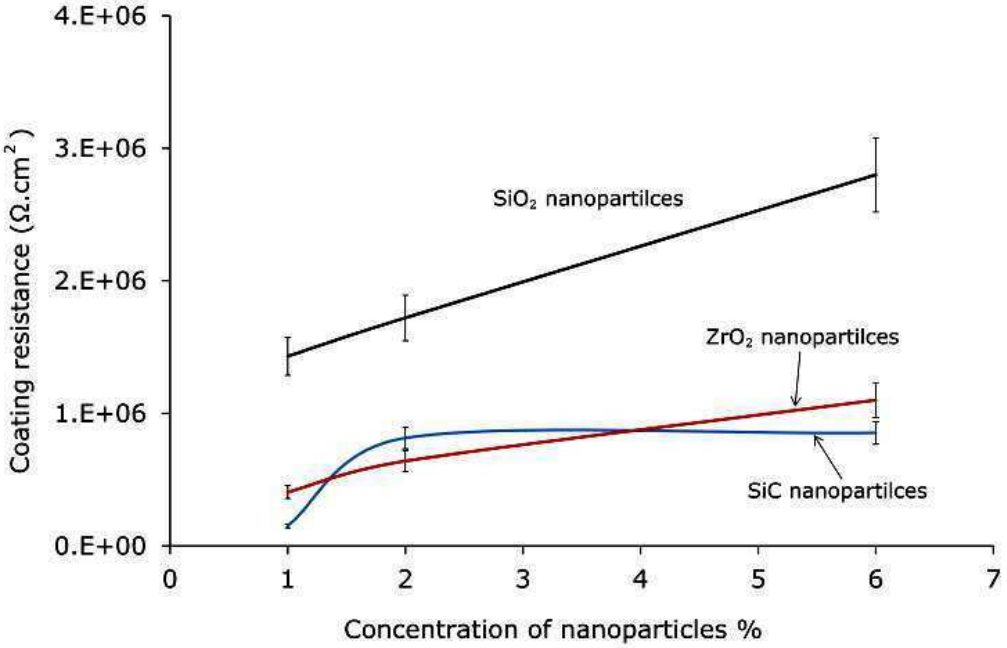

Figure 4.21: The effect of the nanoparticles on the corrosion resistance of the aluminium sample coated with silica film

The development of the passive aluminium silica layer is found also by V. Palanivel [126], this layer suppresses the corrosion reaction of the aluminium substrate coated with SiO_2 nanoparticles-doped silica film.

4.2.2.4 Crack-free silica film

Non-doped silica films with thickness of 4 micrometers were applied on the aluminium samples as in figure 4.22-a. Cracks are observed in these films (see figure 4.22-b). The cracks can be attributed to the shrinkage of the silica film which increases the in-plane tensile stress in the film. Also the different in the

thermal coefficient between the silica film and the substrates can be a reason for film-cracks.

Crack-free coating with thicknesses of 9 μm is obtained for the silica films modified by nanoparticles (Figure 4.22-c). The shrinkage in the nanoparticles-doped silica films is less than the non-doped films, which reduces the in-plane tensile stress of the film and crack-free silica film is formed. This result is observed for the three kinds of the nanoparticles tested in this work, SiO_2; SiC and ZrO_2.

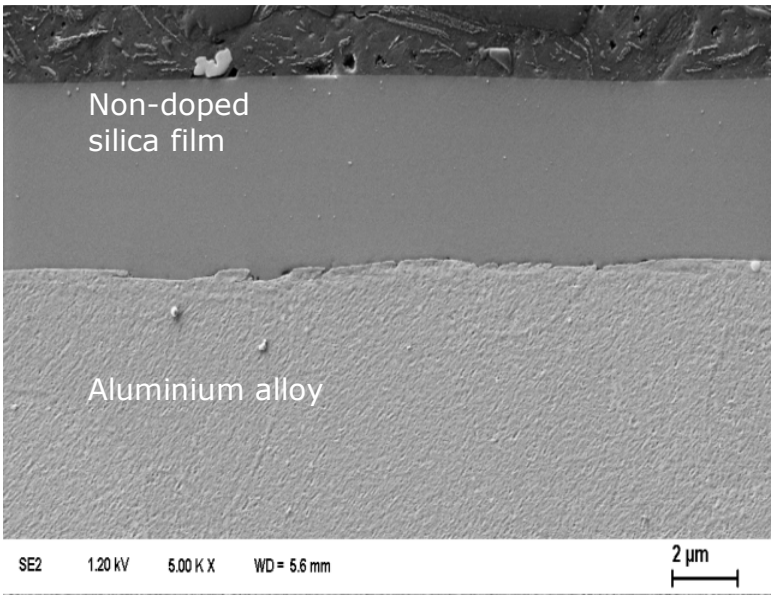

(a)

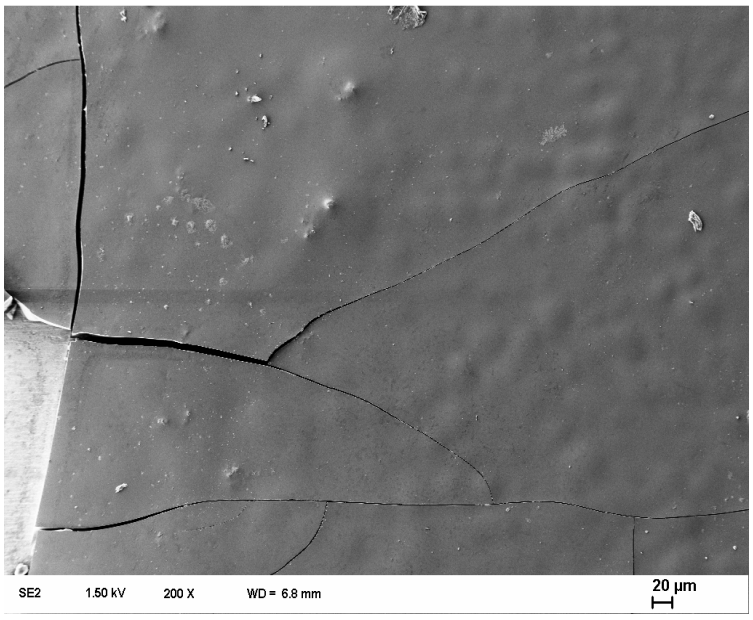

(b)

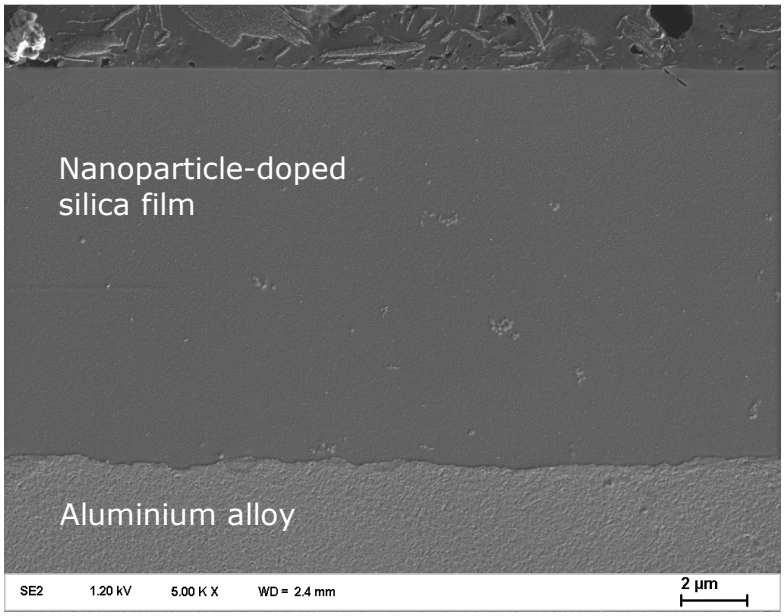

(c)

Figure 4.22: SEM for silica film on aluminium substrate, a) cross-section of the non-doped film; b) cracks in the non-doped film; c) cross-section of the 2 % SiO_2 nanoparticles-doped film

The conclusion can be drawn that the thickness and barrier properties are increased for the silica films modified by nanoparticles, which leads to the decreasing in the cracks of the silica film. The coating delamination is observed for the samples with nanoparticles at concentrations higher than 8 %. The high concentrations of nanoparticles reduce the surface of the aluminium substrate that bonds to silica film, and low-adherence film is formed. This behaviour is observed for SiO_2; ZrO_2 and SiC nanoparticles-doped silica film.

The samples with SiO_2 nanoparticles showed better corrosion resistance than the samples with ZrO_2 or SiC, it can be related to the formation of the aluminium silica layer at the aluminium substrate surface which suppresses the corrosion reaction.

4.2.3 Self-healing characteristics

Self-healing is an important aspect to improve the stability of aluminium and magnesium samples in corrosive solution. The easiest way to prepare inhibitor-doped silica film is the simple mixing of the corrosion inhibitors with the water-based sol. The silica film acts as a reservoir of corrosion inhibitors. When a defect appears in the corrosion inhibitors-doped silica film, the corrosion inhibitors leach out of the coating to the defect area under the capillary forces [135]. A layer of the corrosion inhibitors forms on the aluminium or magnesium substrate at the defect area.

In order to evaluate the self-healing, it is always important to consider the size of the defect in the silica film. A defect width of 50 μm in the silica film is determined by Shchukin to study the self-healing of the aluminium substrate coated with corrosion inhibitors-doped silica film [154]. Lamaka prepared a defect with size of 50X50 μm^2 in the corrosion inhibitors-doped silica film to generate the self-healing [155]. An artificial defect with width of 5 μm is used by Trenado to evaluate the self-healing of the aluminum sample coated with cerium nitrate-doped silica film. [156].

Benthem reported on the relation between the defect size and the description of the defect. The micro-scale defects are associated with the bond breakage; the crack in the film reaches the aluminium substrate, while the macro-scale defect leads to rupture and delamination of the film at the defect area as seen in Figure 4.23. [131]

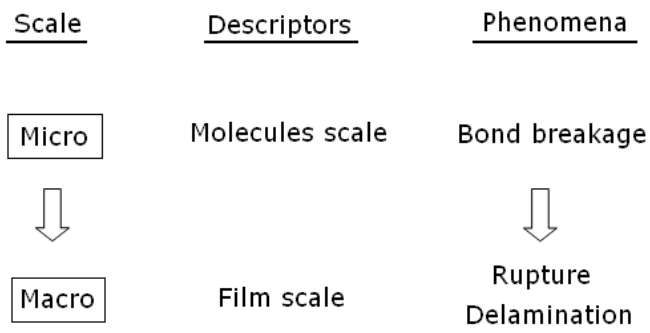

Figure 4.23: The scale of the defect in thin films [131]

The recovery of the macro-scale defect can be achieved by de-lamination of the film, a new silica film need to be applied at the defect area. The corrosion inhibitors in the thin film are able to recover the macro-scale defect, but high concentrations of the corrosion inhibitors as a dopant is needed which reduces the barrier property of the silica film [140; 141]. The micro-scale defect is recovered by the layer of the corrosion inhibitors formed in the defect area. [131]

In this chapter, the corrosion inhibitors and SiO_2 nanoparticles-doped silica film was deposited on the aluminium 6082-T6 substrates. The coated samples were defected to generate the self-healing. The size of the defect is chosen to be 10.000 X 150 μm^2 which is 600 times bigger than the defect of 50 X 50 μm^2 used by other literatures [154; 155]. The aim is to test the ability of the coating system to heal the defect of macro-size which is an advantage in this work. The defect in the samples was characterised before and after the healing process. Electrochemical impedance spectroscopy (EIS) was used to evaluate the protection performance, the EIS spectra were fitted with the appropriate equivalent circuit for better understanding of the self-healing. The healing qualification was estimated by monitoring the defect surface profile using a contact stylus instrument. The scanning electron microscope (SEM) LEO 1455VP was used to characterise the layer formed in the defect after the healing process.

4.2.3.1 Selection of the corrosion inhibitors

The corrosion inhibitors were selected in this work according to the effectiveness and the solubility in aqueous media. The effect of a mixture of corrosion inhibitors on the self-healing ability was also studied.

The effectiveness of the corrosion inhibitors, the corrosion inhibitors are added to the silica film to act as anodic or cathodic inhibitors. The anodic inhibitors are implemented to reduce the anodic corrosion reaction. The cathodic inhibitors are added to block the cathodic corrosion sites.

The corrosion inhibitors tested in this work can be seen in the table 4, the most effective corrosion inhibitors are:

- Cerium nitrate is added to the water-based sol as a cathodic corrosion inhibitor. When a defect occurs in the silica film, cerium ions leach out from the film to defect area, cerium oxide is formed by the reaction of cerium ions with the hydroxide ions (see equations 33; 34). [157]

Cathodic corrosion reaction $$O_2 + 2H_2O + 4e^- \rightarrow 4OH^- \quad (33)$$

Formation of cerium oxide at the cathodic sites
$$Ce^{3+} + 3OH^- \rightarrow Ce(OH)_3$$
$$2Ce(OH)_3 \rightarrow Ce_2O_3.3H_2O \downarrow \quad (34)$$

Cerium oxide has low solubility in aqueous media; it precipitates at the cathode area which blocks the cathodic sites. Therefore, cerium nitrate is used in this work to act as a cathodic inhibitor.

- Benzotriazole (BTAH) is added to the water-based sol as an anodic corrosion inhibitor. Literatures proposed that the inhibition mechanism of the BTAH is related to the adsorption of BTAH on the aluminium substrate surface to form a layer of $[BTA]_{ads}$:Al. [158]

  The adsorption of BTAH can be explained by the removal of hydrogen from the nitrogen atom of benzotriazole to form BTA^-. BTA^- links to the aluminium ions to form $[BTA]_{ads}$:Al at the substrate surface. Therefore, benzotriazole is added as an anodic corrosion inhibitor. [159]

When one kind of corrosion inhibitor is added to the silica film, the amount of the corrosion inhibitor leaches out of the silica film to the defect area is limited by the solubility of this inhibitor in the corrosive aqueous media, which leads to low concentrations of the corrosion inhibitor in the defect area and low self-healing ability.

Mixture of corrosion inhibitors-doped silica film: a mixture of corrosion inhibitors were added to the silica film in this work, the aim is to enhance the concentration of the corrosion inhibitors in the defect area for better self-healing ability. Figure 4.24 shows comparison between EIS spectra of aluminium sample coated with cerium nitrate-doped silica film and EIS spectra of aluminium sample coated with

(cerium nitrate and benzotriazole)-doped silica film. The sample was defected to generate the self-healing. It is clear that the sample with mixture of corrosion inhibitors show better corrosion protection than the sample with one kind of corrosion inhibitor. The development in the corrosion protection can be explained in terms of the mixture of the corrosion inhibitors-doped silica film enhances the barrier property of the corrosion inhibitors layer in the defect area of the sample. Therefore, mixture of cerium nitrate and benzotriazole-doped silica film is used in this work for better self-healing ability.

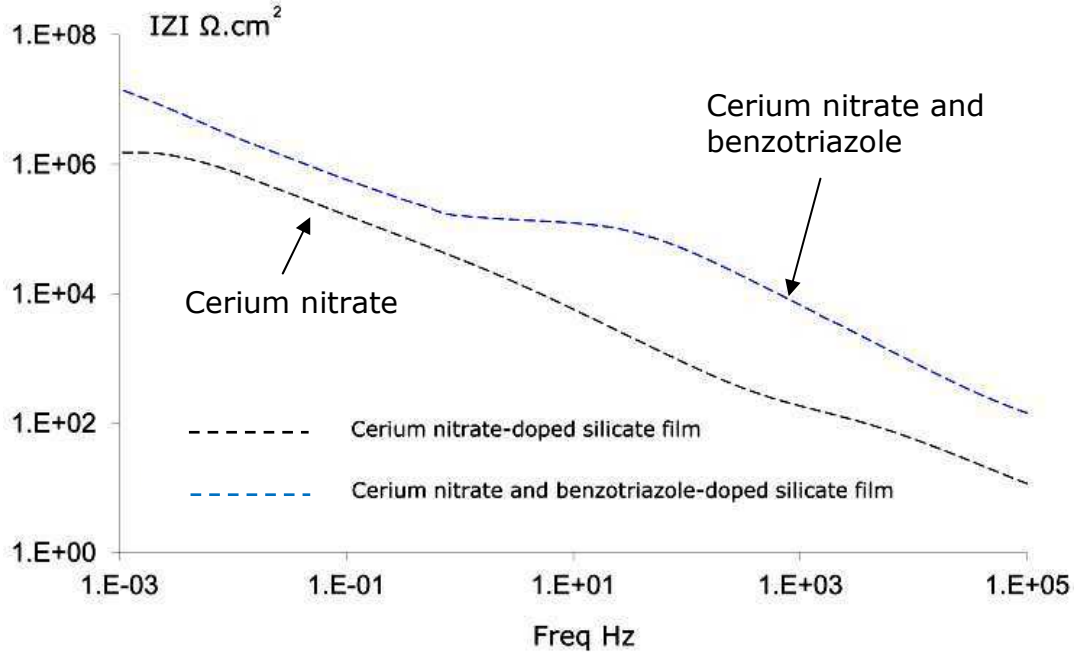

Figure 4.24: Effect of a mixture of corrosion inhibitors on the corrosion protection

The solubility of the corrosion inhibitors

The self-healing is achieved in this work by using organic and inorganic corrosion inhibitors. Cerium nitrate is added as an inorganic inhibitor, the solubility of cerium nitrate in water is 234 g/ 100 ml, benzotriazole is incorporated in the silica film as an organic inhibitor, and the solubility of benzotriazole in water is 20 g/ 100 ml.

When a defect appears in the (cerium nitrate and benzotriazole)-doped silica film, the corrosive aqueous media penetrates in the structure of the silica film. Cerium nitrate has higher solubility in aqueous media than benzotriazole, cerium

ions leaches out of the film under the capillary forces to form the corrosion inhibitors layer in the defect. However, due to the low solubility of benzotriazole in aqueous media, benzotriazole leaches out of the silica film under the capillary forces at low concentration. This ensures two important points:

1- Improvement of the barrier property of the corrosion inhibitors layer in the defect due to leach of the benzotriazole out of the silica film to the defect area.

2- reducing the quick lack of corrosion inhibitor (benzotriazole) from the silica film due to the low solubility of this inhibitor in aqueous media. Hence, benzotriazole leaches out of the film in low concentrations.

The conclusion can be drawn that the both aspects self-healing ability and reducing the lack of corrosion inhibitors can be achieved by improving the barrier property of the corrosion inhibitor layer in the defect of the sample. This point will be proven in this chapter by means of the healing efficiency of the sample.

The protection efficiency of each corrosion inhibitor is tested in this work, and then a mixture of the effective corrosion inhibitors is incorporated in the silica film to evaluate the self-healing of the coated aluminium samples.

Effect of cerium nitrate $Ce(NO_3)_3$

Cerium nitrate $Ce(NO_3)_2$ was added to the silica film as a cathodic corrosion inhibitor, different concentrations of cerium nitrate were tested 0.1 – 20 g/l. Figure 4.25 demonstrated that the impedance response of the aluminium sample 6082-T6 coated with cerium nitrate-doped silica film. It is obvious that the cerium nitrate has strongly improved the corrosion protection. The corrosion protection was enhanced by higher concentrations of cerium nitrate. The best corrosion protection was measured for the samples with 20 g/ l cerium nitrate.

It can be concluded that cerium nitrate improves the corrosion protection of the sample at all studied concentrations; and cerium nitrate has no negative effects on the barrier properties of the silica film.

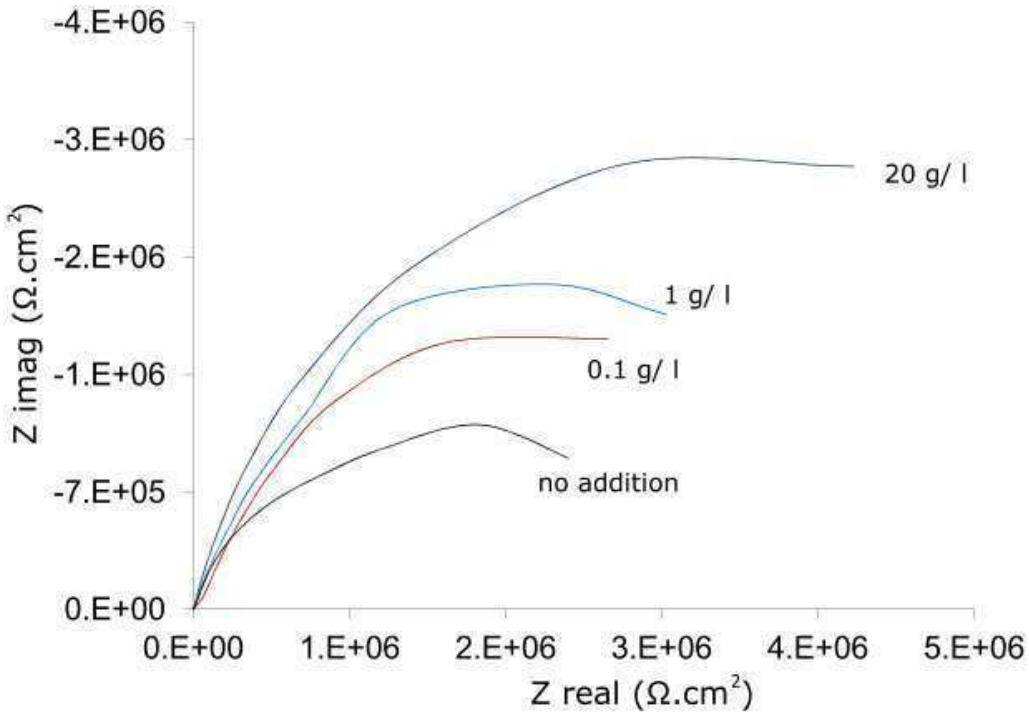

Figure 4.25: EIS spectra as a Nyquist plot for aluminium substrate coated with cerium nitrate-doped silica film

Effect of 1, 2, 3-benzotriazole

1, 2, 3-benzotriazole was used as an anodic corrosion inhibitor at concentrations of 0.5, 1 and 2 g /l. The amount of the benzotriazole in the water-based sol is limited by the solubility of this inhibitor. For 1 g /l benzotriazole, the amount was dissolved in the water-based sol and homogenous silica film was formed. At concentrations of 2 g/l benzotriazole, the solubility limit of the corrosion inhibitor is exceeded, the barrier property of the silica film is reduced. This can be explained in the terms of the strong influence of benzotriazole on the hydrolysis/polymerization processes during the coating preparation [140].

Figure 4.26 illustrates the effect of benzotriazole concentrations on the protection efficiency. The corrosion resistance of the aluminium samples coated with benzotriazole-doped silica film is improved with additions of more than 0.5 g/l. The best corrosion protection was obtained at 1 g/l benzotriazole.

The conclusion can be drawn that benzotriazole at concentrations more than 1 g/l reduces the barrier property of the silica film. Therefore, benzotriazole is added to the water-based sol at concentration 1 g/l.

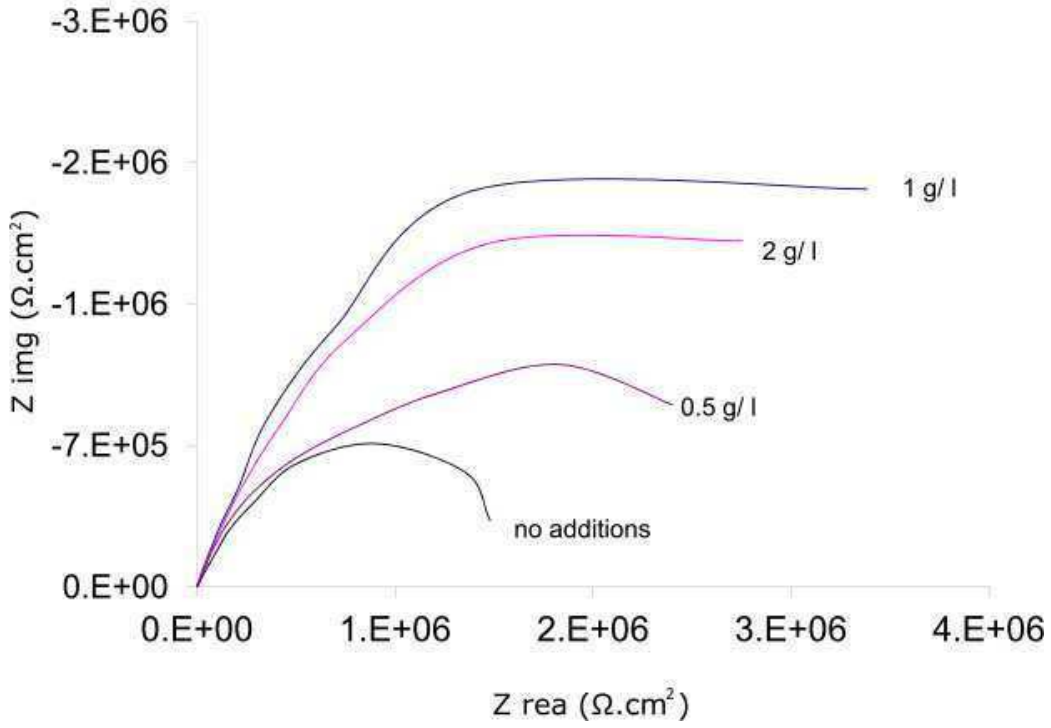

Figure 4.26: Nyquist plot of aluminium samples coated with benzotriazole-doped silica film

4.2.3.2 Electrochemical characterisation of the self-healing effect

The aluminium samples coated with silica film were defected to generate the self-healing. The defect size was (10.000 x 150) μm^2. The electrochemical characterisation of the self-healing was carried out after a specific immersion period of the defected samples in 0.5 M NaCl, the immersion periods of the samples were 48; 96; 192 until 700 hours.

The silica film is made up of three different regions. They are from outside to inside, the crosslinked silica film with the Si-O-Si bonds, interfacial layer dominant with Si-O-Al and Si-O-Si bonds, inner layer of Al oxide on the aluminium alloy substrate as discussed before in Figure 4.14.

After an immersion period of 96 hours of the aluminium samples coated with the 2 % SiO_2 nanoparticles-doped film, the corrosive electrolyte causes the growth of the original defects in the coating. This opens pathways for the corrosive solution toward the aluminium surface. An active corrosion process occurs and an

apparent drop in the total impedance value can be seen after 196 hours as in figure 4.27-a

Figure 4.27-b shows EIS spectra of frequency versus phase shift. The three regions of the silica film are clearly seen. After an immersion period of 196 hours, time constant (TC1) at high frequencies is appeared, this can be attributed to the degradation in the barrier property of the silica film due to the corrosion process. The time constant (TC2) is shown at frequencies less than 10^3 Hz which relates to the degradation in the structure of the interfacial layer of the silica film, especially for Al-O-Si bonds due to the corrosion process. Time constant (TC3) is presented at low frequencies; it demonstrates the corrosion products formed at the aluminium surface.

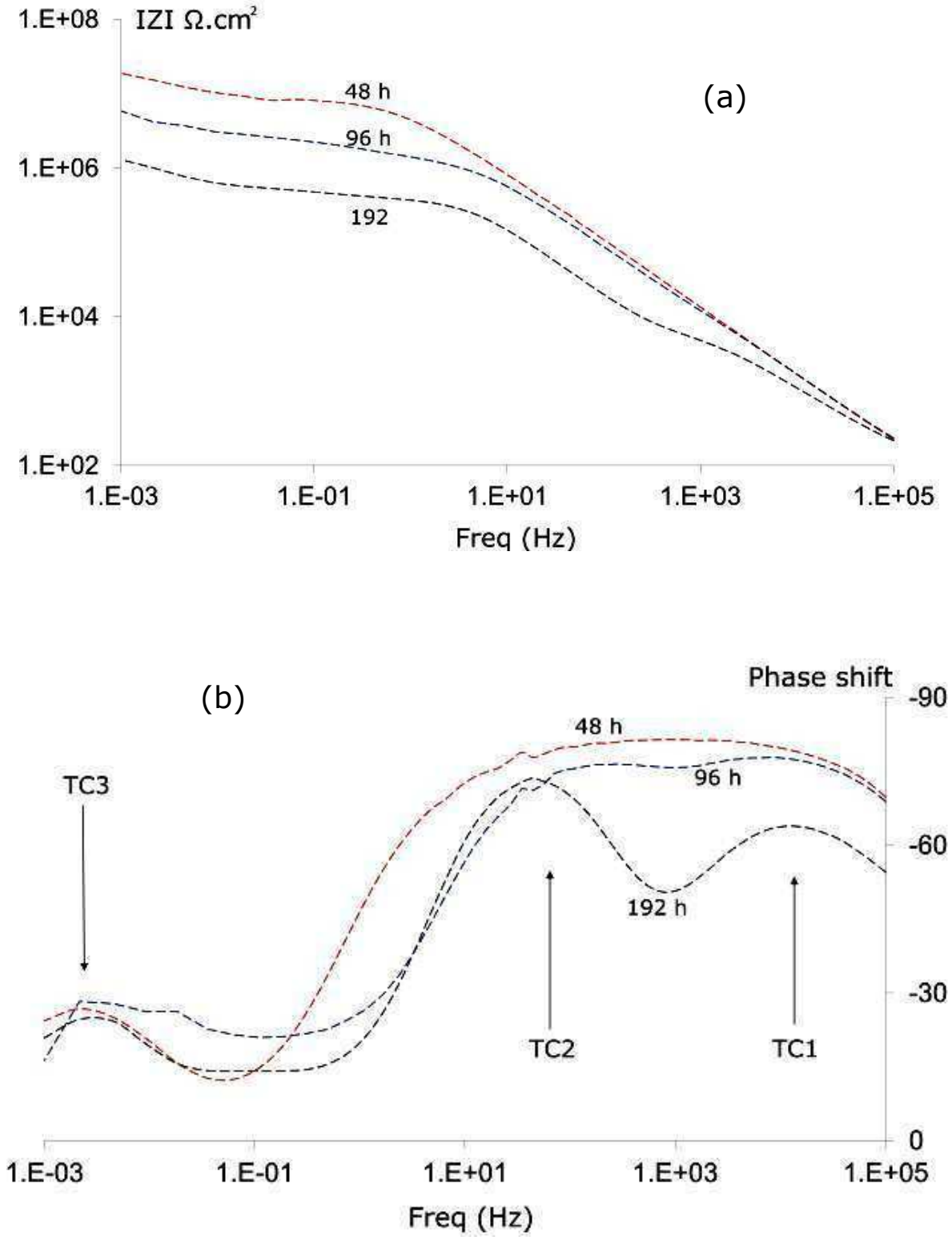

Figure 4.27: Impedance spectra as a Bode plot to evaluate the self-healing of aluminium 6082-T6 coated with 2 % SiO_2 nanoparticles-doped film after different immersion periods in chloride solution. spectra (a) describes the development in the impedance value, spectra (b) shows the development in value of phase shift

Different corrosion inhibitors at varying concentrations were used in this work. The best corrosion protection was obtained for samples with cerium nitrate and benzotriazole at concentrations of 20 g/l and 1 g/l respectively. Figure 4.28 demonstrates the EIS spectra of the aluminium substrates coated with the 2 % SiO_2 nanoparticles and corrosion inhibitors-doped silica film. The samples showed better stability in chloride solution than the samples without corrosion inhibitors.
Due to the defect in the corrosion inhibitors-doped film, the impedance value at high is decreased after an immersion period of 196 hours (Figure 4.28-a). The corrosion inhibitors leach out of the silica film to defect area. The corrosion inhibitor layer is formed in the defect which keeps the impedance of the coated aluminium sample stable during the immersion period.
The time constant TC2 (Figure (4.28–b)) demonstrates the development of the corrosion inhibitors layer in the defect of the sample. It is clear that the TC2 appears after an immersion period of 96 hours. TC2 is shifted to lower frequencies after immersion period of 192 hours which refers to the development in the corrosion inhibitors layer during the immersion period in chloride solution. It is important to indicate that the phase shift value of the TC2 is increased during the immersion period; this can be explained by the development of the barrier property of the corrosion inhibitor layer in the defect due to the leaching of the corrosion inhibitor out of the silica film to the defect area.

The conclusion can be drawn that a layer of corrosion inhibitors is formed in the defect area of the aluminium sample coated with corrosion inhibitors-doped silica film. The barrier property of the corrosion inhibitors layer is developed during the immersion period in chloride solution. This behaviour is attributed to the leachability of the corrosion inhibitors out of the silica film to the defect area, which keeps the impedance of the sample stable during the immersion period in chloride solution.

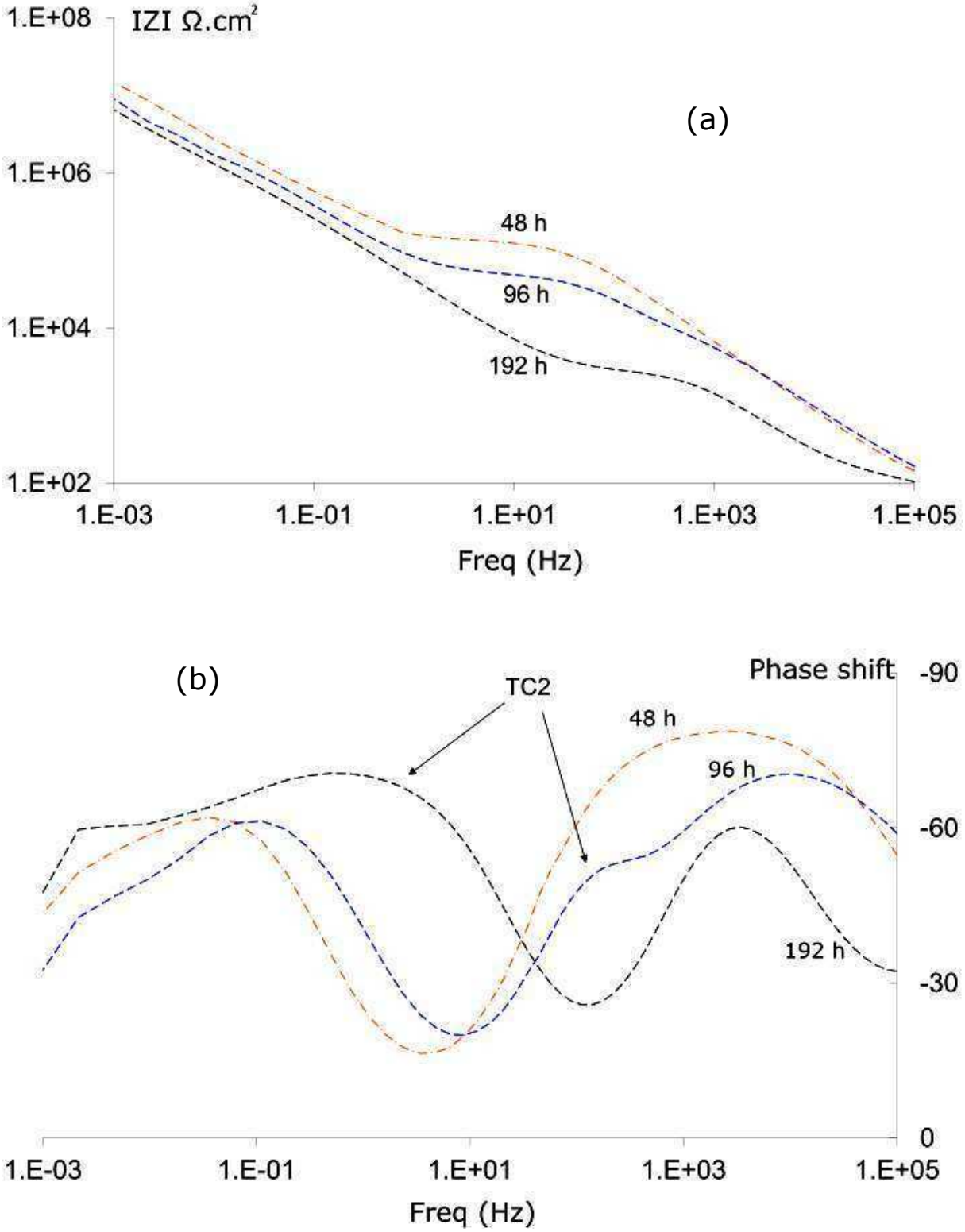

Figure 4.28: Impedance spectra as a bode plot to evaluate the self-healing of aluminium 6082-T6 coated with 2 % SiO_2 nanoparticles and inhibitor-doped silica film after different immersion periods in chloride solution. spectra (a) describes the development in the impedance value and spectra (b) shows the development in the value of the phase shift

The long-term stability of coated aluminium sample in corrosive solution is proven in this work by means of healing efficiency. The healing efficiency (η) is calculated from the equation 36. [160]

$$\eta = \frac{R_{Healed}}{R_{Virgin}} \times 100 \tag{36}$$

Where R_{Healed}, R_{Virgin} are the coating resistance of the defected sample and the corrosion resistance of the undefected sample respectively. The values of R_{Healed} and R_{Virgin} are obtained by the fitting of the EIS spectra with suitable electrical circuit (table 11).

Figure 4.29 presents the healing efficiency of the coated aluminium samples at different immersion periods. It is clear that the samples with corrosion inhibitors demonstrate higher healing efficiency than the samples without corrosion inhibitors. After immersion period of 96 hours, the healing efficiency of aluminium sample with corrosion inhibitors is 11.2 %, while the sample without corrosion inhibitors has healing efficiency of 2.8 %.

The healing efficiency of the samples with corrosion inhibitors is nearly stable during the immersion periods between 96 and 700 hours as in Figure 4.29, this behaviour is attributed to the development of the barrier property of the corrosion inhibitors layer in the defect, which is attributed to the leachability of the corrosion inhibitors out of the film to the defect area.

The conclusion can be drawn that the development of barrier property of the corrosion inhibitors layer in the defect of the sample reduces the penetration of the corrosive solution to the 1) defect area and 2) into the structure of the silica film. This behaviour ensures 1) development in the corrosion resistance of the layer in the defect for long-term corrosion protection and 2) decreasing the amount of the corrosion inhibitors leach out of the silica film to the defect area under the capillary forces which hinders the quick lack of corrosion inhibitors.

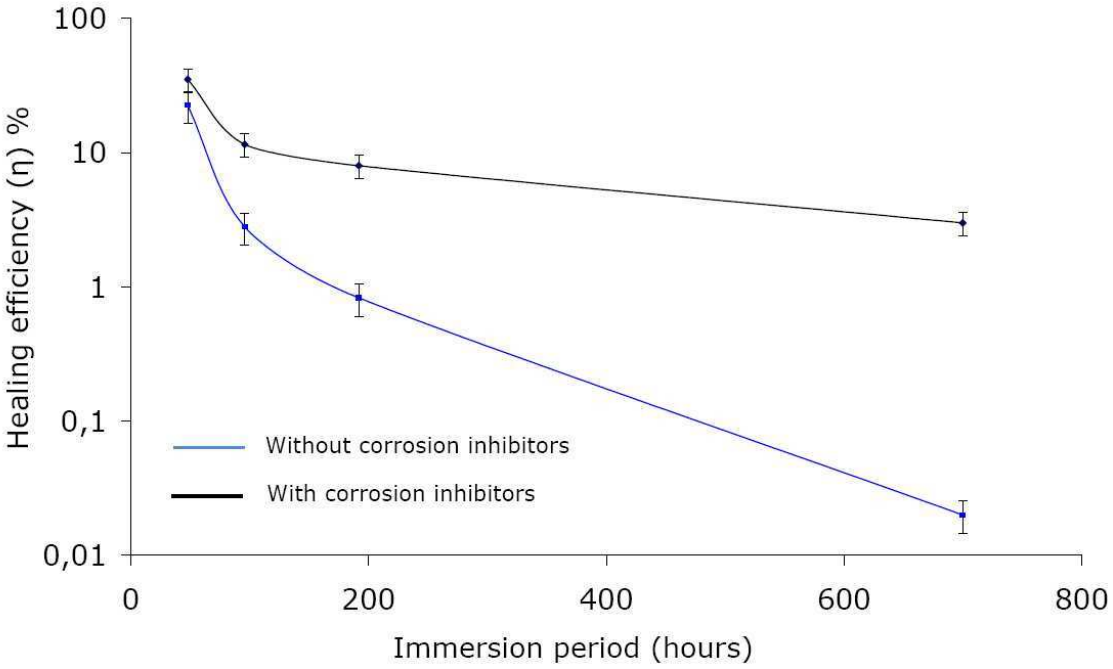

Figure 4.29: Effect of the corrosion inhibitors on the healing efficiency of aluminium sample coated with silica film

4.2.3.3 Characterisation of the defect surface profile

The defect of the silica films was qualitatively studied by SEM investigations. The surface profile exploration showed that the defect before the healing process was quite rough; cracks at the defect edges can be distinguished (Figure 4.30-a). After an immersion period of 700 hours in chloride solution, full recovery of the defect surface was obtained for the samples coated with 2 % SiO_2 nanoparticles and corrosion inhibitors-doped film. A layer was formed in the defect and on the cracks at the defect edges (Figure 4.30-b). The samples coated with the 2 % SiO_2 nanoparticles-doped silica film were destroyed and pitting corrosion was observed as in Figure 4.30-c.

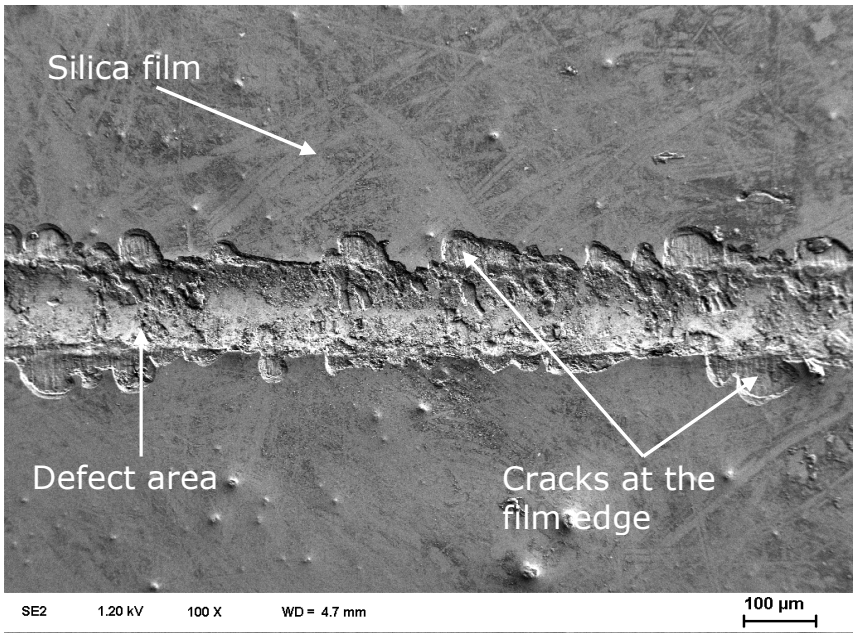
Silica film
Defect area
Cracks at the film edge
SE2 1.20 kV 100 X WD = 4.7 mm
100 µm

(a)

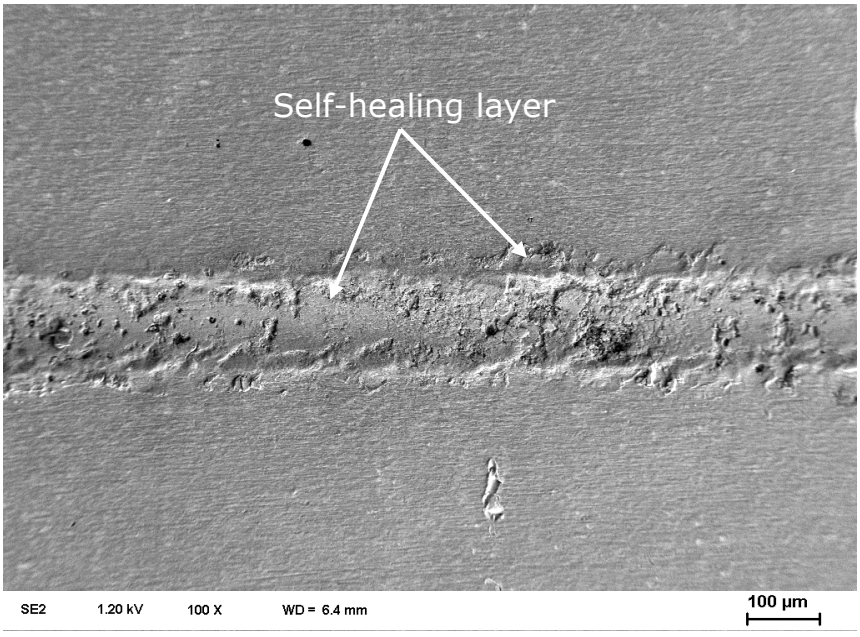
Self-healing layer
SE2 1.20 kV 100 X WD = 6.4 mm
100 µm

(b)

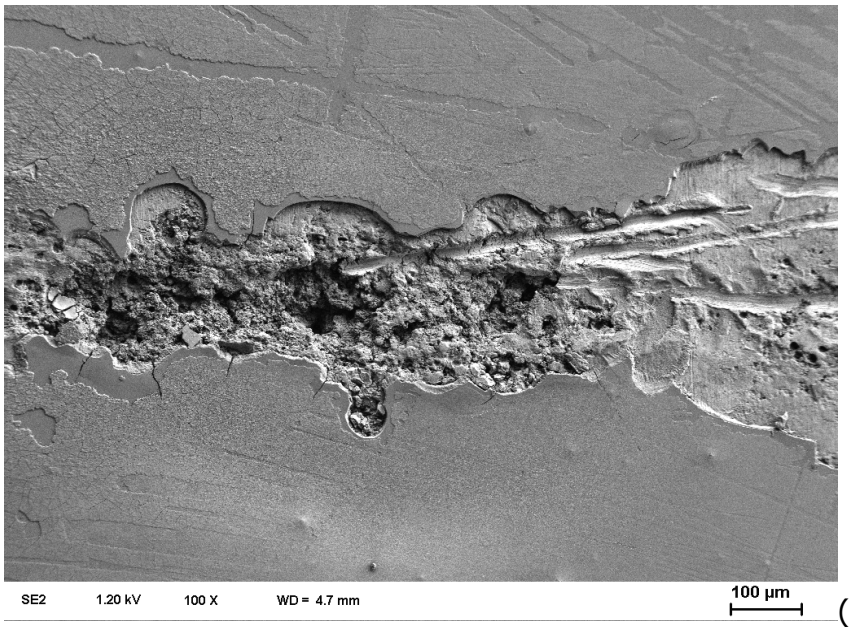

(c)

Figure 4.30: SEM images of the defects: a) sample coated with 2 % SiO_2 nanoparticles and inhibitors-doped film before the test; b) after 700 h immersion in NaCl solution; c) sample coated with non-doped film after 700 h in NaCl

The defect surface profile by means of the contact stylus instrument was carried out to characterise the precipitated materials in the defect as a criterion for the healing quality of the samples. Figure 4.31 shows the surface profile of the different defects. After the immersion test, the defect in the samples coated with the 2 % SiO_2 nanoparticles and inhibitors-doped film is smaller than the defect in the untested sample. The reduction in the defect depth and width confirms the precipitation of the corrosion inhibitors through the self-healing process. The aluminium samples coated with the 2 % SiO_2 nanoparticles-doped film have the biggest defect dimensions after the corrosion test because of the intensive corrosion process in the defect area; this corroborates the results observed by the electrochemical measurements and SEM investigations.

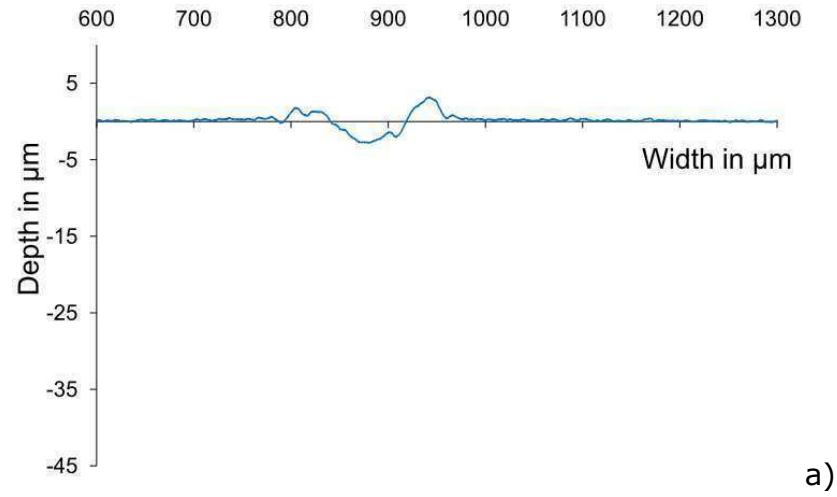

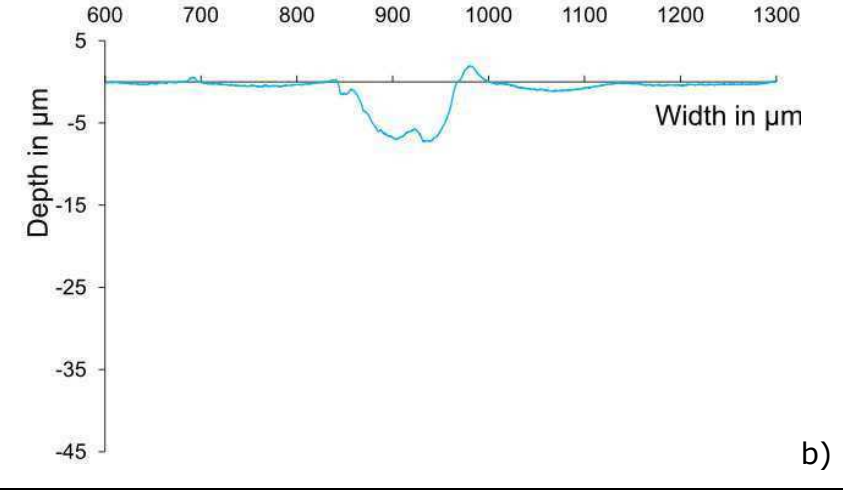

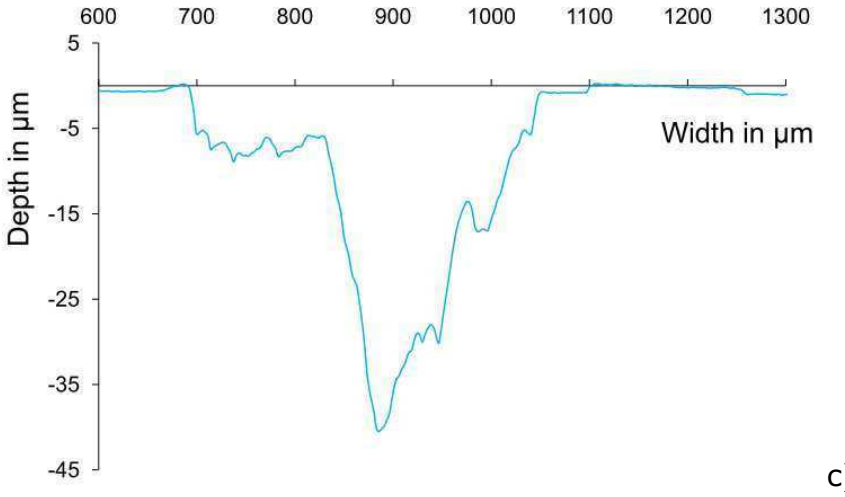

Figure 4.31: Surface profile of different defectes: a) sample coated with 2 % SiO_2 nanoparticles and corrosion inhibitors-doped film before the test and b) after 700 h immersion in NaCl solution; c) sample coated with non-doped film after 700 h immersion in NaCl solution

4.2.4 Fitting of the electrochemical impedance spectroscopy spectra

The electrochemical impedance spectroscopy (EIS) is used in this work as a useful techniques for better understanding of the following points:

1- The electrochemical characterization of the coated aluminium and magnesium samples. The silica film is made up of thee regions as discussed in before in nanoparticles-doped silica film, the development of the corrosion protection of each region needs to be clarified for better understanding of the corrosion process,

2- investigation of the reactions mechanisms of aluminium silica layer for aluminium sample coated with SiO_2 nanoparticles-doped silica film,

3- evaluation the development of the self-healing property of the coated sample, fitting of the EIS spectra is needed to measure the corrosion resistance of the self-healing layer in the defect of the silica film.

4- estimation of the healing efficiency which is needed to investigate the long-term corrosion protection,

5- The electrochemical impedance spectroscopy is non-destructive method; a small amplitude AC signal is applied without significantly disturbing the properties being measured.

The electrochemical impedance spectroscopy experiments are usually run under potentiostate mode. The potentiostate is maintained the required DC potential to the corrosion cell, while the instrument measures the impedance for a range of frequency. The EIS tests are carried out at the open circuit potential (OCP) of the electrochemical cell, the voltage of the OCP is held on the cell while the impedance tests progresses.

Different methods are available to study the corrosion protection such as cyclic voltammetric and salt spray tests. These methods are destructive and destroy the studied sample. The unique advantage of the impedance technique is to evaluate the protection performance of the coating in non-destructive manner. The spectra measured via impedance technique are modelled by an appropriate equivalent circuit. The fitting of the spectra is carried out by available commercial

software. Detailed information about the protection performance, the porosity and the adhesion of the coating to the metal substrate can be obtained from the fitted spectra. [148]

The development in the corrosion protection of the aluminium or magnesium samples coated with silica film can be read roughly from EIS spectra, the fitting of the EIS spectra is carried out in this work for the following reasons:

1- Silica film made up of thee regions, fitting of the EIS spectra is needed to evaluate the corrosion resistance of each layer which is helpful for better understanding of the corrosion process,

2- investigation of the formation of aluminium silica passive layer, fitting of EIS spectra is required to estimate the effect of this layer on the corrosion protection of the sample,

3- calculation of the healing efficiency is required to examine the long-term corrosion protection of the aluminium or magnesium samples coated with corrosion inhibitors-doped silica film,

4- Fitting of the EIS spectra is important to estimate the development in the barrier property of the corrosion inhibitors layer in the defect of the aluminium or magnesium sample coated with corrosion inhibitors-doped silica film,

5- Studying the effect of the corrosion products beneath the silica film on the corrosion protection leads to better understanding through the fitting of the EIS spectra, as discussed before in the ZrO_2 nanoparticles-doped silica film,

Several equivalent electrical circuits were constructed for the fitting of EIS spectra. Information about the studied coating system such as porosity, single or multilayer is needed to draw the suitable equivalent circuit model. Figure 4.32 exhibits the equivalent electrical circuits which used in this work to model the impedance spectra. The model (A) is usually used for uncoated metal substrate; it is also useful for the substrate coated with high protective films.

When cracks and defects appear in the film, the fitting of the coating system is carried out by the model (B). The corrosive solution penetrates in the defect of the film, and two layers can be detected by the impedance spectra; one is double layer at the metal surface which in contact with the corrosive solution in the

defects area; the second layer is the coating layer. It is clear that the equivalent circuit model consists of the coating capacitance C_c in parallel with the coating resistance R_c, the values C_c and R_c are useful to measure the barrier properties of the film. The model (B) also consists of the double layer capacitance C_{dl} is in parallel with the double layer resistance R_{dl} which gives information about the electrochemical reactions at the metal surface, the solution resistance R_s refers to the resistance of the corrosive solution. An interfacial layer is seen in this work by the samples coated with nanoparticles-doped silica film, interfacial layer dominants with Si-O-Al and Si-O-Si bonds. The capacitance of the interfacial layer C_{int} is parallel to the resistance of the interfacial layer R_{int} as in Figure 4.32-c. The components in the Cc and Rc are related to the silica film, while Cdl and Rdl refer to the double layer at the metal surface. [147]

The constant phase element CPE is commonly used in the fitting of the impedance spectra. CPE is a frequency dependence value as in equation 37. The capacitor in EIS experiments often do not behave ideally because of surface roughness, varying in the thickness or the composition of the coating. Therefore, the CPE is used instead of the perfect capacitor. [146]

$$Z_{CPE} = \frac{1}{T(j\omega)^n} \qquad (37)$$

Z_{CPE} Impedance of constant phase element

T Constant

$j = \sqrt{-1}$ Imaginary part

$\omega = 2\pi f$ Radial frequency in radian/second

f Frequency in Hertz

The EIS spectra of the self-healing tests were successfully fitted by the equivalent circuit in Figure 4.32-d, the corrosion resistance of the layer formed in the scratch R_{sc} was used to evaluate the self-healing of the sample.
Figure 4.33 exhibits some examples of the fitted impedance spectra. It is evident that the EIS spectra in this work fit very well with low error.

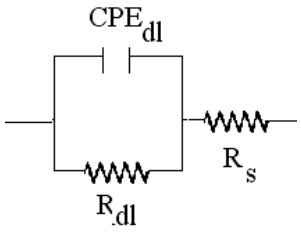

(a)

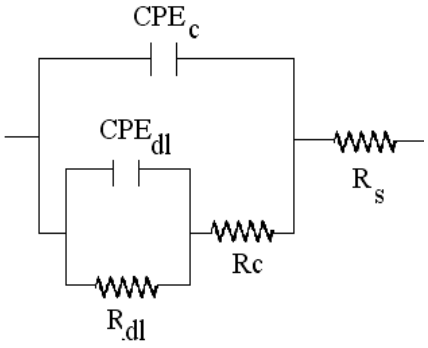

(b)

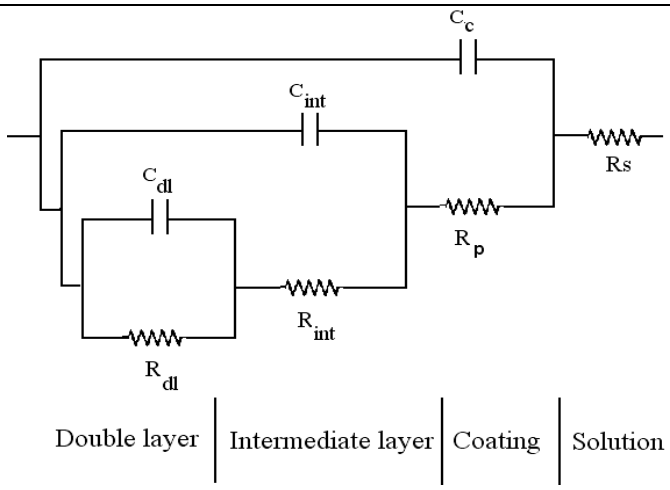

(c)

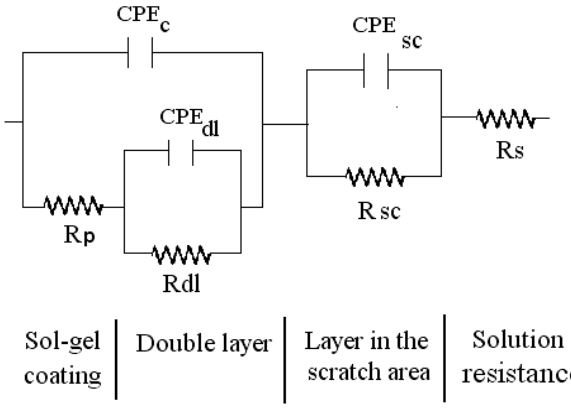

(d)

Figure 4.32: The equivalent circuits for the fitting of EIS spectra

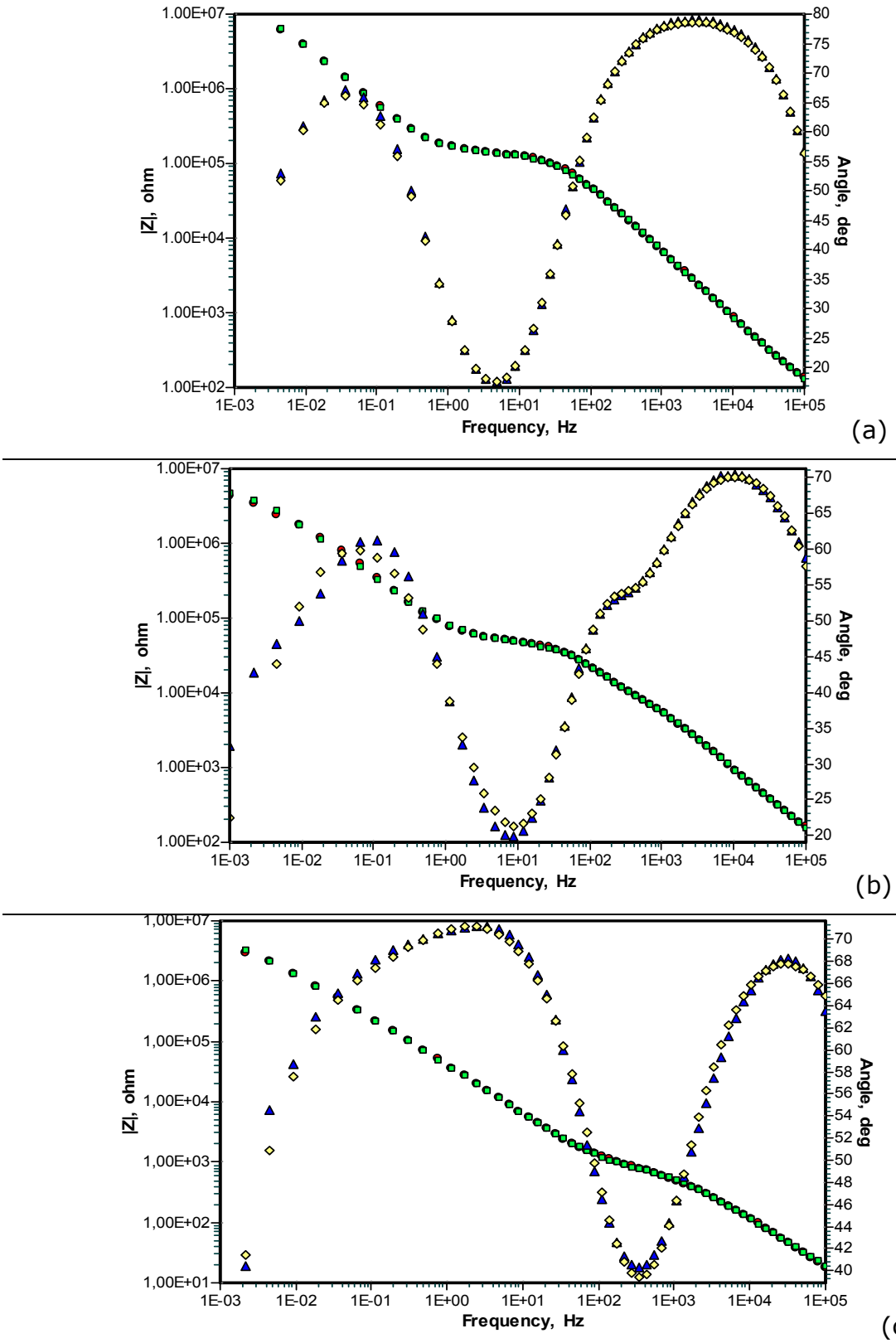

Figure 4.33: The fitted EIS spectra with the appropriate equivalent circuit, (a) Al sample coated with silica film, (b) Al sample coated with cerium nitrate and benzotriazole-doped film after immersion period of 96 hours in NaCl solution, (c) Al sample coated with cerium nitrate-doped silica film

Tables 8; 9; 10; 11 demonstrate the fitting data of the EIS spectra using the appropriate equivalent circuit models.

Table 8: Fitting EIS data for the silica film-coated sample

	Silica film			*Double layer*		
	Q_c	Q_c-n	R_c	Q_{dl}	Q_{dl} -n	R_{dl}
Effect of aging period of the sol						
1 day	3.64E-6	0.64	1.20E6	5.60E-7	0.89	1.00E4
3 day	3.50E-6	0.73	3.80E6	4.93E-7	0.88	3.15E4
5 day	2.80E-6	0.70	4.00E6	5.00E-7	0.88	3.40E4
Effect of the heat treatment of the aluminium substrate coated with silica film						
1 hour	3.90E-6	0.63	2.12E6	5.84E-7	0.90	2.03E4
3 hour	3.50E-6	0.73	3.80E6	4.83E-7	0.88	3.15E4
5 hour	4.00E-6	0.70	4.03E6	4.34E-7	0.80	4.34E4
Non-coated aluminium substrate						
	----	----	----	7.14E-6	0.92	2.00E3

Table 9: Fitted EIS data for the aluminium substrated coated with nanoparticles-doped silica film

Nanoparticles	*Silica film*		*Interfacial layer*		*Double layer*	
	C_c	R_p	C_{int}	R_{int}	C_{dl}	R_{dl}
Aluminium substrate coated with SiC nanoparticles-doped film						
1 %	2.01 E-9	1.10 E7	1.20 E-6	4.62 E5	2.57 E-6	1.52 E5
2 %	1.63 E-9	1.20 E7	7.40 E-7	1.21 E6	5.73 E-6	8.14 E5
6 %	1.47 E-9	1.62 E7	3.73 E-9	1.56 E6	5.46 E-7	8.53 E5
aluminium substrate coated with ZrO_2 nanoparticles-doped film						
1 %	2.67 E-9	7.22 E6	2.33 E-7	7.40 E5	1.47 E-6	4.06 E5
2%	2.58 E-9	9.10 E6	9.42 E-9	2.00 E6	3.20 E-6	6.40 E5
6%	2.52 E-9	9.95 E6	1.02 E-8	1.72 E6	9.32 E-7	1.10 E6

aluminium substrate coated with SiO_2 nanoparticles-doped film						
1 %	2.80 E-9	1.77 E7	4.40 E-9	2.75 E6	3.11 E-6	1.43 E6
2%	2.03 E-9	2.53 E7	4.40 E-7	3.00 E6	3.60 E-6	1.72 E6
6%	1.16 E-9	2.73 E7	1.62 E-9	2.90 E6	3.90 E-7	2.80 E6

Table 10: Fitting EIS data for the aluminium substrate coated with corrosion inhibitors-doped films

Corrosion inhibitors	*Silica film*			*Double layer*		
	Q_c	Q_c-n	R_p	Q_{dl}	Q_{dl} -n	R_{dl}
Effect of cerium nitrate on the corrosion protection						
1 g/l	4.60E-6	0.60	3.74E6	4.45E-7	0.85	9.50E3
10 g/l	4.13E-6	0.92	3.85E6	4.24E-7	0.80	1.00E4
20 g/l	5.16E-6	0.80	5.10E6	8.55E-7	0.83	1.10E4
Effect of benzotriazole on the corrosion protection						
0.5 g/l	4.80 E-6	0.90	3.70E6	6.40E-7	0.74	----
1 g/l	1.85E-6	0.93	7.80E6	4.00E-6	0.72	----
2 g/l	5.62E-6	0.82	7.14E6	6.00E-6	0.80	----
Effect of zinc phosphate on the corrosion protection						
0.1 g/l	3.44E-6	0.55	7.60E6	7.40E-7	*0.84*	6.40E4
0.3 g/l	1.84E-6	0.63	2.70E6	2.40E-7	*0.91*	2.80E4

Table 11: Fitting EIS data to evaluate the self healing of the sample

Immersion period	*Silica film*			*Interfacial layer*			*Double layer*		
	Q_c	Q_c-n	R_p	Q_{sc}	Q_{sc}-n	R_{sc}	Q_{dl}	Q_{dl}-n	R_{dl}
Aluminium substrate coated with non-doped silica film									
0	2.53E-6	0.84	1.01E7	8.80E-8	0.80	8.00E5	5.80E-8	0.90	1.34E5
96	2.05E-6	0.83	1.25E6	5.40E-8	0.90	4.65E4	1.00E-8	0.84	4.54E4
192	5.80E-6	0.80	3.70E5	1.90E-7	0.96	2.80E3	3.72E-7	0.94	1.11E3
700	1.12E-5	0.90	8.60E3	6.15E-6	0.23	1.24E2	1.31E-5	0.90	2.32E2
Aluminium substrate coated with corrosion inhibitors and 2 % SiO_2 nanoparticles-doped silica film									
0	3.50E-8	0.90	4.46E7	1.60E-6	0.70	4.50E6	1.04E-7	0.95	7.40E6
96	4.50E-8	0.90	5.14E6	4.14E-6	0.60	1.84E6	6.30E-7	0.82	1.21E6
192	1.30E-7	0.95	3.50E6	1.15E-6	0.60	1.50E6	1.30E-7	0.81	3.70E5
700	8.10E-5	0.32	2.20E5	6.55E-5	0.64	1.04E5	1.16E-6	1	8.50E3

4.2.5 Sealing of anodized aluminium in water-based sol

Natural aluminium oxide is unstable in corrosive environments. The aluminium alloy needs a protective coating to resist the corrosion effect. The anodizing process (ANOX) is commonly applied to enhance the corrosion protection of the aluminium alloys. Porous ANOX structure is formed because of the aluminium alloy impurities and the different in the oxide growth at the metal surface during the anodizing process.

The aluminium metal alloy coated with porous ANOX film has usually a low corrosion protection. The corrosive ions penetrate into the pores which enhances the corrosion process. Sealing the porous of the anodized aluminium is needed to close the pores and to hinder the negative effect of the anions on the aluminium metal sample.

Aluminium samples Al 6082 were anodized at room temperature using DC current of 2 A/dm^2 for 1.5 h to obtain the anodized layer (anox) with a thickness

of 45 µm. The samples were sealed in water-based sol. The samples were then cured at 150 °C for 3 hours. The experiment showed that a silica film of a thickness of 5 µm is formed on the anodized aluminium as seen in figure 4.34.

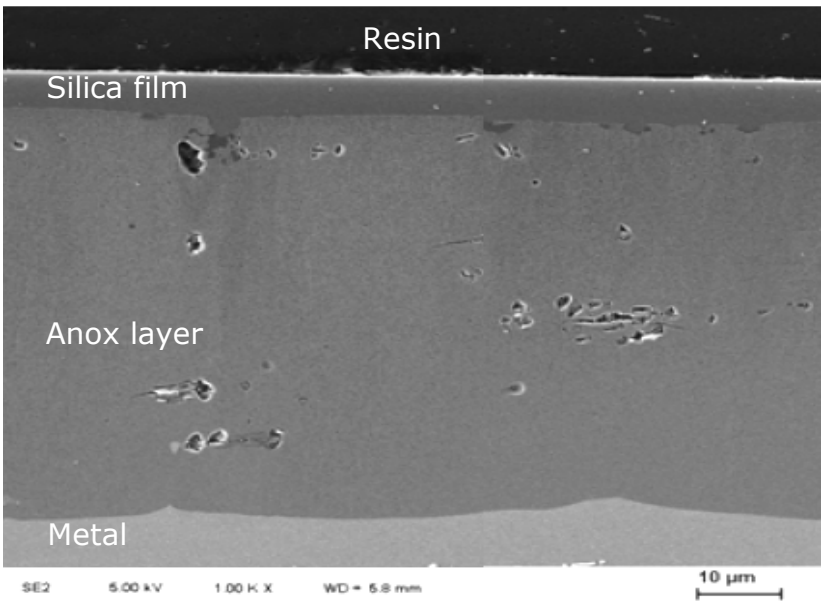

Figure 4.34: Cross-section of anodized layer sealed in water-based sol

The SEM and EDX investigations on the cross-section of the ANOX sample sealed in water-based sol showed that the silica film is formed in the pores, the silica materials are detected by EDX at the points where the pores are cut (see figure 4.35). Figure 4.36 demonstrates EDX analysis spectra of the materials in the pores of the ANOX sealed in water-based sol in comparison to the spectra of unsealed ANOX. EDX spectra show that the silica materials are formed in the pores.

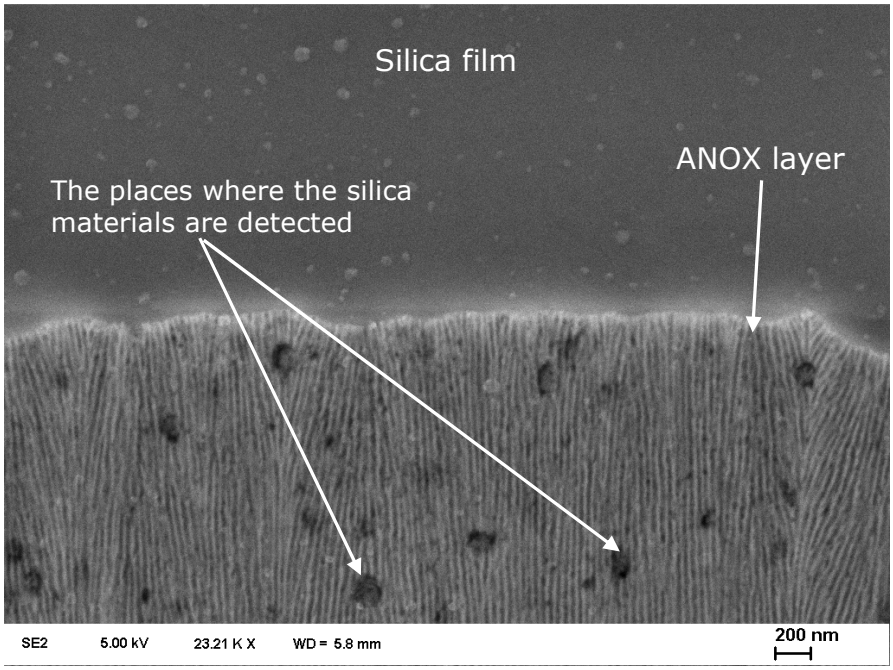

Figure 4.35: SEM image at the cross-section of anodized aluminium sealed in the sol

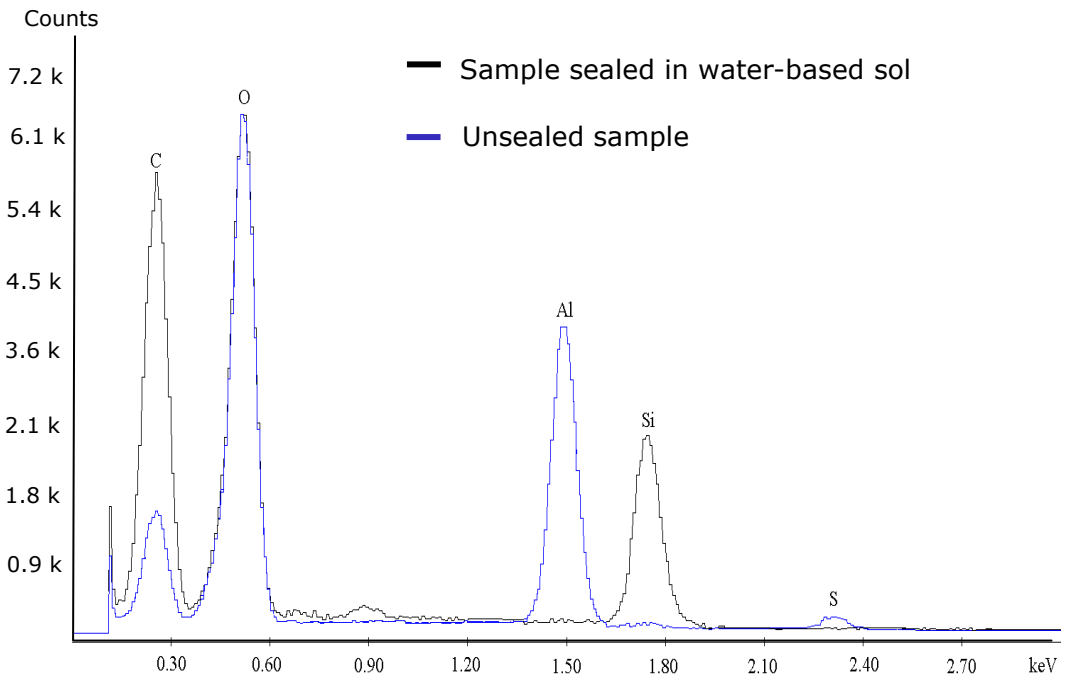

Figure 4.36: EDX analysis of the material in the pores of the anodized aluminium

The aluminium and anodized aluminium samples have low stability in base solutions, the aluminium oxide reacts with alkali, forming $[Al(OH)_4]^-$ as in the equation 38 and 39. [162].

$$2Al + 6H_2O \rightarrow 2Al(OH)_3 + 3H_2 \quad (38)$$

$$Al(OH)_3 + NaOH \rightarrow Na^+ + [Al(OH)_4]^- \quad (39)$$

The reaction products migrate to the solution, and the formation of aluminium hydroxide layer on the aluminum surface is prevented. Figure 4.37 presents ANOX samples immersed in 0.1 M NaOH for 12 hours, it is clear that the unsealed ANOX layer is dissolved in the NaOH solution. While, the ANOX layer sealed in water-based sol shows no signs of metal oxide dissolution due to the barrier property of the silica film, which hinders the contact between the corrosive solution and the ANOX layer.

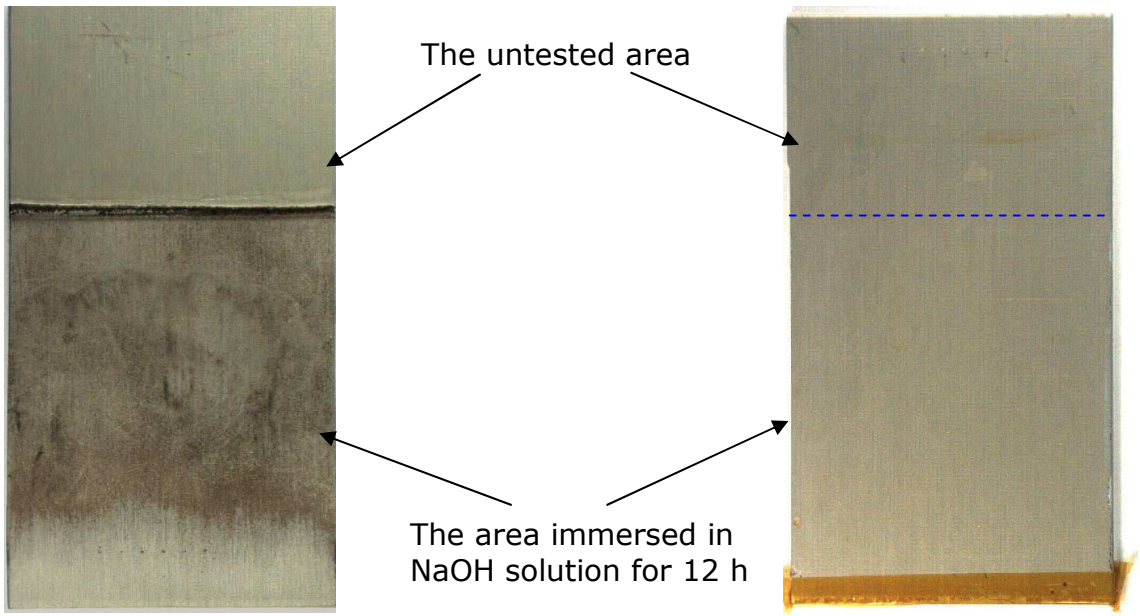

Figure 4.37: Anodized aluminium after 12 h of immersion in 0.1 M NaOH, a) sealed in water-based sol, b) unsealed sample

4.3 Magnesium alloy AZ 31 coated with silica film

Magnesium alloys are widely used in automotive industry, computer parts, cellular phones and the aerospace industry, where weight reduction is needed. Because of the electrochemical activity of magnesium metal, the protective coating is needed to inhibit the contact of the magnesium alloy surface with metal alloys or the corrosive environment. [11]

4.3.1 Multi-silica films treated magnesium alloy

The natural magnesium oxide on the magnesium alloy surface is stable at pH values higher than 11.5 as in Figure 4.38 [11]. When the magnesium alloy AZ31 is immersed in the water-based sol, the magnesium oxide dissolves in the sol due to the low pH value of the sol used in this work (pH=4.5). For that reason, failures appear in the silica film. Therefore, multi-silica films are needed to recover the failures may appear during the deposition of the silica film on magnesium alloy AZ31.

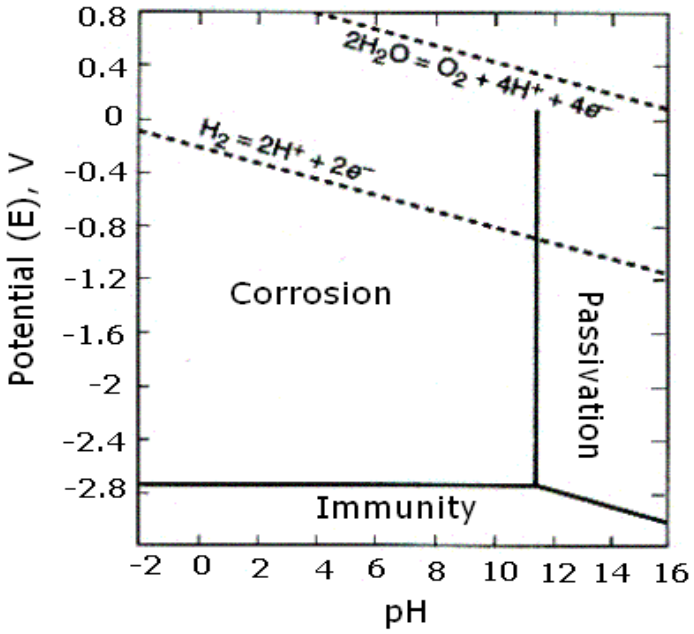

Figure 4.38: Pourbaix diagram of magnesium metal [11]

2 % SiO_2 nanoparticles-doped multi-silica films were deposited on magnesium alloy AZ31. The heat treatment of the coated magnesium samples was carried out for cross-linking of the silica film. Figure 4.39 shows EIS spectra of magnesium ally AZ31 coated with 2 % SiO_2 nanoparticles-doped multi-silica films. The impedance value of the magnesium sample coated with three layers is 3E5 Ω.cm^2 at frequency of (10E-3 Hz), the impedance value is increased to 8E6 Ω.cm^2 for the samples coated with four silica films. This indicates that the application of multi-layers recovers the defects of the silica film.

Low stability was seen for multi-silica films with five layers due to the film-cracks. Hence, silica film with four layers is determined in this work for the coating of magnesium alloy AZ31.

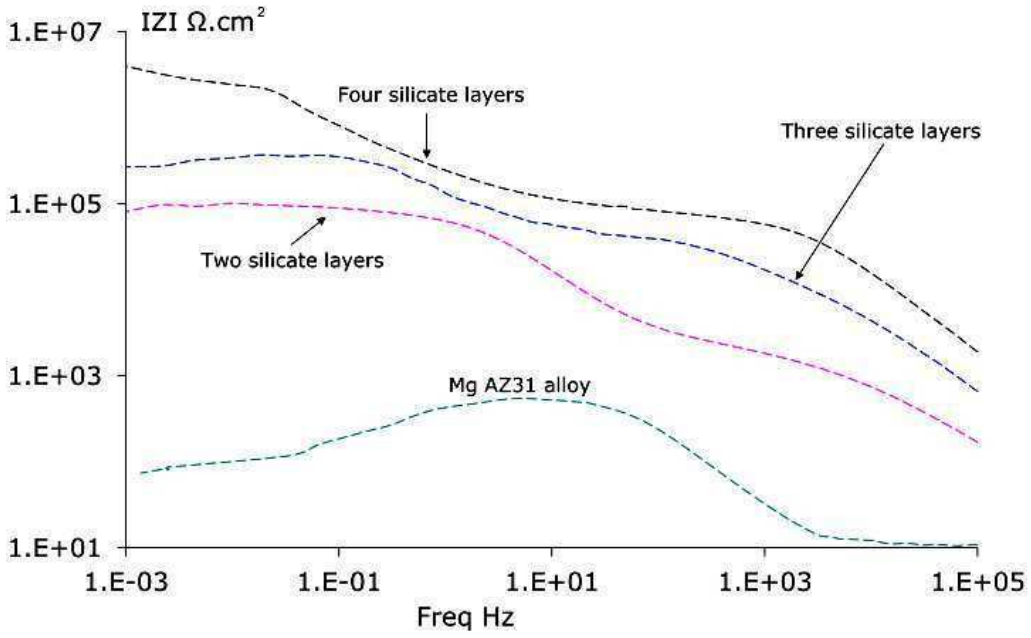

Figure 4.39: Effect of multi-silica films on the corrosion protection of Mg AZ31

4.3.2 Self-healing of magnesium alloy AZ31

Multi-silica films were applied on the magnesium alloy, the multi-silica films were defected by means of scratch test instrument to generate the self-healing, the size of the defect was 10.000 x 150 µm^2. The electrochemical characterisa-tion of the self-healing was carried out after a specific immersion period of the defected samples in 0.5 M NaCl. The immersion periods were 0, 48 and 96 hours.

Figure 4.40 demonstrates the effect of the corrosion inhibitors on the electrochemical behaviour of magnesium metal alloy AZ31 coated with silica film. The corrosion protection of the sample without corrosion inhibitors destroyed after 96 hours immersion period in 0.5 M NaCl. The impedance module of the fresh prepared sample (0 hours) is 5.10E5 $\Omega.cm^2$ at frequency of 10E-3 Hz. The impedance module of the sample reduces 500 times to value of 10E-3 $\Omega.cm^2$ after an immersion period 96 hour in chloride solution.

The conclusion can be drawn that the corrosion resistance of the magnesium sample coated with non-doped silica film reduces 500 times after immersion period of 96 hours in chloride solution, this can be explained in terms of high chemical activity of the magnesium metal, and no protective layer is formed in the defect area of the sample to reduce the corrosion process.

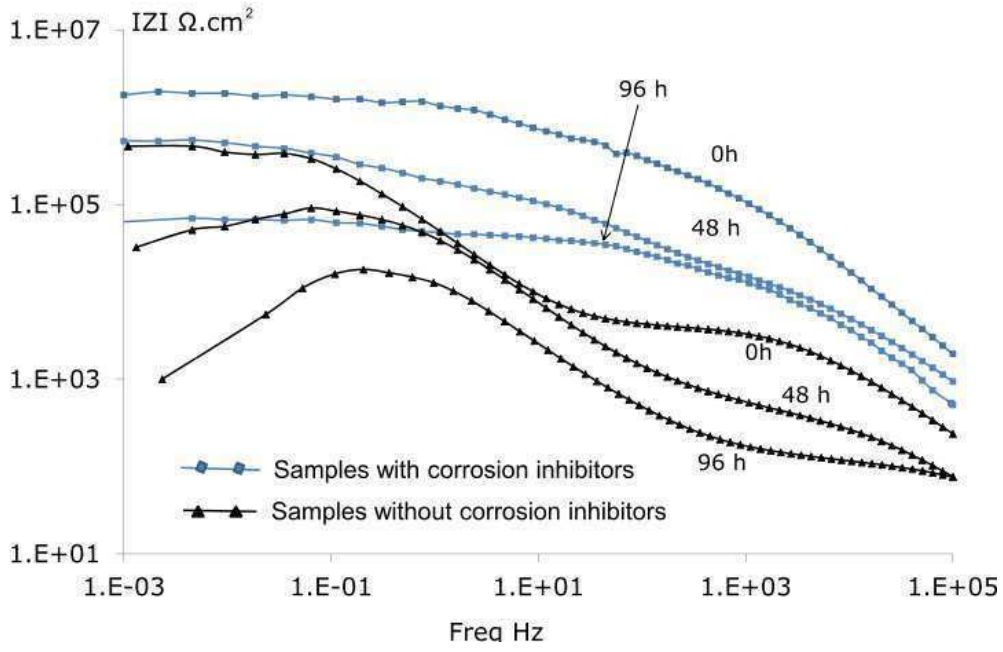

Figure 4.40: The electrochemical behavior of magnesium sample coated with silica film during the immersion period in chloride solution and the self-healing effect

The EIS spectra of the magnesium sample coated with SiO_2 nanoparticles and corrosion inhibitors-doped multi-silica films showed better stability in the chloride solution than the samples without additions. The impedance module (at 10E-3 Hz) of the fresh prepared samples (0 hours) is 1.8E6 $\Omega.cm^2$. This value is reduced 28.4 times to reach 6.32E4 $\Omega.cm^2$ after an immersion period of 96 hours in chloride solution.

It is clear from Figure 4.40 that the decreasing in the impedance of the samples with corrosion inhibitors is less than the samples without corrosion inhibitors especially after 96 hours immersion period in chloride solution. This can be attributed to the self-healing effect of the corrosion inhibitors-doped film, a layer of the corrosion inhibitors is formed in the defect of the sample which reduces the penetration of the corrosive solution toward the substrate surface and decreases the corrosion process.

The conclusion can be drawn that the corrosion resistance of the magnesium sample coated with corrosion inhibitors-doped silica film reduces 28 times after an immersion period of 96 hours in chloride solution. While, the corrosion resistance of the magnesium sample without corrosion inhibitors reduces 500 times. This result can be explained in terms of a corrosion inhibitors layer is formed in the defect of the magnesium samples coated with corrosion inhibitors-doped film which reduces the corrosion process.

4.3.3 Sealing of the PEO magnesium

Plasma electrolytic oxidation (PEO) of light-weight metals is widely accepted as an environmental friendly method to form a ceramic coating on magnesium alloys. Pores and defects usually appear over the ceramic layer; the corrosion protection of PEO layer on magnesium alloy is not good enough to be used as a single layer, post-treatment is needed for better barrier property of the coated magnesium sample.

In this work, PEO process was applied on magnesium alloy AZ31, pores and defects can be seen on the substrate surface as in Figure (4.41-a). The PEO layer was sealed in 2 % SiO_2 nanoparticles and corrosion inhibitors-doped water-based sol, the aim is to form the silica film in the defect and the pores of the PEO layer for better corrosion protection. Figure (4.41-b) demonstrates PEO layer after the sealing process, the pores of the PEO layer are closed which improves the corrosion resistance of the sample.

SEM investigations on the cross-section of the PEO layer demonstrates that the pores of the PEO layer reach the substrate surface which is the reason for low corrosion resistance (see figure (4.42-a)). Silica film is formed in the pores of the

PEO layer after sealing in water-based sol, and thin silica film also deposited on the surface of the sample for better corrosion protection as in figure (4.42-b).

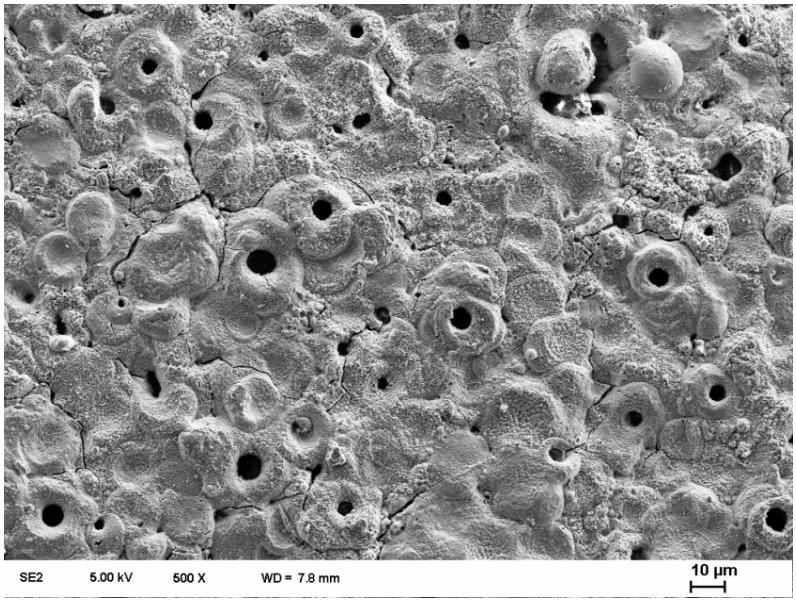

Figure 4.41: SEM for PEO of magnesium a) before sealing and b) after sealing

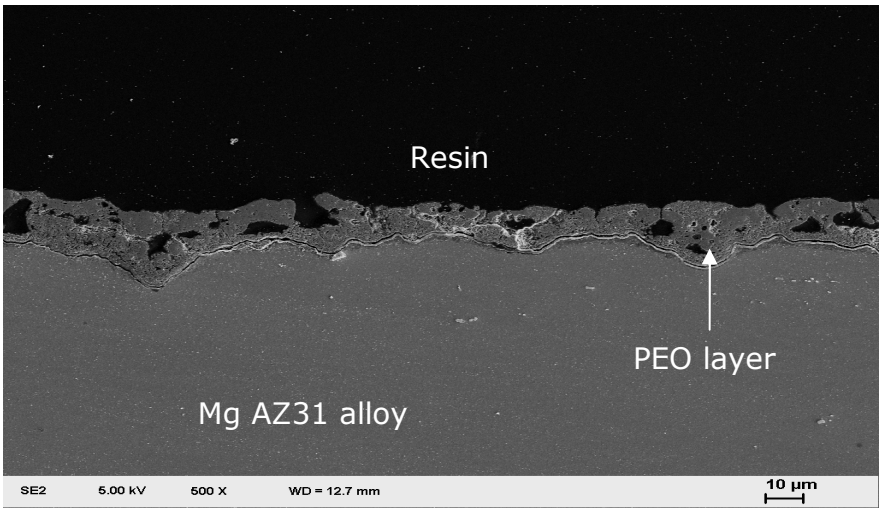

(a)

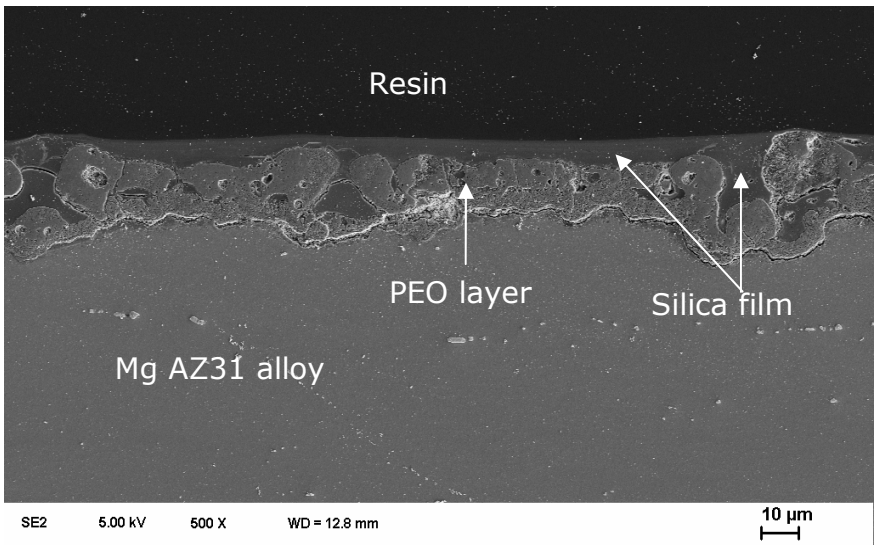

(b)

Figure 4.42: Cross-section in the PEO layer of magnesium a) before sealing and b) after sealing

Figure 4.43 demonstrates EIS measurements of PEO of magnesium alloy AZ31; the impedance module IZI of the PEO of magnesium alloy (at frequency of 10E-3 Hz) is 1E5 $\Omega.cm^2$, which is rises to 1E7 $\Omega.cm^2$ for PEO sample sealed in water-based sol. This indicates that the impedance module of the sample is increased 100 times after the sealing in the water-based sol. The development in the impedance value is related to the barrier silica film formed in the defects and pores of the PEO layer.

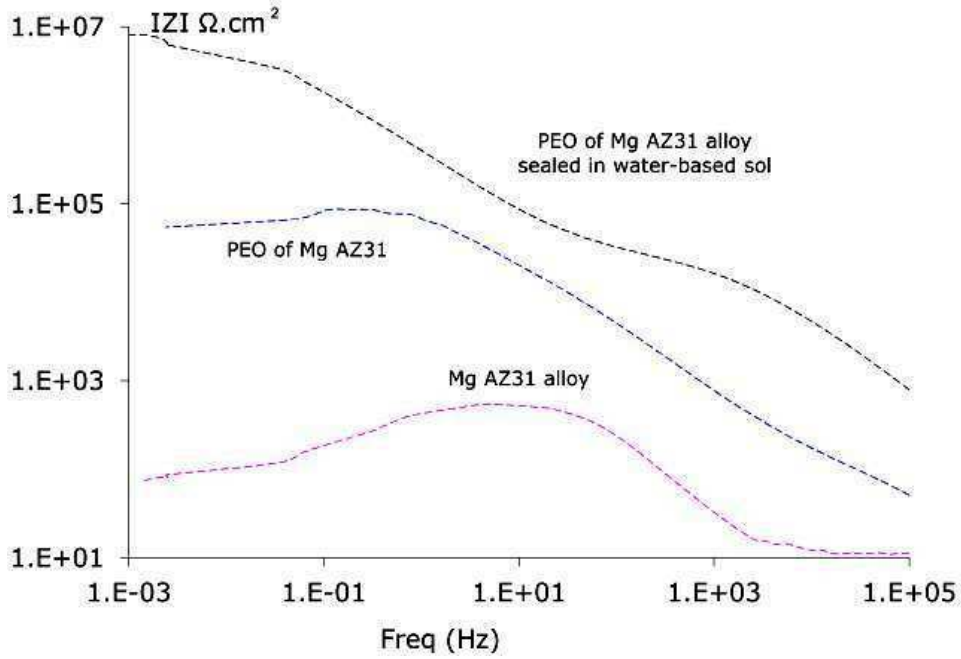

Figure 4.43: Effect of the sealing in water-based sol

The stability of the sealed PEO layer in water-based sol was tested by salt spray test. Figure 4.44 shows that no signs of corrosion were observed after 135 hours for the sealed samples (sample A). Corrosion spots were seen on the unsealed PEO layer (sample B). While, the uncoated magnesium alloy AZ31 (sample C) is destroyed.

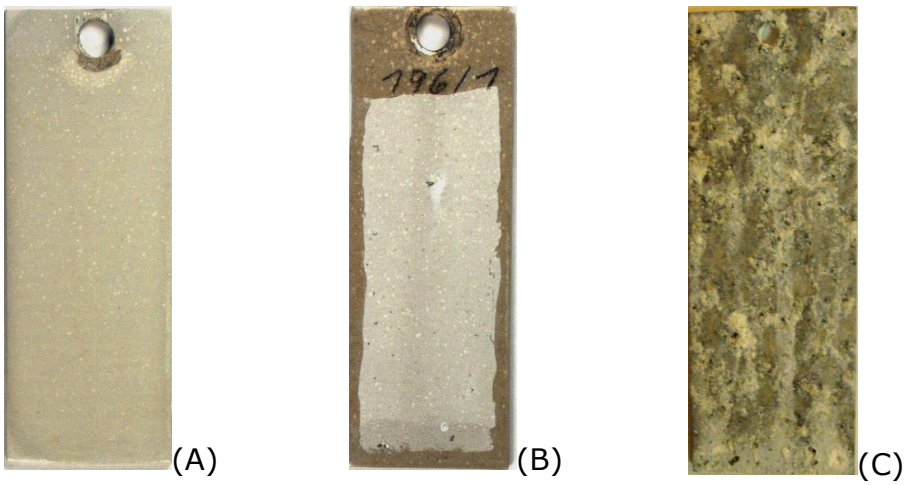

Figure 4.44: Magnesium alloy AZ31 after 135 hours in salt spray test, A) PEO sealed in water-based sol (multi-layers), B) unsealed PEO layer and C) uncoated magnesium sample

4.4 The stability of the sol

The control of the stability during the synthesis, storage, and transportation is known to be one of the most challenging problems of the water-based sols. In practice, it is noticed that the stability of the sol is depend on the pH value. Table 12 demonstrates the sol stability at various concentrations. The clear sol is considered as a stable. The sol starts to loss the stability when the hazy colour is visible. The hazy colour is a result of the condensation reactions of the Si-OH in the sol which leads to low sol stability.

As a result, the water-based sol at concentration of 5 % and pH 4.5 was stable for 6 days, the hazy colour of this sol was visible after one week. The solid phase of the sol was seen after a period of 3 weeks, which is a result of the polymerisation of the silanes molecules. The continuous visual inspection of 50 % water-based sol at the composition 25: 25: 50 (GPTM: TEOS: H_2O) with 2 % SiO_2 nanoparticles at pH value of 4.5 showed that the sol is stable after one year. No traces of hazy colour are observed.

The stability of the water-based sol can be controlled by the surface charges of the particle-to-particle interaction, which is governed by the pH value of the sol.

The hydrolysis reaction of the alkoxy groups is expressed as in the equation 40

$$Si - OR + H_2O \rightarrow Si - OH + ROH \qquad (40)$$

At low pH values, Si-OH is reacted with H^+ as in the equation 41 to form Si-OH_2^+. Sol particles with positive surface charge are obtained, repulsing level between the sol particles becomes higher and low agglomeration is occurred. Thus, sol particles with small sizes are formed at low pH values.

$$Si - OH + H^+ \rightarrow Si - OH_2^+ \qquad (41)$$

At neutral and slight alkaline sols, the Si-OH is reacted with OH^- as in the equation 42 to form Si-O^-, the attraction between the different charges in the sol is occurred (Si-OH^{2+} and the Si-O^-). Degradation in the sol stability is observed due to the agglomeration of the molecules.

$$Si-OH+OH^{-}\rightarrow Si-O^{-}+H_2O \qquad (42)$$

At high pH values, the repulsing between the negatively charged particles becomes higher. Thus, the agglomeration at high pH values is low and the water-based sol is stable.

Table 12: The stability of the sol at different concentrations and pH values

Per-cent volume ratio of the sol TEOS:GPTM	pH value	Test period	Sol stability
3:3	4.5	6 days	Hazy colour
5:5	4.5	6 days	Hazy colour
10:10	4.5	60 days	Hazy solution
25:25	4.5	360 days	Clear solution
25:25	7	20 days	Hazy solution
5:5	11	30 days	Clear solution
10:10	11	30 days	Clear solution
5:5	2	60 days	Clear solution

The result can be drawn that the best corrosion protection and the best sol stability were obtained from the sols at concentration of 25:25 (TEOS: GPTM) % and the pH value of 4.5.

5 Discussion and validation

To evaluate the advantage and disadvantage of this work, the results need to be discussed with respect to the most important literature reviews. The comparison can be drawn as follow:

5.1 Aging parameter of the sol:

The aging of the sol is needed to obtain a protective cross-linked silica film rather than an oily film. During the aging period, hydrolysis reactions take place. OR groups are hydrolysed into OH groups. Different aging periods determined in the literature. Wang reported that the optimal aging period of the water-based sol is 3 days [125]. V. Palanivel aged the sol at room temperature for 2 days [126].

The aging period of the water-based sol was studied in this work. The experiment showed that the best aging period of the water-based sol is 3 days. Longer aging period did not show important changes on the effectiveness of the sol, This can be explained in terms of the most of the OR groups in the water-based sol are hydrolyzed after the aging period of 3 days and no important hydrolysis reactions occur after this aging period.

5.2 Heat treatment of the coated sample

The heat treatment of the aluminium or magnesium sample coated with silica film is needed for crosslinking of the film. Schem treated the aluminium sample coated with water-based silica film for 4h at 120°C [137]. Zhu found that the corrosion protection of the Aluminium alloy coated with silica film enhances when the heat treatment period rises from 1 to 4 hours at 100 °C [26].

Gerard treated the aluminium sample coated with silica film at 300 °C for 1.5 hours [150]. The heat treatment at temperature of 300 °C leads to changes in

the microstructure of the aluminium and magnesium alloys which results by a different in the properties of the metal alloy.

In this work, the heat treatment of aluminium and magnesium samples coated with silica film was carried out at 150 °C. The experiment showed that the best corrosion protection was measured at the treatment period of 3 hours. The heat treatment for a period more than 3 hours did not show a development in the corrosion protection of the coated sample. This can be explained in terms of the most of OR and OH groups in the silica film are condensed after the heat treatment at 150 °C for 3 hours.

5.3 Nanoparticles-doped silica film

Liu prepared aluminium sample coated with SiO_2 nanoparticles-doped silica film [162]. The study of Liu concluded that the thickness and the barrier property of the silica film are enhanced when SiO_2 nanoparticles added to the silica film. The best corrosion protection is obtained at 7.10^{-5} g /l of SiO_2 nanoparticles. The barrier property of the silica film reduces at concentrations higher than 10^{-4} g /l of SiO_2 nanoparticles.

In the present thesis work, the thickness and the barrier property of the silica film are enhanced when SiO_2 nanoparticles were added to the silica film. 10 g/l SiO_2 nanoparticles-doped silica film showed better barrier properties than the non-doped film. The silica film began to loose the barrier properties at 80 g/l SiO_2 nanoparticles. This can be explained in terms of the high concentration of nanoparticles reducing the surface of the aluminium substrate that bonds to silica film, which leads to low-adherence silica film.

It can be concluded that the concentrations of SiO_2 nanopartles in the present thesis are higher than the concentrations of SiO_2 nanopartles employed by the work of Liu [162]. This can be related to the difference in the structure of the silica film due to the dissimilar sol composition and the different in the application parameter of the silica film. However, the SiO_2 nanoparticles in both studies improve the barrier property of the silica film which can be related to decreasing in the cracks of the nanoparticles-doped silica film.

5.4 Self-healing

The size of the defect

It is always important to consider the size of the defect in the silica film to estimate the self-healing ability of the coated sample. An artificial defect with size of 50 X 50 μm^2 in the film is determined by S. Lamaka to generate the self-healing [155]. The quinolinol and benzotriazole are added to the silica film as corrosion inhibitors. The experiment showed that the corrosion activity is reduced, indicating that the recovery of the defect (50 X 50 μm^2) is possible by using quinolinol and benzotriazole as a corrosion inhibitors.

A scratch width of 5 µm is used by C. Trenado to study the self-healing of the aluminium sample coated with cerium salt-doped silica film. The scratch area of the sample is successfully healed. [156]

In the present work, the defect area of 10.000 X 150 μm^2 was prepared in the silica film. The size of the defect is 600 times bigger than the defect size determined by literatures [154; 155; 156]. The aim is to evaluate the ability of the studied coating system to heal macro-defect sizes. The experiment showed that the defect was successfully healed. A layer of the corrosion inhibitors was formed in the defect area of the aluminium and magnesium samples coated with corrosion inhibitors-doped silica film.

Self-healing of the coated sample

The easiest way to obtain corrosion inhibitors-doped silica film is the simple mixing of the corrosion inhibitors with the water-based sol. D. Raps studied the stability of aluminium sample coated with benzotriazole (at concentration of 30 g/ l)-doped silica film [140]. The experiment demonstrates that benzotriazole reduces the barrier property of the silica film. D. Raps proposed in his work the using of microcapsules-doped film to eliminate the interaction between benzotriazole and the components of the silica film.

In present thesis work, the effect of benzotriazole on the stability of the silica film was investigated. The benzotriazole-doped water-based sol was prepared by

a simple mixing of the corrosion inhibitors with the sol. The corrosion protection of the coated sample was enhanced at concentration of 1 g/l of benzotriazole. The barrier property of the silica film was reduced at concentrations of 2 g/l benzotriazole. This can be explained in the term of the strong influence of benzotriazole on the hydrolysis/condensation processes during the coating preparation [140]. The effectiveness of benzotriazole on the corrosion protection depends also on the structure of the silica film which can be controlled by the composition and the application parameters of the silica film. The conclusion can be drawn that benzotriazole at concentrations less than 2 g/ l shows no negative effects on the barrier property of the silica film. The samples with benzotriazole showed better corrosion protection than the non-doped samples.

Electrochemical characterization

M. Zheludkevich studied the electrochemical characterization of the aluminium sample coated with cerium nitrate-doped silica film [163]. After an immersion period of 48 hours as in Figure 5.1, the impedance module of the sample is 10E6- $\Omega.cm^2$ at a frequency of 10E3- Hz. However, the impedance module of the sample prepared in our work is 10E7- $\Omega.cm^2$ even after 192 hours immersion period as seen in Figure 5.2. The development in the impedance of the sample in our work can be explained in terms of the using of a mixture of the corrosion inhibitors (cerium nitrate and benzotriazole) which enhances the concentration of the corrosion inhibitors in the defect area of the aluminium and magnesium samples coated with silica films.

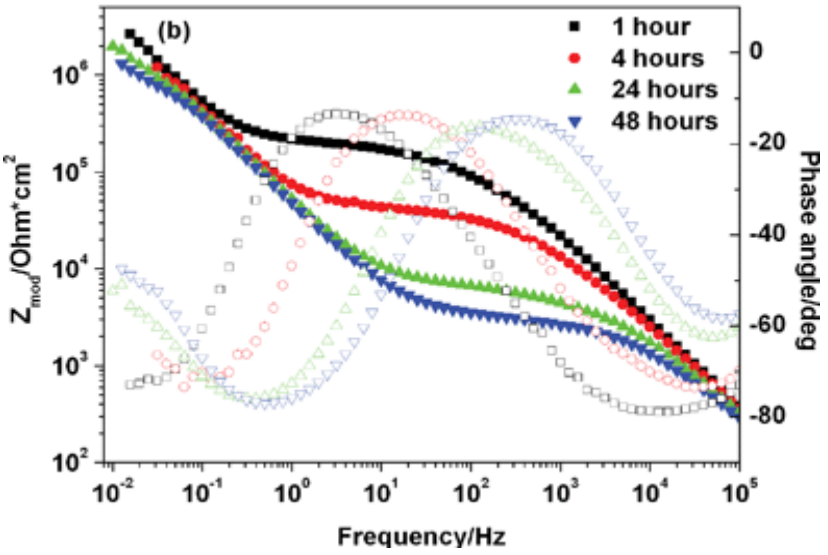

Figure 5.1: Effect of immersion period on the corrosion protection of cerium nitrate-doped silica film [163]

The EIS measurements in the work of Zheludkevich and in our work demonstrate the same electrochemical behaviour as seen in Figures 5.1 and 5.2. The impedance of the aluminium sample is reduced at high frequencies due to the corrosion in the defect of the sample. The layer of corrosion inhibitors forms in the defect area which keeps the impedance of the sample stable.

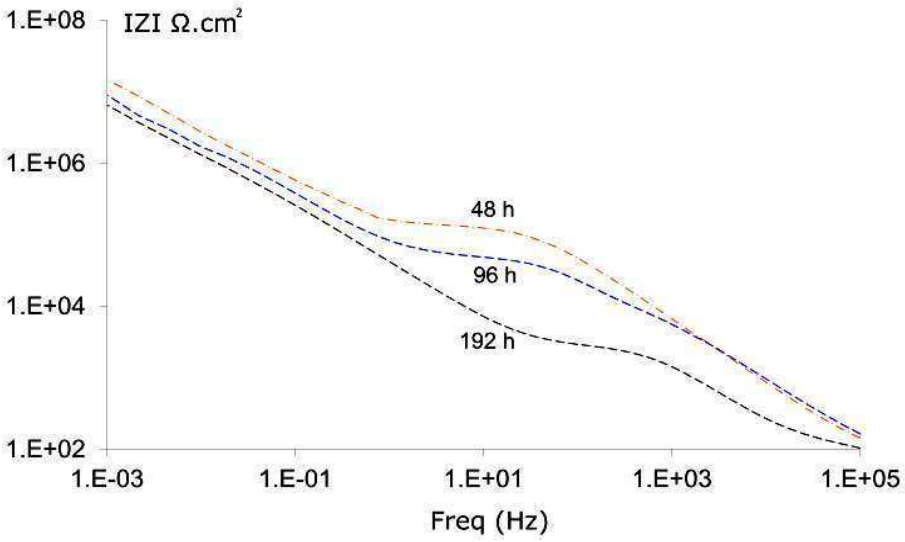

Figure 5.2: Effect of immersion period on the corrosion protection of aluminium sample 6082-6 coated with cerium nitrate and benzotriazole-doped silica film

5.5 Sealing of the PEO in sol

Shi treated the magnesium alloy by the micro-arc oxidation technique (MAO). The MAO layer is sealed in TiO_2 sol prepared by sol–gel process. Multi-silica films are applied on the MAO layer. The electrochemical measurements showed that the corrosion resistance of the sample increased 30 times after the sealing process. [164]

Bestetti applied multi-layers of SiOx produced by sol–gel process on magnesium samples anodized by micro-arc technique. The result showed that corrosion current density of the sealed sample is three times less than the corrosion current density of the unsealed sample. [165]

In our work, plasma electrolytic oxidation (PEO) was applied on magnesium alloy AZ31. The pores and the cracks of the PEO layer were sealed in water-based sol. The experiment showed that impedance of the sealed samples is 100 times higher than the impedance of the unsealed samples, which is related to the barrier silica film formed in the defects and pores of the sealed sample.

5.6 The price of the sol

Zhu prepared alcohol-based sol using Bis-[triethoxysilylpropyl]-tetrasulfide as an organo-silica material. The costs of one litre sol can be estimated to be 198 Euro/litre + the cost of the 900 ml alcohol as a solvent to make one litre sol. [26]

Palanivel synthesised the water-based sol using vinyltriacetoxysilane as an organo-silica materials. The cost of one litre is 222 Euro/litre sol. [126]

To reduce the cost of the sol, mixture of organo-silica materials can be used. In our work, the best result is measured for silica film from the sol composition TEOS: GPTM: water at the concentrations (25:25: 50) ml to prepare 100 ml water-based sol. The cost of this sol is estimated to be 130 Euro/Litre.

6 Conclusion

The water-based silica films were successfully applied on the aluminium alloy 6082-T6 and magnesium alloy AZ31. The water-based sol was prepared from GPTM, TEOS, water as a solvent and acid as a catalyst. The aim of the work is to obtain cost-efficient water-based sols, protective silica film and cracks-free film with self-healing property. The conclusion of the work can be drawn as follows

The composition of the water-based sol

The water-based sol is prepared from GPTM, TEOS, water and hydrochloric acid as a catalyst. The pH value of the sol is adjusted by the catalyst to a value of 4.5. The water-based sol showed low stability at pH values higher than 4.5. The sol at pH values less than 4.5 demonstrates stability for more than one year, but low barrier property is observed for the silica films deposit from this sol, this can be explained in terms of the dissolution of the metal oxide at the surface of aluminium or magnesium substrate in the acid sol.

Different concentrations of GPTM and TEOS in the sol were tested. The sol with TEOS only showed low barrier property of the silica film. Hence, GPTM was added to the sol to improve the hydrophobicity due to the organic part in the structure of the GPTM. The best barrier property is measured for silica film from the sol composition TEOS: GPTM: water at concentrations of (25: 25: 50) ml to prepare 100 ml sol. The cost of this sol is estimated to be 130 Euro/Litre, which is less than the cost of sols mentioned by other literatures.

The application parameters of the silica film

The aging period of the water-based sol showed an important effect on the structure and the barrier property of the silica film. Through the aging period, the hydrolysis and the condensation reactions of alkoxy groups happen

simultaneously. The viscosity of the sol increases due to the condensation reactions in the water-based sol.

The experiment demonstrates that the aging of the sol for a period of 3 days shows the best protection efficiency; this indicates that the most of alkoxy groups (OR) are hydrolysed to hydroxyl groups (OH) after the aging period of 3 days. No further development in the protection efficiency is measured after aging the sol more than 3 days. This can be explained in terms of no important hydrolysis reactions happen after aging period more 3 days.

This result is observed for sols with different concentrations which indicate that the aging period has no important relation with the concentration of the sol. The aging period of the sol can be decreased by using higher amounts of the catalyst which accelerates the hydrolysis reaction.

The heat treatment is needed for drying and crosslinking of the silica film, OH and OR groups are condensed during the heat treatment to form the structure of the silica film. In this work, the fully cross-linked film structure is obtained at the heat treatment 3 hours at 150°C. Longer heat treatment period did not show further development in the protection performance of the coated aluminium and magnesium samples. This can be explained in the terms of the most of the OH and OR groups in the silica film are condensed after heat treatment 3 h at 150 °C.

For heat treatment at temperatures higher than 150°C for example 300°C, fully cross-linked silica film can be obtained. But the microstructure and the properties of the aluminium and magnesium alloys will be different after the treatment at 300°C. Therefore, heat treatment temperatures higher than 150°C are avoided. To reach the fully cross-linked silica film at heat treatment temperature less than 150 °C for example 100 °C, long heat treatment period is needed for the condensation of OH and OR groups in the silica film.

Pitting corrosion

The cyclic voltammetry (CV) measurements showed pitting corrosion for uncoated aluminium and magnesium metal alloys in chloride solution. While no signs of pitting corrosion were seen on the surface of the substrate coated with

silica film. The corrosion current density of the uncoated aluminium substrate 6082-T6 is 5.2E-5 mA.cm^2. The corrosion current density increases up to 76 times to reach 3.96E-3 mA.cm^2 for aluminium sample 6082-T6 coated with silica film. The protection efficiency of the coated aluminium sample reaches 98.68 %.

The high protection efficiency of the coated aluminium sample with silica film can be explained by:

1) Physical barrier layer of the fully cross-linked silica film, the barrier silica film hinders the effect of the corrosive solution on the aluminium or magnesium substrates,

2) bonding of the silica film to the aluminium and magnesium substrates through the covalent bond, which ensures the adhesion of the silica film on the substrate,

3) functional molecules-doped silica film such as corrosion inhibitors can improve the stability of the sample in corrosive solution due to the self-healing effect.

Crack-free silica film

Cracking is one of the major drawbacks of the silica film. The cracks are generated during the cross-linking of the water-based silica film by the heat treatment. The volume of the silica film is reduced during the heat treatment due to a) evaporation of the water, b) shrinkage of the silica film through the polycondensation reactions of OH and OR groups. The decreasing in the volume of the silica film raises the in-plane tensile stress in the silica film and cracks can be formed.

In this work nanoparticles-doped silica film was successfully applied on aluminium alloy 6082-T6 and magnesium alloy AZ31. Different nanoparticles at varying concentrations were used. The corrosion protection of the aluminium samples coated with non-doped films is 3.5E6 Ω.cm^2. The corrosion protection increases 5 times to reach 1.8E7 Ω.cm^2 for aluminium samples coated with 2 % SiO_2 nanoparticle-doped films. The thickness of the silica film is enhanced from 2 µm for the non-doped film to 9 µm for 2 % SiO_2 nanoparticle-doped films.
The conclusion can be drawn that the thickness and the barrier property of the silica film are enhanced when 2 % SiO_2 nanoparticles are doped in the film. This can be explained by a reduction of the cracks in the silica film due to the doping of the nanoparticles in the film. The shrinkage of the nanoparticles-doped silica

film is less than the shrinkage in the non-doped silica film, which leads to less in-plane tensile stress in the silica film and less cracks.

The coating delamination is observed for the coatings with SiO_2 or SiC or ZrO_2 nanoparticles at concentrations higher than 8 %. High concentrations of nanoparticles reduce the surface of the aluminium or magnesium substrate that bonds to the silica film. Thus, silica film has low adhesion on the substrate.

The samples coated with SiO_2-nanoparticle-doped films showed better corrosion protection than the samples coated with ZrO_2 or SiC-nanoparticle-doped films. The silicon dioxide nanoparticles in the films react with the cathodically generated OH ions to form Al-silica compounds; the passive silica layer suppresses the corrosion process. No evidence for the formation of magnesium-silica layer is seen by the magnesium alloy coated with SiO_2 nanoparticles-doped silica film, which can be explained by the high corrosion rate of the magnesium metal alloy.

Self-healing

The size of the defect

The size of the defect in the silica film is an important aspect to evaluate the self-healing feature. The size of the defect in this work was 10.000 x 150 μm^2 which is 600 times bigger than the defect of 50 x 50 μm^2 used by several literatures. The aim is to test the ability of the coating system to heal the defect of macro-size.

Choosing of the corrosion inhibitors

Different corrosion inhibitors were used in this work, the most effective corrosion inhibitors were cerium nitrate and benzotriazole. The silica film acts as reservoir for corrosion inhibitors, when a defect appears in the corrosion inhibitors-doped silica film. The corrosion inhibitors leach out of the coating to the defect area under the capillary forces. A layer of the corrosion inhibitors forms on the aluminium or magnesium substrate at the defect area which reduces the corrosion process.

Cerium nitrate as a dopant in the silica showed no negative effects on the barrier properties of the silica film in all concentrations. The corrosion resistance of aluminium sample coated with 1 g/l cerium nitrate-doped silica film is 3.74E6 $\Omega.cm^2$, this value increases to 5.10E6 $\Omega.cm^2$ at concentration 20 g/l of cerium nitrate-doped film.

Benzotriazole at concentrations higher than 2 g/l decreases the barrier properties of the silica film. The corrosion resistance of the coating (Rc) of the sample with 1 g/l of benzotriazole is 7.80E6 $\Omega.cm^2$, the corrosion resistance of the coating is reduces to 7.14E6 $\Omega.cm^2$ at concentration 2 g/l of benzotriazole. This behaviour can be explained by the influence of benzotriazole on the hydrolysis/condensation processes during the coating preparation.

It can be concluded that cerium nitrate at concentration of 20 g/l and benzotriazole at concentration 1 g/l showed the best corrosion protection. The corrosion inhibitors at these concentrations have no negative effects on the barrier property of the silica film.

Long-term corrosion protection and lack of corrosion inhibitors

The experiment demonstrated that a mixture of (cerium nitrate and benzotriazole)-doped silica film showed better self-healing ability than the cerium nitrate-doped silica film. This indicates that the concentration of the corrosion inhibitors in the defect area of the sample enhances when a mixture of corrosion inhibitors is doped in the silica film.

Enhancing the concentrations of the corrosion inhibitors in the defect of the sample enhances the barrier property of the layer in the defect which has two advantages:

1- Hindering the penetration of the corrosive solution to the defect area of the sample which is needed to reach the long-term corrosion protection,

2- reducing the penetration of the corrosive solution into the structure of the silica film. This decreases the leaching of the corrosion inhibitors out of the silica film under capillary forces which hinders the quick lack of corrosion inhibitors.

The healing efficiency of the aluminium sample coated with 2 % SiO_2 nanoparticles and corrosion inhibitors-doped film reaches to 11.2 % after

immersion period of 96 hours in chloride solution, while healing efficiency for the non-doped aluminium sample is 2.8 % after the same immersion period. The difference in the healing efficiency can be explained in terms of the self-healing layer formed in the defect of the substrates coated with corrosion inhibitors-doped film which enhances the healing efficiency.

The healing efficiency of the aluminium sample coated with 2 % SiO_2 nanoparticles and corrosion inhibitors-doped film is nearly stable at the immersion period between 96 and 700 hours. This behaviour can be explained by the long-term corrosion protection of the coated aluminium sample in corrosive solution, which is attributed to the developing in the barrier property of the corrosion inhibitors layer in the defect of the sample.

The qualification of the healing process was evaluated by monitoring the defect surface profile before and after the immersion test in chloride solution. The defect dimensions of the aluminium samples coated with the inhibitors-doped film were small due to the precipitation of the corrosion inhibitors in the defect area; full recovery of the defect area and the cracks at the defect edges was achieved. The samples coated with the non-doped film showed low stability in chloride solution, the defect size was considerably bigger after the corrosion test. The defect depth and width of the samples coated with the non-doped film increased several times and pitting corrosion occurred.

Corrosion protection of magnesium alloy Mg AZ31

Multi-silica films were applied on the magnesium alloy AZ31, Multi-films is needed to recover the failures may appear during the deposition of the silica film on magnesium alloy AZ31, the failures in the silica film can be attributed to the dissolution of the magnesium oxide layer in the water-based sol at pH value of 4.5 which is used in this work.

After an immersion period of 96 hours in chloride solution, the impedance module (at 1E-3 Hz) of the magnesium sample coated with corrosion inhibitors-doped multi-silica films is 6.32E4 $\Omega.cm^2$, while the impedance module of the magnesium sample coated with non-doped silica film is 1E3 $\Omega.cm^2$. This indicates that the impedance of the sample with corrosion inhibitors is 60 times higher than the impedance of the sample without corrosion inhibitors. The result can be

explained in terms of the corrosion inhibitors layer forms in the defect of the sample; the barrier property of this layer reduces the effect of the corrosive solution on the magnesium alloy.

The impedance module (at 1E-3 Hz) of the magnesium sample with corrosion inhibitors is reduced from 1.80E6 $\Omega.cm^2$ for fresh prepared samples to a value of 6.32E4 $\Omega.cm^2$ after immersion period of 96 hours in chloride solution. This indicates that the corrosion process at the defect area of the sample is faster than the self-healing process. This behaviour is explained by the high chemical activity of magnesium metal.

The conclusion can be drawn that the magnesium samples coated with corrosion inhibitors-doped silica film showed better corrosion resistance than the samples without corrosion inhibitors. This behaviour can be explained in terms of the self-healing. The barrier property of the corrosion inhibitors layer in the defect need to be improved for better corrosion protection which can be achieved by using more water-soluble corrosion inhibitors.

Sealing of the samples in water-based sol

Sealing of the anodized aluminium is needed to close the pores which hinder the effect of the corrosive solution on the aluminium metal substrate. The anodized aluminium alloy 6082-T6 samples were sealed in water-based sol. Silica film with a thickness of 5 µm is formed on the anodized aluminium; silica film is also presented in the pores of the anodized aluminium layer.

The anodized aluminium samples sealed in water-based sol shows no signs of metal oxide dissolution after 12 hours immersion period in 0.1 NaOH solutions, this behaviour can be explained in terms of the barrier property of the silica film on the anodized aluminium sample which hinders the effect of the base solution on the aluminium oxide layer. However, the unsealed aluminium oxide layer is dissolved in the NaOH solution after the immersion period of 12 hours.

The ceramic layer was formed on the surface of magnesium alloy AZ31 by plasma electrolytic oxidation (PEO) technique. Pores and defects were observed over the ceramic layer. The corrosion protection provided by PEO layer on magnesium alloy is not good enough to be used as a single layer. Sealing of PEO layers in SiO_2 nanoparticles and corrosion inhibitors-doped water-based sol was

successfully closed the pores and the defects of the PEO layer. The impedance of the sealed PEO samples is 100 times higher than the impedance of the unsealed PEO samples. This result can be explained in terms of the barrier silica film is formed in the pores of the sealed sample which reduces the effect of the corrosive solution.

The conclusion can be drawn that sealing of the anodized aluminium and PEO of magnesium in water-based sol improves the corrosion protection of the sample in corrosive solution; this result can be attributed to the silica film formed in the defect and pores of the sealed coating.

Stability of the water-based sol

The control of the stability during the synthesis, storage, and transportation is known to be one of the most important needs of the water-based sols. In practice, it is noticed that the stability of the sol depends on the pH value. The study demonstrates that the water-based sol at the concentration of 25: 25: 50 (GPTM: TEOS: H_2O) with 2 % SiO_2 nanoparticles and pH value of 4.5 is stable after one year at the room temperature. The stability of this sol composition is reduced at pH value of 7, which can be attributed to the attraction between the different charges in the sol (Si-OH^{2+} and the Si-O^-). The sol showed also long-term stability at pH values less than 4.5, but the silica films obtained from this sol are not protective due to the dissolution of the metal oxide at the aluminium or magnesium metal substrate surface in the acid sol, where the stable metal oxide layer is needed on the metal substrate to form protective silica film.

The achievement of the work

The achievement of the work can be summarized as follow:

- The price of the water-based sol in this work is 133 euro/l which is 60 % less than the price of the water-based sol used in the literature [19; 125]
- The using of the water-based sol reduces the amount of the alcohols in the sol. The 6 % water-based sol contains 4.5 % alcohols; the alcohols are produced by the hydrolysis of GPTM and TEOS. However, 6 % alcohol-based sol contains 90 % alcohols as solvent to achieve the homogeneity of the sol [19].
- The corrosion inhibitors-doped silica film proposed in this work is able to heal a defect with size of 600 times bigger than the defect size used by literatures [154; 155]
- The corrosion resistance of aluminium sample coated with SiO_2 nanoparticles-doped silica film is 7 % higher than the corrosion resistance of aluminium sample coated with ZrO_2 or SiC nanoparticles-doped silica film, due to the formation of aluminium silica layer at the substrate surface.
- The healing efficiency of the aluminium sample coated with corrosion inhibitors-doped silica film is stable at 11.2 % during the immersion period between (96-700) hours in chloride solution. This indicates the long-term corrosion protection due to the development in the barrier property of the corrosion inhibitors layer in the defect of the sample.
- The impedance of the magnesium sample AZ31 coated with silica film increases 60 times when the corrosion inhibitors are doped in the silica film.
- Sealing of PEO layer of magnesium alloy AZ31 in water-based sol improves the impedance of the sample 100 times, due to the formation of silica film in the defects, which hinders the effect of the corrosive solution.
- The water-based sol at the composition GPTM: TEOS: Water (25: 25: 50) to make 100 ml sol is stable for more than 12 months at pH value of 4.5.

6 References

[1] Feng, Z.; Liu, Y.: Sol–gel coatings for corrosion protection of 1050 aluminium alloy. Electrochimica Acta Volume 55, Issue 10 (2010), P. 3518–3527.

[2] Li, Y.; Mahmood, M.: An environmentally friendly coating for corrosion protection of aluminum and copper in sodium chloride solutions. Electrochimica Acta Volume 53, Issue 27 (2008), P. 7859-7862.

[3] Corriu, R.: Molecular chemistry of sol-gel derived nanomaterials. John Wiley & Sons (2009) ISBN 0470721170, P. 120-155.

[4] Zak, A.; Majid, W.: Effect of solvent on structure and optical properties of PZT nanoparticles prepared by sol–gel method, in infrared region. Ceramics International Volume 37, Issue 3 (2011), P. 753-758.

[5] Ghosh, S.: Self-healing materials: fundamentals, design strategies, and applications. Wiley-VCH Verlag GmbH & Co. KgaA (2008) ISBN 3527318291, P. 210-255.

[6] Moynot, V.; Gonzalez, S.; Kittel, J.: Self-healing coatings: An alternative route for anticorrosion protection. Progress in Organic Coatings Volume 63, Issue 3 (2008), P. 307-315.

[7] Jackson, A.: Novel encapsulation technology for small size scale self-healing applications. Materials Science and Engineering in the Graduate College of the University of Illinois at Urbana-Champaign (2011), P. 78-95.

[8] Schütze, M.; Wieser, D.; R, Bender: Corrosion Resistance of Aluminium and Aluminium Alloys. Wiley-VCH (2010) ISBN 3527330011, P. 591-395.

[9] Schweitzer, P.: Fundamentals of metallic corrosion: atmospheric and media corrosion of metals. CRC press (2007) ISBN 0849382432, P. 250-280.

[10] Sastri, V.; Ghali, E.; M. Elboujdaïni: Corrosion prevention and protection: practical solutions. John Wiley & Sons (2007) ISB N047002402X, P. 50-85.

[11] Ghali, e.; Revie, R.: Corrosion Resistance of Aluminum and Magnesium Alloys. Wiley-VCH (2010) ISBN 978-0-471-71576-4, P. 31-43.

[12] Davis, J.; Corrosion: understanding the basics. ASM International (2000) ISBN 0871706415, P. 120-155.

[13] Stansbury, E.; Buchanan, R.: Fundamentals of electrochemical corrosion. ASM International (2000) ISBN 0871706768, P. 210-222.

[14] Mccafferty, E.: Introduction to Corrosion Science. Springer Science and Business Media (2010) ISBN 978-1-4419-0454-6, P. 21-35.

[15] Beneke, H.: Lexikon der Korrosion und des Korrosionsschutzes. Vulkan-Verlag GmbH (2000) ISBN 3-8027-2-918-8, P. 169-225.

[16] Baboian, R.: Corrosion tests and standards: application and interpretation. ASTM International (2005) ISBN 0-8031-2098-2, P. 205-210.

[17] Vargel, C.: Corrosion of aluminium. Elsevier Ltd (2004) ISBN 008-0444954, P. 113-114.

[18] Heidersbach, R.; Heidersbach, B.: Metallurgy and Corrosion Control in Oil and Gas Production. John Willey, sons Inc (2011) ISBN 978-0-470-24848-5, P. 68-88.

[19] Bardal, E.: Corrosion and protection. Springer-Verlag London Limited (2004) ISBN 1852337583, P. 110-120.

[20] Revie, R.: Uhlig's Corrosion Handbook. Wiley-Interscience (2000) ISBN-13**:** 978-0471157779, P. 14-42.

[21] Cicek, V.; Al-Numan, B.: Corrosion Chemistry. Serivener Publishing LLC (2011) ISBN 978-0-470-94307-6, P. 55-70.

[22] Landolt, D.: Corrosion and surface chemistry of metals. EPFL Press (2007) ISBN 0849382335, P. 312-320.

[23] Meng, G.; Wei, L.: Effect of microcrystallization on pitting corrosion of pure aluminium. Corrosion Science Volume 51, Issue 9 (2005), P. 2151–2157.

[24] Buchheit, P.; Moran, J.: Corrosion and corrosion prevention of low density metals and alloys. Electrochemical Society Inc. (2001) ISBN 1-56677-290-7, P. 229-233.

[25] Schmuki, P.: Pits and pores II: formation, properties, and significance for advanced. Electrochemical Society Inc. (2001) ISBN 1-56677-292-3, P. 409-416.

[26] Zhu, D.: Corrosion protection of metals by silane surface treatment. PhD Thesis, University of Cincinnati (2005), P. 19-30.

[27] Shifler, D.: Corrosion in marine and saltwater environments II. Electrochemical Society Inc. (2005) ISBN 1-56677-457-8, P. 321-326.

[28] Possart, W.: Adhesion, current research and applications. Wiley-VCH (2005) ISBN 3527312633, P. 518-527.

[29] Pietschmann J., Filiform corrosion of organically coated aluminium. Part 1, Aluminium, Volume 69 (1993), P. 1019–1023.

[30] Davis, R.: Corrosion of aluminum and aluminum alloys. ASM International (1999) ISBN 0-87170-629-6, P. 55-59.

[31] Anyadike, N.: Aluminium: The Challenges Ahead. Woodhead Publishing Limited (2002) ISBN 1-8557-3591-1, P. 137-141.

[32] Steele, D.: Filiform corrosion on architectural aluminium. Anti Corrosion Materials and Methods Volume 41(1994), P. 8–12.

[33] Ambat, R.; Dwaarkadasa, S.: Effect of hydrogen in aluminium and aluminum alloys: Bulletin of Materials Science volume 19 (1996), p. 103–114.

[34] Afsetha, A.; Nordlienb, H.; Scamansc, G.; Nisancioglu, K.: Filiform corrosion of binary aluminium model alloys. Corrosion Science Volume 44, Issue 11 (2002), P. 2529-2542.

[35] Ireland, R.: Arronche, L.; Saponara,V.: Electrochemical investigation of galvanic corrosion between aluminum 7075 and glass fiber/epoxy composites modified with carbon nanotubes. doi:10.1016/j.compositesb (2011).

[36] Coya, A.; Viejob, P.; Skeldonc, P.; Thompson, G.: Susceptibility of rare-earth-magnesium alloys to micro-galvanic corrosion. Corrosion Science Volume 52, Issue 12 (2010), P. 3896-3906.

[37] Liua, C.; Chena, C.; Bholea, S.; Caob, X.; Jahazib, M.: Polishing-assisted galvanic corrosion in the dissimilar friction stir welded joint of AZ31 magnesium alloy to 2024 aluminum alloy. Materials Characterization Volume 60, Issue 5 (2009), P. 370-376.

[38] Gebharda, A,; Bayerlb, T.; Friedrichb, K.: Galvanic corrosion of polyacrylnitrile (PAN) and pitch based short carbon fibres in polyetheretherketone (PEEK) composites. Corrosion Science Volume 51, Issue 11 (2009), P. 2524-2528.

[39] Veraa, R.; Verdugob, P.; Orellanaa, M.; Muñoza, E.: Corrosion of aluminium in copper–aluminium couples under a marine environment: Influence of polyaniline deposited onto copper. Corrosion Science Volume 52, Issue 11 (2010), P. 3803-3810.

[40] Avedesian, M.; Baker, H.: Magnesium and magnesium alloys. ASM International (1999) ISBN 0871706571, P. 150-166.

[41] Kainer, K.: Magnesium: eigenschaften, anwendungen, potentiale. Wiley-VCH Verlag GmbH (2000) ISBN 3-527-29979-3, P. 258-259.

[42] Kainer, K.: Magnesium: Proceedings of the 7th International Conference on Magnesium. Wiley-VCH Verlag GmbH (2007) ISBN 978-527-31764-6, P. 721-726

[43] Gupta, M; Sharon, N.: Magnesium, Magnesium Alloys, and Magnesium Composites. John Wiley and Sons (2011) ISBN 978-0-470-49417-2, P. 87-96.

[44] Qua, Q.; Maa, J.; Wanga, L.; Lib, L.; Dinga, Z.: Corrosion behaviour of AZ31B magnesium alloy in NaCl solutions saturated with CO_2. Corrosion Science Volume 53, Issue 4 (2011), P. 1186-1193.

[45] Tanga, M; Liu. M; Zhu, L: Effect of zirconia sol in electrolyte on the characteristics of microarc oxidation coating on AZ91D magnesium. Materials Letters Volume 65, Issue 3 (2011), P. 413-415.

[46] Bierwagena, G.; Brownb, R.; Battocchia, D.; Hayes, S.: Active metal-based corrosion protective coating systems for aircraft requiring no-chromatenext term pretreatment. Progress in Organic Coatings Volume 68, Issues 1-2 (2010), P. 48-61.

[47] Philip A. Schweitzer, E.: Paint and coatings applications and corrosion resistance. CRC press (2006) ISBN-10: 1574447025, P. 250-266.

[48] Streitberger, H. Dössel, K .: Automotive paints and coatings. WILEY-VCH Verlag GmbH & Co. KGaA (2008) ISBN-10: 3527309713, P. 190-233.

[49] Gilleo, K.: Coating technology handbook. Taylor & Francis Group LLC (2006) ISBN-10: 1574446495, P. 420-455.

[50] Talbert, R.: Paint Technology Handbook. CRC Press (2007) ISBN 1574447033, P. 143-160.

[51] Gardner, H.: Paint Technology and Tests. Nabu Press (2011) ISBN 1172770336, P. 120-177.

[52] Davis, J.: Surface engineering for corrosion and wear resistance. ASM International (2001) ISBN 0-87170-700-4, P. 120-110

[53] Rufe, P.: Fundamentals of manufacturing supplement. Society of Manufacturing Engineers (2005) ISBN 0-87263-7476, P. 75-80.

[54] George, F.: Voort, V.: Metallography, principles and practice. ASM International (1999) ISBN 0-87170-672-5, P. 178-185.

[55] Aerts, T.; Jorcin, J.; Graeve, I.; Terryn, H.: Comparison between the influence of applied electrode and electrolyte temperatures on porous anodizing of aluminium. Electrochimica Acta Volume 55, Issue 12 (2010), P. 3957-3965.

[56] Giovanardia, R.; Fontanesib, C.; Dallabarbac, D.: Adsorption of organic compounds at the aluminium oxide/aqueous solution interface during the aluminium anodizing process. Electrochimica Acta Volume 56, Issue 9 (2011), P. 3128-3138.

[57] Aerts, T.; Graeve, I.; Terryn, H.: Anodizing of aluminium under applied electrode temperature: Process evaluation and elimination of burning at high current densities. Surface and Coatings Technology Volume 204, Issues 16-17 (2010), P. 2754-2760.

[58] Asoh, H.; Nishio, K.; Nakao,: Conditions for fabrication of ideally ordered anodic porous alumina using poretextured Al. Journal of The Electrochemical Society, 148-4 (2001), P. 152-156.

[59] Zaitseva, E.; Donskoi, A.: Sealants based on polysulfide elastomers. Polymer Science Series Volume 1 (2008), P. 289-297.

[60] Escudero, E.; López, E.; Bartolomé, J.; González, A.: Behaviour of anodised aluminium in very long-term atmospheric exposure. Surface and Coatings Technology Volume 201, Issues 16-17 (2007), P. 7303-7309.

[61] Cao, Z.; Cao, X.; Sun, L.; He, Y.: Surface Morphologies of Sealed Film on Anodized Al Alloy. Advanced Materials Research Volume 239 (2011), P. 2034-2037.

[62] Xingwen, Y,; Chunan, C.; Zhiming, Y.: Application of rare earth metal salts in sealing anodized aluminum alloy. Journal of Materials Science Letters Volume 19, Number 21 (2000), P. 1907-1908.

[63] Robert, B.; CEFA, M.; Clark, S.; Klingenberg, M.; Berman, E.; VoevodinN.: Alternatives to dichromate sealer in anodizing operations. Metal Finishing Volume 109, Issues 4 (2011), P. 25-32.

[64] Leea, J.; Kima, Y.; Janga, H.; Jungb, H.; Chung, W.: Cr_2O_3 Sealing of Anodized Aluminium Alloy by Heat Treatment. Procedia Engineering Volume 10 (2011), P. 2803-2808.

[65] Kim, S.; Kim, G.; Okido, M.: Sealing effects of anodic oxide films formed on Mg-Al alloys. Korean Journal of Chemical Engineering Volume 21 (2004), S. 915-920.

[66] Guo, J.; Wang, L.; Wang, S.; Xue, Q.; Yan, F.: Preparation and performance of a novel multifunctional plasma electrolytic oxidation composite coating formed on magnesium alloy. Journal of Materials Science Volume 44, Number 8 (2009), P. 1998-2006.

[67] Srinivasan, P.; Liang, J.; Blawert, C.; Störmer, M.; DietzelA, W.: Preliminary study of calcium containing plasma electrolytic oxidation coatings on AM50 magnesium alloy. Journal of Materials Science Volume 45, Number 5 (2010), P. 1406-1410.

[68] Arrabal, R.; Matykina, E.; Skeldon, P.; Thompson, G.: Incorporation of zirconia particles into coatings formed on magnesium by plasma electrolytic oxidation. Journal of Materials Science Volume 43, Number 5 (2008), P. 1532-1538.

[69] Pokhmurskii, V.; Nykyforchyn, H.; Klapkiv, M.; Pokhmurska, H.; Wielage, B.; Grund, T.; Wank, A.: Plasma electrolytic oxidation of arc-sprayed aluminum coatings. Journal of Thermal Spray Technology Volume 16, Numbers 5-6 (2007), P. 998-1004.

[70] Ferreira, T.: Corrosion protection of magnesium AZ31 alloy sheets by polymer coatings. Fakultät III – Prozesswissenschaften Der Technischen Universität Berlin (2011) PhD Thesis.

[71] Meng, Q. Frankel, S.: Characterization of chromate conversion coating on AA7075-T6 aluminium alloy. Surface and Interface Analysis Volume 36, Issue 1 (2004), P. 30–42.

[72] Steven, L.; Scala, J.: Determination of hexavalent chromium in NAVAIR trivalent chromium process coatings and process solutions. Metal Finishing Volume 107, Issue 5 (2009), P. 28-34.

[73] Grillia, R.; Bakera, M.; Castlea, J.; Dunnb, E.; Wattsa, J.: Corrosion behaviour of a 2219 aluminium alloy treated with a chromate conversion coating exposed to a 3.5% NaCl solution. Corrosion Science Volume 53, Issue 4 (2011), P. 1214-1223.

[74] Kulinich, S.; Akhtar, A.; Susac, D.; Wong, P.; Wong, K.; Mitchell, K.: On the growth of conversion chromate coatings on 2024-Al alloy. Applied Surface Science Volume 253, Issue 6 15 (2007), P. 3144-3153.

[75] Zhang, W.: Formation and corrosion inhibition mechanism of chromate conversion coatings on aluminium and AA2024-T3. Ohio State University Department of Materials Science and Engineering, PhD Thesis (2002), P. 75-90.

[76] Pöllmann, H.; Auer, S.: Cr^{6+}-containing phases in the system $CaO–Al_2O_3–CrO_4–H_2O$ at 23 °C. Journal of Solid State Chemistry, In Press (2011), doi:10.1016/j.jssc.2011.10.022

[77] Pokhmurskii, V.; Zin M.; Vynar, M.; Bily, L.: Contradictory effect of chromate inhibitor on corrosive wear of aluminium alloy. Corrosion Science Volume 53, Issue 3 (2011), P. 904-908.

[78] Vasquez, M.; Halada, G.; Clayton, G.; Longtin, J.: On the nature of the chromate conversion coating formed on intermetallic constituents of AA2024-T3. Surface and Interface Analysis Volume 33 (2002), P. 607–616.

[79] Pietschmann, J.: Industrielle Pulverbeschichtung: Grundlagen, Anwendungen, Verfahren. Vieweg and Teubner Verlag (2009) ISBN 3834804630, P. 310-340.

[80] Konietzko, J.: Arbeitsbedingte Erkrankungen, Ätiologie. Diagnose. Therapie. Hnadbuch für die ärztliche Praxis. Ecomed Verlag (2001) ISBN 3609201932, P. 55-70.

[81] Gentner, A.: Berufsgenossenschaftliche Grundsätze für arbeitsmedizinische Vorsorgeuntersuchungen. Gentner Alfons Verlag (2004) ISBN-10: 3872476351, P. 430-455.

[82] Kaatsch, P.; Katalinic, A.: Krebs in Deutschland 2005/2006 Häufigkeiten und Trends. Robert Koch-Instituts und der Gesellschaft der epidemiologischen Krebsregister in Deutschland (2010) ISBN 978-3-89606-207-9, P. 50-66.

[83] Björn, D.: Die zweite Konversionsschicht–Nachbehandlung dreiwertiger Konversionsschichten mit chrom(III)basierten Nachtauchlösungen. Eugen G. Leuze Verlag, Galvanotechnik Volume 99 (2008), P. 1080-1096.

[84] Protsenkoa, V.; Danilova, F.; Gordiienkoa, V.; Kwonb, S.; Kimb, M.: Electrodeposition of hard nanocrystalline chrome from aqueous sulfate trivalentchromium bath. Thin Solid Films Volume 520, Issue 1 (2011), P. 380-383.

[85] Zenga, Z.; Zhanga, Y.; Zhaoa, W.; Zhang, J.: Role of complexing ligands in trivalent chromium electrodeposition. Surface and Coatings Technology Volume 205, Issue 20 (2011), P. 4771-4775.

[86] Hamid, Z.: Electrodeposition of black chromium from environmentally electrolyte based on trivalent chromium salt. Surface and Coatings Technology Volume 203, Issue 22 (2009), P. 3442-3449.

[87] Zenga, Z.; Lianga, B.; Zhang, B.: Electrochemical corrosion behavior of chromium–phosphorus coatings electrodeposited from trivalent chromium baths. Electrochimica Acta Volume 53, Issue 24 (2008), P. 7344-7349.

[88] Chu, J.; Klos, P.: High-performance, eco-friendly alternative coating process for fasteners. Fastener Technology International (2009).

[89] Yua, H.; Chena, B.; Shia, X.; Suna, X.; Li, B.: investigation of the trivalent-chrome coating on 6063 aluminum alloy. Materials Letters Volume 62, Issues 17-18 (2008), P. 2828-2831.

[90] Bhatt, H.; Manavbasi, A.; Rosenquist, D.: Trivalent chromium for enhanced corrosion protection on aluminum surfaces. Metal Finishing Volume 107, Issue 6 (2009), P. 39-47.

[91] Shi, H.; Liu, F.: Characterization of self-assembled nano-phase silane-based particle coating. Transactions of Nonferrous Metals Society of China Volume 20, Issue 10 (2010), P. 1928-1935.

[92] Palanivel, V.: Modified silane thin films as an aternative to chromates for corrosion protection of AA2024-T3 alloy. University of Cincinnati, MS.c Thesis (2003), P. 75-88.

[93] Ciriminna, R.; Carà, P.; Sciortino, M.; Pagliaro.; M.: Catalysis with Doped Sol-Gel Silicates. Volume 353, Issue 5 (2011), P. 677–687.

[94] Wittmar, A.; Caparrotti, H.; Veith, V.: Simple preparation routes for corrosion protection hybrid sol-gel coatings on AA 2024. Surface and Interface Analysis (2011) in press DOI: 10.1002/sia.3771.

[95] Tavandashti, N.; Sanjabi, S.; Shahrabi, T.: Evolution of corrosion protection performance of hybrid silica based sol–gel nanocoatings by doping inorganic inhibitor. Materials and Corrosion Volume 62, Issue 5 (2011), P. 411–415.

[96] Li, D.; Huang, F.: Sol–gel preparation and characterization of nanoporous ZnO/SiO_2 coatings with broadband antireflection properties. Applied Surface Science Volume 257, Issue 23 (2011), P. 9752-9756.

[97] Belleville. P.: Functional coatings: The sol-gel approach. Comptes Rendus Chimie Volume 13, Issues 1-2 (2010), P. 97-105.

[98] Yasuda, Y.; Nishikawa, K.; Furukawa, S.: Structural colors from TiO_2/SiO_2 multilayer flakes prepared by sol–gel process. Dyes and Pigments Volume 92, Issue 3 (2011), P. 1122-1125.

[99] Parralejoa, A.; Orti, A.: Effect of type of solvent alcohol and its molar proportion on the drying critical thickness of ZrO_2–3 mol % Y_2O_3 films prepared by the sol–gel method. Surface and Coatings Technology Volume 205, Issue 11 (2011), P. 3540-3545.

[100] Weng, W.; Chen, H.; Tsai, S.; Wu, J.: Thermal property of epoxy/ SiO_2 hybrid material synthesized by the sol–gel process. Journal of Applied Polymer Science Volume 91 (2004), P. 532–537.

[101] Acrylic polymer/silica organic–inorganic hybrid emulsions for coating materials: Role of the silane coupling agent. Journal of Polymer Science Part A: Polymer Chemistry Volume 44, Issue 16 (2006), P. 4736–4742.

[102] Zhao, J.; Milanovab, M.; Warmoeskerkena, M.; Dutschk, V.: Surface modification of TiO_2 nanoparticles with silane coupling agents. Colloids and Surfaces A: Physicochemical and Engineering Aspects In Press (2011), doi:10.1016/j.colsurfa.2011.11.033.

[103] Binker, C. Scherer, G.: Sol-gel science-the physics and chemistry of the sol-gel processing. Academic press INC Elsevier (1999) ISBN 0121349705, P. 255-293.

[104] Sakka, S.; Handbook of Sol-Gel Science and Technology: Processing, Characterization and Applications. Springer US; Auflage (2005) ISBN 1402079699, P. 755-772.

[105] Sol-Gel Chemistry and technology (2001), www.solgel.com

[106] Zeigler, J.; Fearon, F.: Silicon-Based Polymer Science: A Comprehensive Resource (Advances in Chemistry Series). American Chemical Society (1989) ISBN 0841215464, P. 550-588.

[107] CASTRO, Y.; FERRARI, B. MORENO, R.; DUR, D.: Silica Sol-Gel Coatings on Metals Produced by EPD. Journal of Sol-Gel Science and Technology Volume 26 (2003), P. 735–739.

[108] Yeh, J.; Hsieh, C.; Yeh, C.: Organic base-catalyzed sol–gel route to prepare PMMA–silica hybrid materials. Polymer International Volume 56 (2007), P. 343–349.

[109] Didier, B.: Preparation of Polyimide/Silica Hybrid Material by Sol–Gel Process under Basic Catalysis: Comparison with Acid Conditions. Wiley InterScience Polymer Physics Volume 46 (2008), P. 1891–1902.

[110] Cesar, R.; Airoldi, C.: Acid and Base Catalysts in the Hybrid Silica Sol–Gel Process. Journal of Colloid and Interface Science Volume 195, Issue 2 (1997), P. 381-387.

[111] Romano, A.; Fedel, M.: Silane sol–gel film as pretreatment for improvement of barrier properties and filiform corrosion resistance of 6016 aluminium alloy covered by cataphoretic coating. Progress in Organic Coatings Volume 72, Issue 4 (2011), P. 695-702.

[112] Klein, L.: Sol-Gel Technology for Thin Films, Fibers, Performs, Electronics and Specialty Shapes. William Andrew Verlag (1989) ISBN 081551154X, P. 220-256.

[113] Li, Q.; Mihailova, B.: Aging effects on the nucleation and crystallization kinetics of colloidal TPA-silicate-1. Microporoius and Mesporous Materials Volume 43 (2001), P. 51-59.

[114] Wright, J.; Sommerdijk, N.: Sol-Gel Materials: Chemistry and Applications. CRC Press (2000) ISBN 905-6993-267, P. 75-88.

[115] Aegerter, M.; Mennig, M.: Sol-gel technologies for glass producers and users. Springer US (2004) ISBN 1402079389, P. 320-355.

[116] Hsiang, H.; Lin, S.: Effects of aging on nanocrystalline anatase-to-rutile phase transformation kinetics. Ceramics International Volume 34 (2008), P. 557–561.

[117] Klein, L.: Sol-gel optics: processing and applications. Springer US (1994) ISBN 0792394240, P. 320-344.

[118] Hamdy, A.; Butt, D.: Environmentally compliant silica conversion coatings prepared by sol–gel method for aluminum alloys. Surface and Coatings Technology Volume 201, Issues 1-2 (2006), P. 401-407.

[119] Metroke, T.; Apblett, A.: Effect of solvent dilution on corrosion protective properties of Ormosil coatings on 2024-T3 aluminum alloy. Progress in Organic Coatings Volume 51 (2004), P. 36–46.

[120] Roussia, E.; Tsetsekou, A.: Novel hybrid organo-silicate corrosion resistant coatings based on hyperbranched polymers. Surface and Coatings Technology Volume 205, Issue 10 (2011), P. 3235-3244.

[121] Liu, D.; Troczynski, T.: Water-based sol–gel synthesis of hydroxyapatite: process development. Biomaterials Volume 22, Issue 13 (2001), P. 1721-1730.

[122] Hench, L.; Ulrich, R.: Ultrastructure processing of glasses, ceramics and composites. John Wiley & Sons Inc (1984) ISBN 0471896691, P. 320-355.

[123] Brinker, C.: Better ceramics through chemistry II. Materials Research Society (1986) ISBN 0931837391, P. 55-69.

[124] Fedel, M.: Environmentally friendly hybrid coatings for corrosion protection: silane based pre-treatments and nanostrucutred water born coating. University of Trento-Italy, Department of Materials Engineering and Industrial Technology (2010), PhD Thesis, P. 25-30.

[125] Wang, H.; Akid, R.: A room temperature cured sol–gel anticorrosion pre-treatment for Al 2024-T3 alloys. Corrosion Science Volume 49, Issue 12 (2007), P. 4491-4503.

[126] Palanivel, V.; Zhu, D.; Ooij, W.: Nanoparticle-filled silane films as chromate replacements for aluminum alloys. Progress in Organic Coatings Volume 47 (2003), P. 384–392.

[127] Tanglumlert, Supaphol, P.: Hard-coating materials for poly(methyl methacrylate) from glycidoxypropyltrimethoxysilane-modified silatrane via a sol–gel process. Surface and Coatings Technology Volume 200, Issue 8 (2006), P. 2784-2790.

[128] Palanivel, V.: Modified silane thin films as an aternative to chromates for corrosion protection of AA2024-T3 alloy. University of Cincinnati USA, Department of Materials Science and Engineering (2003) Master of Science, P. 20-55.

[129] Wang, Y.: Pretreatment, morphology and properties of organosilane anti-corrosion coatings. University of Cincinnati USA, Department of Chemical and Materials Engineering (2007) PhD Thesis, P. 35-40.

[130] Kurisu, T.; Kozuka, H.: Effects of Heating Rate on Stress Evolution in Alkoxide-Derived Silica Gel-Coating Films. Journal of the American Ceramic Society Volume 89, Issue 8 (2006), P. 2453–2458.

[131] Benthem, B.: Variation in In-Plane Stress during Densification and Crystallization of Titania Gel Coatings Deposited on Different Substrate Surfaces. Journal of the American Ceramic Society Volume 92, Issue 9 (2009), P. 1951–1958.

[132] Kozuka, H.: Stress evolution on gel-to-ceramic thin film conversion. Journal of Sol-Gel Science and Technology Volume 40, Numbers 2-3 (2006), P. 287-297.

[133] Paussa, L.: Thin ZrO_2–based sol-gel films for the protection of aluminium alloy: barrier, adhesion and inhibition abilities. University of Padova Spain, Department of Industrial Engineering (2010), PhD Thesis, P. 213-223.

[134] Fix, D.; Andreeva, D.: Application of inhibitor-loaded halloysite nanotubes in active anti-corrosive coatings. Advanced Functional Materials Volume 19, Issue 11 (2009), P. 1720–1727.

[135] Hosseini, S.; Jafari, A.: Self-healing corrosion protection by nanostructure sol–gel impregnated with propargyl alcohol. Electrochimica Acta Volume 54, Issue 28 (2009), P. 7207-7213.

[136] Tavandashti, N.; Sanjabi, N.: Corrosion study of hybrid sol–gel coatings containing boehmite nanoparticles loaded with cerium nitrate corrosion inhibitor. Progress in Organic Coatings Volume 69, Issue 4 (2010), P. 384-391.

[137] Schem, M.; Schmidt, T.: CeO_2-filled sol–gel coatings for corrosion protection of AA2024-T3 aluminium alloy. Corrosion Science Volume 51, Issue 10 (2009), P. 2304-2315.

[138] Kozeij, M.; Orel, B.: Method for producing sol-gel anti-corrosion coatings for solar absorbers. WIPO Patent Application (2010) WO/2010/112481.

[139] Standke, B.; Wassmer, C.: Water-dilutable sol-gel composition. United States Patent Application, (2009) WO/2009/0022898

[140] Raps, D.; Hack, T.: Electrochemical study of inhibitor-containing organic–inorganic hybrid coatings on AA2024. Corrosion Science Volume, 51 Issue 5 (2009), P. 1012-1021.

[141] Shchukin, D.; Zheludkevich, M.: Layer-by-layer Assembled nanocontainers for self-healing corrosion protection. Advanced MaterialsVolume 18, Issue 13 (2006), P. 1672–1678.

[142] Lamaka, S.; Zheludkevich, M.: Nanoporous titania interlayer as reservoir of corrosion inhibitors for coatings with self-healing ability. Progress in Organic Coatings Volume 58, Issues 2-3 (2007), P. 127-135.

[143] Shi, H.; Liu, F.; Han, E.: Corrosion behaviour of sol–gel coatings doped with cerium salts on 2024-T3 aluminium alloy. Materials Chemistry and Physics Volume 124, Issue 1 (2010), P. 291-297.

[144] Hack, T.; Raps, D.; Anti-corrosion layer for aluminum and magnesium alloys. WIPO Patent Application (2010) WO/2010/081757.

[145] Marcus, P.; Marcus, M.: Corrosion mechanisms in theory and practice. Taylor & Francis (2002) ISBN 0824706668, P. 520-555.

[146] Kelly, R.; Scully, J.: Electrochemical techniques in corrosion science and engineering. CRC Press (2002) ISBN 0824799178, P. 320-380.

[147] Barsoukov, E.; Macdonald, J.: Impedance spectroscopy: theory, experiment, and applications. John Wiley and Sons (2005) ISBN 0471647497, P. 175-230.

[148] Orazem, M.; Tribollet, B.: Electrochemical impedance spectroscopy. John Wiley and Sons (2008) ISBN 0470041404, P. 75-120.

[149] Scully, J.; Silverman, D.: Electrochemical impedance: analysis and interpretation. American Society for Testing and Materials (1993) ISBN 0803118619, P. 307-315.

[150] Gerard, C.; Rene, M.: Fluoropolymer-containing sol-gel coating. (2004) WO2004/076570.

[151] Cui, Y.; Qian, G.: Enhanced thermal stability of optical nonlinearity for anilino–silane derived inorganic–organic hybrid thin films. Optics Communications Volume 270, Issue 2 (2007), P. 414-418.

[152] Weres, O.; Tsao, L.: The activity of NaOH buffered by silicate solids in molten sodium acetate-water at 317 °C. Journal of Solution Chemistry Volume 17, Number 8 (1988), P. 777-790.

[153] Yamasaki, N.; Korablova, I.: Formation of a Highly Protective Amorphous Aluminum Silicate Layer on Steel during Granite–Dry Steam Interaction. Journal of the American Ceramic Society Volume 86, Issue 6 (2003), P. 1061–1063.

[154] Shchukin, D.; Mohwald, H.: Corrosion inhibiting pigment comprising nanoreservoirs of corrosion inhibitor. Patent application number: 20090078153 (2009).

[155] Lamaka, S.: The combined use of scanning vibrating electrode technique and micro-potentiometry to assess the self-repair processes in defects on "smart" coatings. Electrochimica Acta (2011) In Press, doi:10.1016/j.electacta.2011.02.048.

[156] Trenado, C.; Wittmar, M.: Multiscale numerical modeling of Ce^{3+} inhibitor release from novel corrosion protection coatings. Modeling Simulation Material Science Engineering Volume 19 (2011) In Press, doi:10.1088/0965-0393, P. 120-155.

[157] Buchheit, R.; Mamidipally, S.: Active Corrosion Protection in Ce-Modified Hydrotalcite Conversion Coatings. Corrosion Volume 58 Number 1 (2002), P. 3-14.

[158] Trornans, D.; Sun, R.: Anodic polarization behavior of copper in aqueous chloride/ benzotriazole solutions. Journal of Electrochemical Society Volume 138 (1991), P. 3235-3244.

[159] Allam, N.; Nazeer, A.: A review of the effects of benzotriazole on the corrosion of copper and copper alloys in clean and polluted environments. Journal of Applied Electrochemistry Volume 39 (2009), P. 961–969.

[160] Kessler, M.: Self-healing: a new paradigm in materials design. DOI: 10.1243/09544100JAERO172. Proc. MechE Volume 221 (2007), P. 479-495.

[161] http://knowledge-storage.com/science/34-science/46-aluminium

[162] Liu, L.; Hu, J.: Improving the formation and protective properties of silane films by the combined use of electrodeposition and nanoparticles incorporation. Electrochimica Acta Volume 52 (2006), P. 538–545.

[163] Zheludkevich, M.; Tedim, J.: Self-healing protective coatings with "green" chitosan based pre-layer reservoir of corrosion inhibitor. Journal of Material Chemistry Volume 21 (2011), P. 4805-4812.

[164] Shi, P.; Ng, W.: Improvement of corrosion resistance of pure magnesium in Hanks solution by microarc oxidation with sol–gel TiO_2 sealing. Journal of Alloys and Compounds Volume 469 (2009), P. 286–292.

[165] Bestetti, M.; Forno, A.: Anodic oxidation and sol–gel coatings for corrosion and wear protection of AM60B alloy. Transactions of the Institute of Metal Finishing Volume 88, Number 1 (2010), P. 57-62.

List of publications

[1] Darwich, S.; Scharf, I.; Lampke, T: Nanostructured coatings for light weight alloy: features and performance. 14. Werkstofftechnisches Kolloquium (2011). ISBN 978-3-00-025648-6.

[2] Darwich, S.; Scharf, I.; Lampke, T.: Sol-gel coating for aluminium alloy: self-healing characteristics. Journal for Electrochemistry and Plating Technology Volume 1, Issue 4, (2011) P. 20-30, ISSN 1866-7406.

[3] Darwich, S.; Lampke, T.; Alisch, G.: Sol-gel coatings doped by corrosion inhibitors for protection of plasma anodized magnesium and magnesium alloy. Galvanotechnik 10 (2010), P. 2252-225. ISSN 0016-4232 B 20696.

[4] Darwich, S.; Azem, F.; Lampke, T.: Concept, structure and performance of sol-gel coatings on anodized light-weight metals. DFO-Tagung Leichtmetall-Anwendungen. 16-17 (2010), P. 47-50. ISBN 978-3-89943-078-3.

[5] Wielage, B.; Nickel, D.; Lampke, T.; Alisch, G.; Podlesak, H.; Darwich, S.; Hockauf, M.: Corrosion characteristics of an ultrafine-grained Al-Mg-Si alloy AA6082. Materials Science Forum Volumes 584-586 (2008), P. 988-993.

[6] Lampke, T.; Darwich, S.; Wielage, B.; Steinhäuser, S.: Cost efficient silica conversion coatings for corrosion protection prepared by sol–gel process. Mat.-wiss. u. Werkstofftech. Volume 39, Number 7 (2008), P. 460 – 465. ISSN 0933-5137.

[7] Lampke, T.; Darwich, S.; Nickel, D.; Wielage, B.: Development and characterization of sol-gel composite coatings on aluminum alloys for corrosion protection. Materialwissenschaft und Werkstofftechnik Volume 39, Issue 12 (2008), P. 914–919, DOI: 10.1002/mawe.200800396.

Presentations

[1] Workshop, Fraunhofer-Institut für Keramische Technologien und Systeme IKTS, 2008.
[2] 11 Werkstofftechnisches Kolloquium, Chemnitz 2008.
[3] 12 Werkstofftechnisches Kolloquium, Chemnitz 2009.
[4] Euro-interfinish conference, Bremen-Germany, 2010.
[5] DFO-Tagung Leichtmetall-Anwendungen, 2010, Rödermark.
[6] 13 Werkstofftechnisches Kolloquium, Chemnitz 2010.
[7] 14 Werkstofftechnisches Kolloquium, Chemnitz 2011.